EFFECT OF SCALE IN PROPPANT TRANSPORT EXPERIMENT USING PGA

A Thesis

by

TAN NHAT TRAN

Submitted to the Office of Graduate and Professional Studies of
Texas A&M University
in partial fulfillment of the requirements for the degree of

MASTER OF SCIENCE

Chair of Committee,	Nobuo Morita
Committee Members,	Kan Wu
	Hiroko Kitajima
Head of Department,	Jeff Spath

August 2018

Major Subject: Petroleum Engineering

ABSTRACT

The present experiment attempts to study the behavior of proppant mixed with fibers in slickwater fracturing using a large-scale flow equipment. Previous experiments have shown that, at small scale, PGA fibers in slickwater proved very effective in suspending proppant. The mixture was successful in creating highly conductive channels in a slot flow experimental setup. However, at such scale, the conditions for creating channels were close to ideal. The study aims at replicating the same results at a larger scale with more practical conditions.

A transparent acrylic panel, 4’ x 16’ x 4.5", with several inlets was fabricated to simulate an open fracture plane.

The results of the study are as follows:

- Large-scale slot-flow experimental setup was designed and constructed.
- The setup could successfully perform experiments to observe proppant distribution.
- Two experiments showed a proppant bank, a phenomenon often observed in previous studies. Experiment 3 showed channels as a result of mixing fibers and proppant.
- The large-scale setup could perform experiments at more rigorous conditions than the small scale and offer more objective results.
- It has 4 times more viewing area.
- The fracture width can be varied from 0.1” – 0.5”.
- The number of inlets is 5.
- It could handle up to 2 psig pressure buildup.
- It could perform experiments with flow rate of up to 24 gpm for 4 vertical foot.
- Mixing mechanism still requires improvement.

CONTRIBUTORS AND FUNDING SOURCES

This work was supported by a dissertation committee consisting of Professor Nobuo Morita [advisor] and Dr. Kan Wu of the Department of [Petroleum Engineering] and Professor Hiroko Kitajima of the Department of [Geology and Geophysics].

All the work for the dissertation was completed in collaboration with Jung Yong Kim

Graduate study was supported by funding from Texas A&M University and Kureha Corporation.

TABLE OF CONTENTS

Page

LIST OF FIGURES

Page

LIST OF TABLES

Page

1. INTRODUCTION

1.1 Hydraulic Fracturing in Shale

Hydraulic fracturing is pumping fluid into the wellbore at a high flow rate so that the reservoir rock will crack open. Continually pumping fluid will propagate the fracture into the reservoir. Then, slurry is pumped into the fracture to create a zone of high permeability. This zone is called a hydraulic fracture. The purpose of proppant is to keep the fracture's surfaces open after pumping operation stops. In shale, a technique called slickwater fracturing is often used. Slickwater fracturing is a method that uses a large amount of water to create conductive fracture networks from low permeability, high net-pay reservoir (Schein 2015).

Frac fluid in slickwater treatment consists mainly of water, friction reducer and a small amount (less than 10 lbm/1,000 gal) of viscosifier (Palisch 2010). Guar gum is the most common viscosifier used (Liang 2015). Slickwater typically has a low proppant concentration, from 0.25-1.0 lbm/gal. Some designs can have up to 3.0 lbm of proppant/gal (Palisch 2010).

1.2 Channel Fracturing

Most of fracturing techniques in the industry aim at creating a proppant pack in the fractures. This method is the easiest and most commonly used. There is another type of fracturing techniques less heard of, channel fracturing. The technology itself is not new, having been proposed since as far back as 1973 (Tinsley 1975) by Halliburton, though they called it "pillar fracturing." The term "channel fracturing" was coined by Schlumberger and Baker Hughes later.

The biggest distinction between conventional fracturing and channel fracturing is that the latter offers much higher conductivity. The operators pump proppant in a way such that they form

"chunks" or "islands" of proppant within the fracture walls. These proppant pillars are then to hold the fracture open in place of a homogeneous proppant pack. Hydrocarbon can flow through these channels.

According to Tinsley (1975), the method is significant in that it opens wide-open space for hydrocarbon to flow. According to their analysis, the ideal conductivity can reach orders of magnitude higher than that in conventional proppant pack. These numbers are due to the channels through which oil and gas flow, unobstructed by damage in the proppant pack. Several ways are used to create channels. One method, which is extensively used by Schlumberger, is to pump sequentially slurries and fibers at a calculated interval. This action leads to the sequential distribution of proppant and proppant-free fluid transport thereby diverting and facilitating islands of proppant within the fracture (Hou 2016). Another method uses slickwater with fiber added as a proppant-carrying agent. A fluid of this composition does not require sequential pumping, is easier to implement, and potentially has better production. The exact nature of fibers is not known due to proprietary property. But based on the observed properties, it seems like they are polylactic acid (PLA).

Early initiations in channel fracturing have yielded excellent results. Medvedev ed (2013) published the following findings from their technical study:

a. Achieve low occurrence of near wellbore screen-outs. Over 99.9% of all treatments achieved 100% proppant placement.
b. Significantly reduce proppant use. In average, the authors found a reduction of 43% proppant than conventional techniques.

c. After fracturing, the average initial and long term well productivity and P_{wf} consistently met or exceeded those of wells completed with conventional fracturing techniques.
d. Achieve heterogeneous proppant placement.
e. Enhanced fracture conductivity and the development of larger fracture area within the reservoir drive the productivity trends.

Rajagopalan (2015) went further in supporting the positive effect of channel fracturing. Since this technique creates high perm highway, it can overcome heterogeneity of the formation (5% - 27% porosity and perm of =< 406 mD). Plus, channel fracturing can overcome formation damage and remove declining production rate due to plugged proppant pack, which is similar to conventional fracturing.

1.3 Overview of PGA

Due to elevated attention in biodegradable polymer in the 1960s, polyglycolic acid (PGA) found its use in surgeries as medical suture. (Gilding 1979) In the late 1980s, Kureha Corporation developed the world's first PGA mass production method. (Kureha 2018). Since then, PGA has been used mostly as frac ball in hydraulic fracturing.

PGA has been applied successfully as lost circulation material (LCM) and fluid loss control material (FLM) in offshore riserless drilling (Jan 2013). The application took advantage of PGA's high tensile strength and biodegradable features to improve drilling mud. The mud formed a thin mud cake to stabilize borehole, plug open fracture and granular zone to prevent fluid loss. PGA also tangle together to be a net that helped suspend cuttings. Since PGA is

biodegradable, there was no permeability damage to the reservoir. The only downside was that PGA could not be used when temperature is above 248ºF (120ºC) (Yoshimura 2014).

Hydrolysis Rate of PGA

Since PGA ultimately degrade by themselves (Yoshimura 2014), if implemented in fracturing fluid, they likely will not contribute to skin damage. In his paper (2014), Yoshimura shows percentage of weight remaining after certain duration in different temperatures of PGA. These trends correspond closely to tensile strength with respect to time exposed to water. Though tensile strength of PGA corrodes significantly with time, they last long enough for a normal fracturing duration.

1.4 Past Experiments with PGA

In 2015, PGA and PLA were applied as fluid loss control material for fracturing fluid. In (Yoshimura 2014), the authors found the PGA and PLA fibers were as effective as silica flour, but they did not incur skin damage. Numerical simulations also showed that these materials could increase productivity by extending fracture length and width. Plus, they are applicable in both conventional and unconventional reservoir. The disadvantages are the same as with drilling mud. PGA and PLA cannot be used when reservoir temperature is above 248ºF (120ºC).

Figure 1. Result From Small Scale Experiment, Reprinted From Tran (2017)

The present thesis aims at extending previous work published by Tan Tran in 2017. The experimental setup had a dimension of 1’ x 4’ x 0.8.” The fracture width was fixed at 0.2.” A ceramic sheet was attached to one side of the fracture to simulate surface roughness. Three inlets, top, center and bottom, were installed to study the effect of injecting location. The fluid composition used in Tran (2017) was as follows

Table 1. Frac Fluid Composition (data from Tran, et al., 2017)

Water	1000 gal
Proppant	826
Guar gum	5
PGA fibers	0 – 5 lbm

The results were:

(1) Instead of using high viscosity gel, PGA fibers can suspend proppant. However, very high concentration of fibers can cause screenouts.

(2) PGA fibers help create island of proppant. The flow rates between these islands are varied. This phenomenon leads to the propagation of non-uniform proppant pack and reduces settling rate of proppant.

(3) The proppant islands remain in place long after the experiment.

Tran (2017)’s experiments, however, have some limitations. The experiment used 30/60 mesh proppant. In fracturing shale, such as the Bakken Shale, producers mostly used 20/40 mesh proppant (Hu 2014), which is heavier than 30/60. The slurry was injected from only 1 inlet. This

is not representative since there are multiple injection points in a fracturing operation. Finally, the fracture half-length was limited to 4 feet.

This thesis attempted to replicate Tran (2017)'s results, but under more rigorous conditions. We would use a large scale experimental setup of 4' x 16' x 4.5", 20/40 proppant, and have multiple injection points. The results in this experiment would better reflect fibers' performance under field conditions.

2. METHODOLOGY

2.1 Laboratory Equipment

In designing the acrylic assembly, we have the following criteria: (1) it must be able to handle up to 5 psig of fluid pressure, (2) the width of the slot must be variable, and (3) it must be larger than the experiment presented in Tran (2017) while keeping the same width to length ratio. Table 2 shows the difference in parameters between this experiment and Tran (2017).

Table 2. Difference between a Small Scale and Large-Scale Setup

	Tran (2017) (Small Scale)	Current Thesis (Large Scale)
Size	1’ x 4’ x 0.8”	4’ x 16’ x 4.5”
Channel Width	0.2”	0.1” - 0.5”
Inlet Number	3	5
Outlet Number	1	5
Maximum Flow Rate	0.61 gpm	24 gpm
Material	Acrylic	Acrylic

Acrylic is chosen as the preferred material because it is widely available. A lot of fabricating shops are familiar with them. They come in a big selection of sizes, offer high rigidity and is the most cost-effective material.

After consulting with plastic specialists, we found that, to withstand 5 psig of fluid pressure, the panel thickness would have to be around 1 inch. Since requirement (3) dictates that the new

panel must be bigger than Tran (2017)'s while keeping the same ratio of width to length; the new panel could be 2' x 8' x 1". That is, the new panel would be 2 feet high, 8 feet long and 1 inch thick. Given the biggest, standard size acrylic panel is 4' x 8', having 2 panels joining each other at the end will give us a 4' x 16' panels, a 1 to 4 ratio. This also satisfies requirement 3. A 4' x 16' view would give us higher resolution than a 2' x 8' view as well. Thus, we decided to have a 4' x 16' x 4.5" setup.

Because proppant is abrasive, damaging the panel's clarity with consecutive experiments was a likely concern. As polycarbonate is scratch-resistant, we decided to add a layer of polycarbonate where the panel meets proppant. We reduced the thickness of the acrylic inner shell from 1" to 0.75" and glued a 0.25" thick polycarbonate on top of it to create a 1" thick panel. Other drawings and specifications are presented in the Appendix.

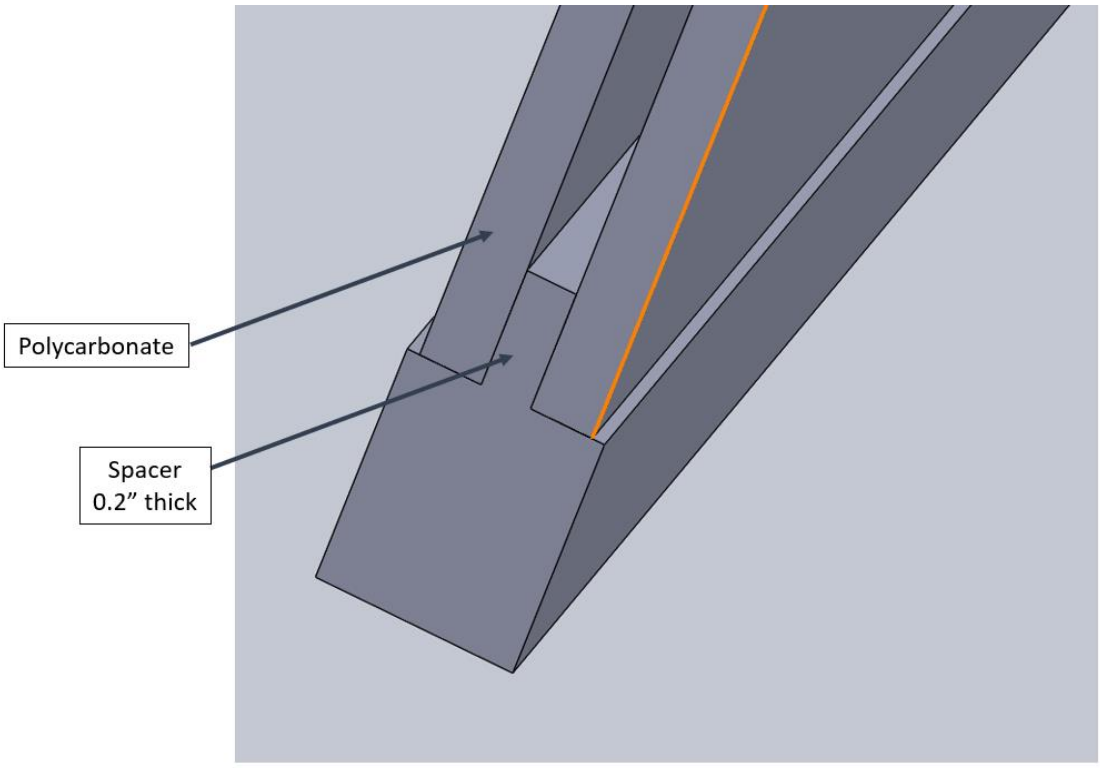

Figure 2. Spacer for Fixing the Width

To satisfy requirement (2), we have a replaceable spacer, as shown in Figure 2. The spacer will be manufactured to exact thickness requirement. If the experiment requires 0.3” fracture slot, a new 0.3” thick spacer will be made. At the same time, the filler’s thickness in Figure 3 will have to be replaced so that the total thickness inside the outer shell is 2.5”. The void space of the filler should completely disappear.

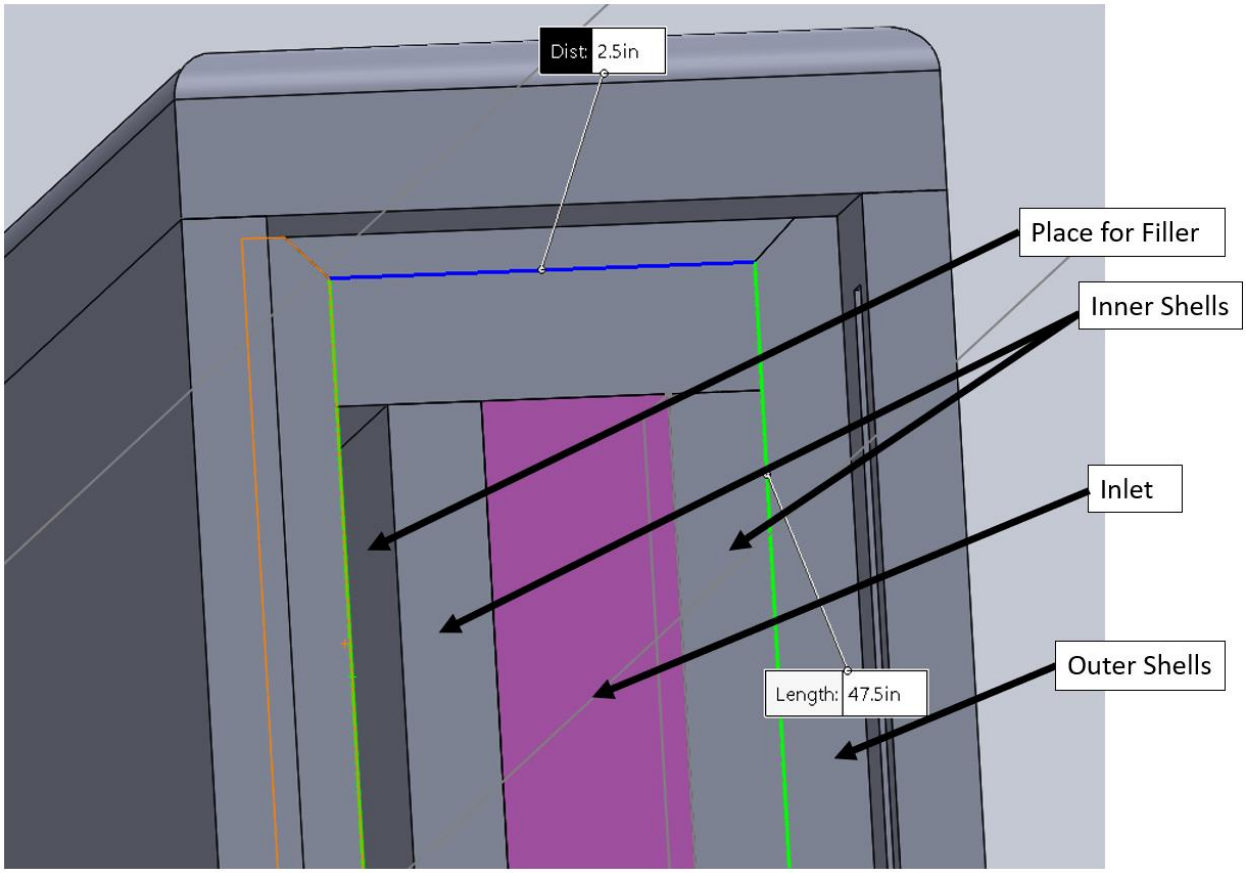

Figure 3. The Inside of the Panels When Put Together.

After designing the panels, we designed a frame to secure them in place. Based on recommendations from our machinist, we chose steel L beams and rectangular beams (Figure 4 and Figure 5). The L beam will cover the panels along the edge while the rectangular beams provide closing pressure. The machinist suggested using 17 steel bars on each side to make sure the setup in secured. Figure 6 shows the frame assembly in Solidworks.

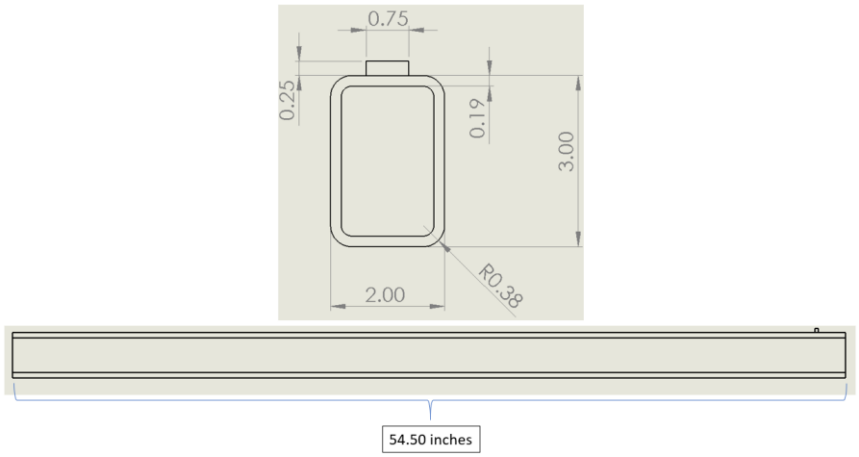

Figure 4. Dimension of a Steel Bar

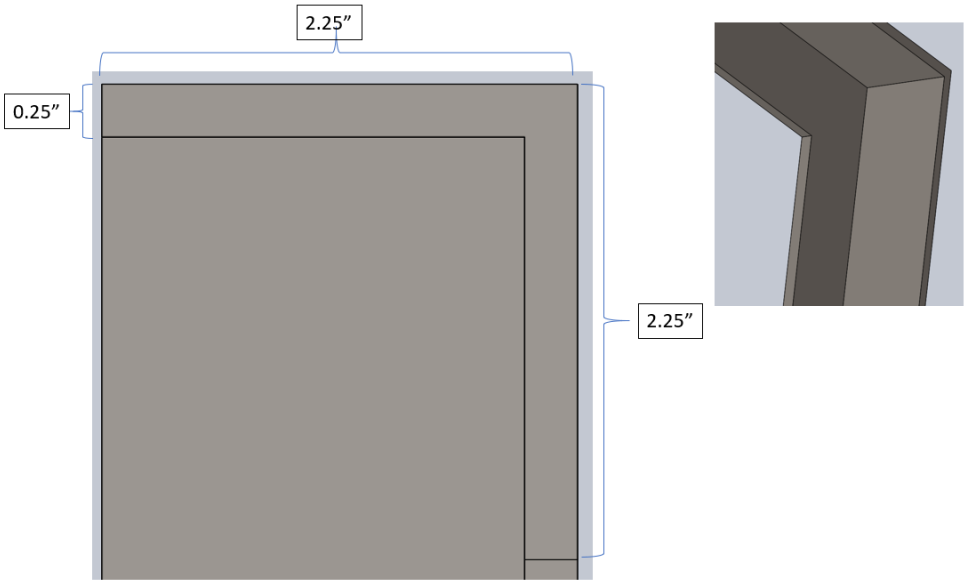

Figure 5. Dimension of the L Beam Frame

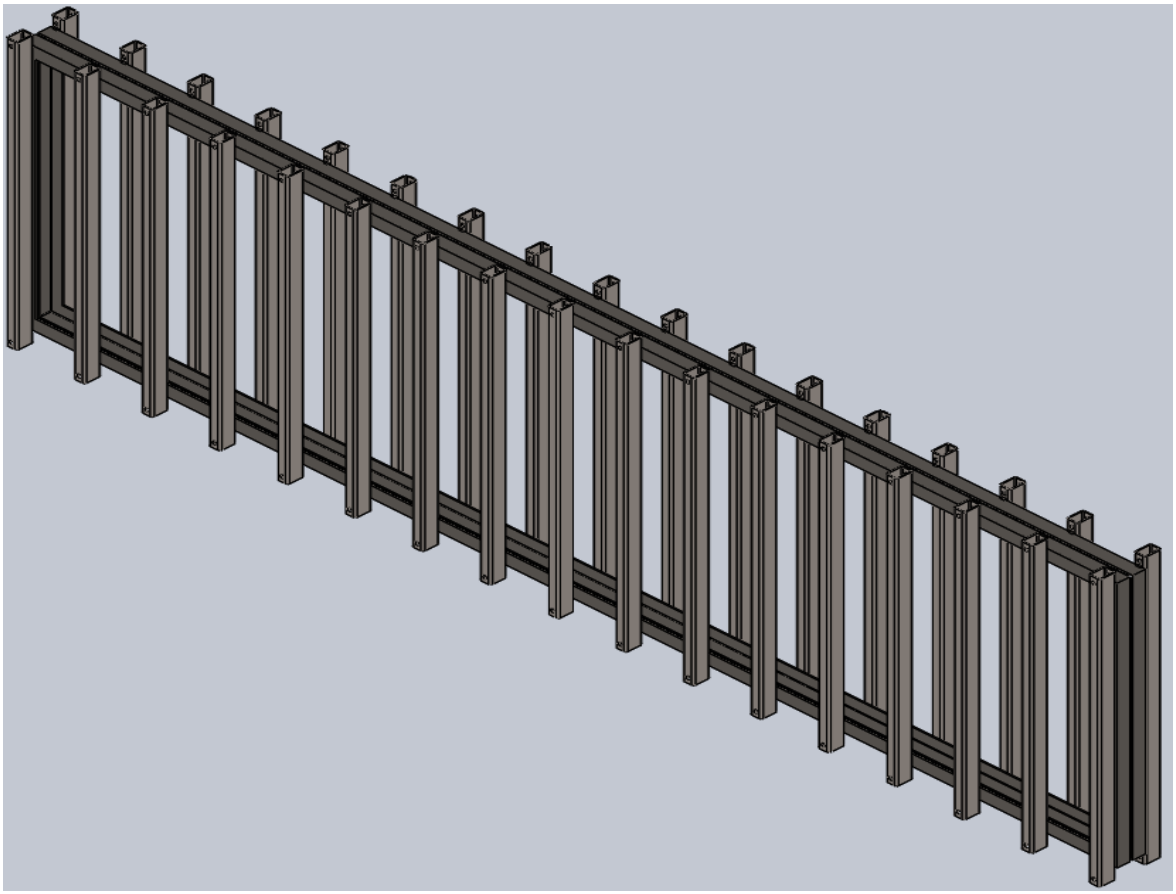

Figure 6. Complete Frame Assembly

We have 5 inlets; all are connected to a common feed. This setup is presentative of how people do fracturing in the field. Choice of pipe size is arbitrary. In this experiment, we chose 0.5" inside diameter (ID). Figure 7 shows the inlet side of the panel.

Figure 7. The Inlet Side of the Panel With Inlets and Pressure Sensor

On the outlet side, we have 5 independent outlets. Each of them flows toward a container that filters out proppant. In a design with our dimension (4’ x 16’ x 4.5”), due to big surface area, a small pressure buildup inside can result in a big amount of force; this force could severely damage the panels. Thus, we need each of the outlet to be free to quickly release the pressure.

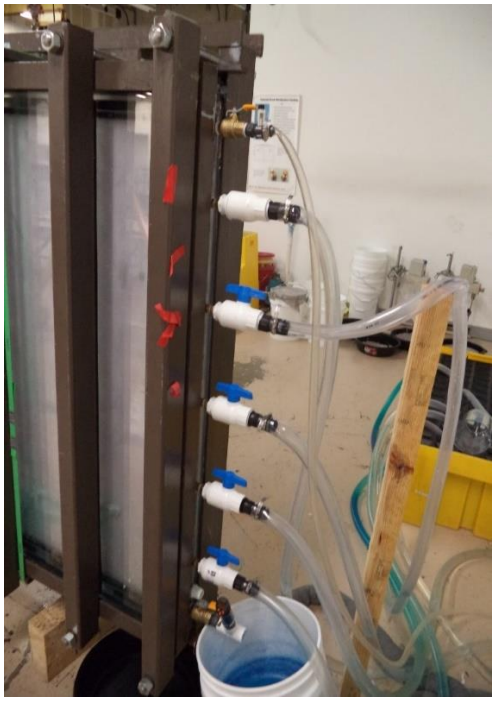

Figure 8. The Outlet Side of the Panel With Pressure Sensor

Our pump selection has three criteria: it must be able to handle fluid with up to 10% solid content; it must have a maximum rate of 20 gallon per minute (gpm); it should be maintenance-friendly; there should be an option for speed control; and lastly, it should be able to handle some pressure. All these criteria lead to the pump shown in Figure 9. Table 3 shows its specifications.

Table 3. Specification of Pumping Equipment

Pump Rate	~ 21 gpm
Power	¾ HP
Motor RPM	1725
Frame	56C

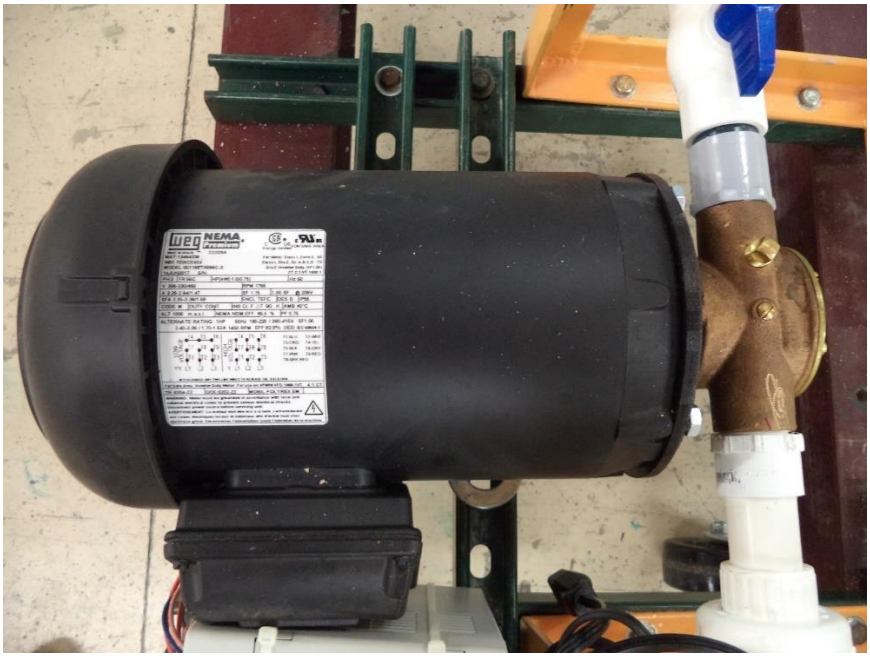

Figure 9. WEB General Purpose Motor

Three-phase motors can be controlled by a variable frequency drive (VFD), so we chose a VFD that has sufficient power to handle the WEB motor. In the future, we are looking at pumping at constant rate or constant pressure, so the VFD we chose had that function as well. The VFD is shown in Figure 10.

Figure 10. Automation Direct GS2-22P0 Variable Frequency Drive

We chose a flow meter that has the following characteristics: having no moving parts; can withstand sand; having a minimum range of 20 gpm; and lastly, having an analog to digital output for data logging. As fracturing fluid carries polymer and proppant, we cannot use flow meter with moving parts. This takes out most of the flow meter that works with an impeller. After consulting with ifm efector, a sensor manufacturer, we were recommended the SA6010. The sensor has no moving mechanism. Its maximum rate covers 20 gpm, and it has an analog output as well. The sensor is shown in Figure 11.

Figure 11. Flow Sensor SA 6010

The pressure sensors we chose required similar criteria. It must be able to handle solids. The working range should be up to 15 psi, a step measurement of 0.01 psi and analog output for data logging. The PN2697 (Figure 12) from ifm efector satisfied these conditions well. It has no moving part. It has an operational range of 0 – 14.5 psi, a step pressure of 0.02 psi and analog output. The step pressure is still acceptable at 0.02 psi.

Figure 12. PN2697 Flow Sensor

Our mixing tank has a capacity of 110 gal (Figure 13). Its cone-shape bottom allows fluid to be drained completely. The path to divert flow on the right is to aid the pump at low flow rate. By experience, we found that our pump is capable of pumping fluid reliably at or above 500 RPM, or 8 gpm. If we reduce the RPM, torque will be too high for the motor to handle, prompting the VFD to shut down. By having a diverting path, we can set the motor speed below 500 RPM and manually adjust the extra valve to achieve a desired rate.

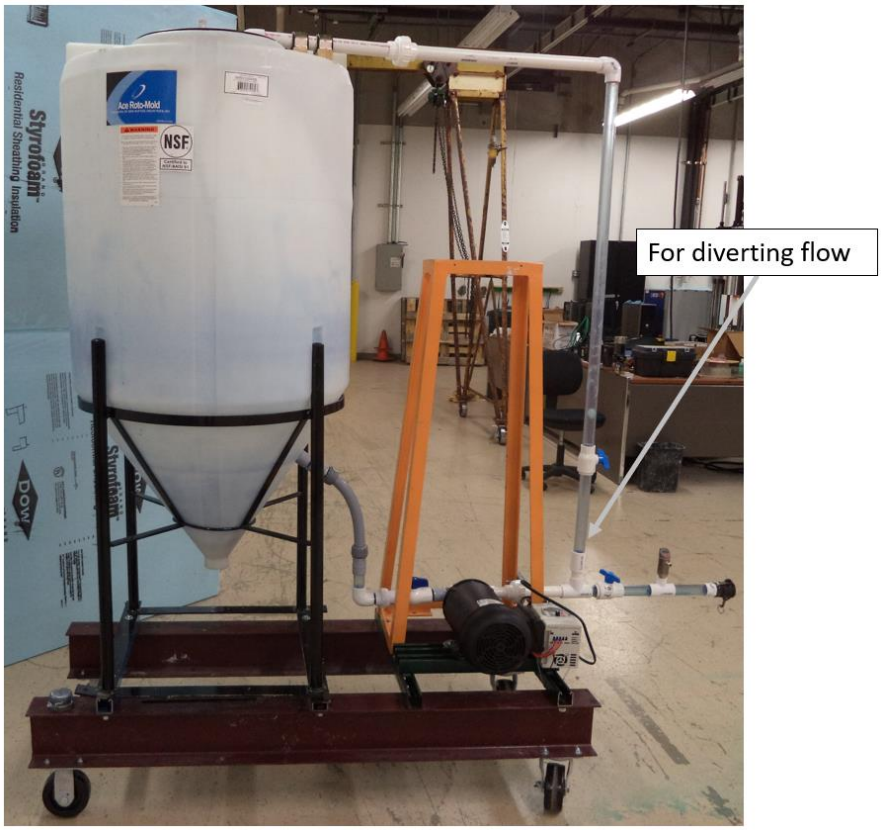

Figure 13. The Mixing Tank, Pump, VFD and Other Equipment

To agitate the fluid, we had a circulating pump placed at the bottom (Figure 14). The pump would suck fluid from the bottom and circulate to the top, creating a uniform solution.

Figure 14. Submersible Pump for Circulating Slurries

We used CARFRAMO RZR50 mixer for making guar solution (Figure 15). The concentrated solutions will be made outside the mixing tank. After we dissolved all the guar amount we needed, we filled up the rest of the tank with water until we had 100 gal.

Figure 15. CARFRAMO RZR50 Fluid Mixer

For measuring viscosity, we use FANN viscometer (Figure 16).

Figure 16. FANN Viscometer

The data acquisition module is necessary for logging pressure and flow rate data throughout the experiment. We use an acquisition module from DATAQ, model DI 1120 (Figure 17). Channel 1 was reserved for flow rate. Its voltage range is from 1 to 5 V for a flow range of 0 – 24 gpm. Channel 2 and 3 are for inlet and outlet pressure. Their ranges are from 0 V to10 V for a range of 0 – 14.5 psig.

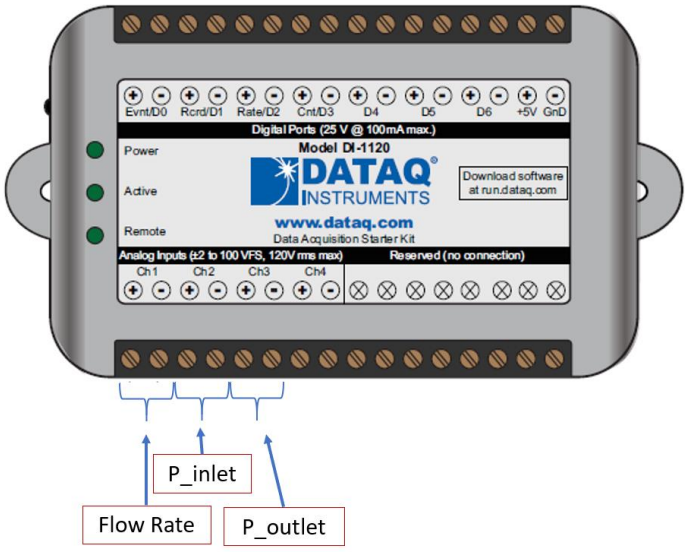

Figure 17. Data Acquisition Module – DI1120

2.2 Experimental Sample

Below, we will show the samples we used during our experiment. We obtained guar gum from ingredi.com (Figure 18).

Figure 18. Guar Gum

Our proppant was 20/40 size (2.69 g/cc or 167.93 lbm/ft^3) provided by CARBO (Figure 19).

Figure 19. CARBO Proppant With Mesh Size 20/40

Figure 20. PGA Fibers Samples Were Degraded

All our fibers were provided by our sponsor company. Since PGA had been severely degraded (Figure 20), we decided to run the experiment with PGA/PLA 50/50 instead (Figure 21). The PGA/PLA sample has been pre-cut to be roughly 0.2".

Figure 21. PGA/PLA 50/50 Fibers Still Maintained Fibrous Form

2.3 Experimental Procedures

2.3.1 Assembling Procedure for the Acrylic Panels

The process starts after all the panels are cleaned of silicon residues and smudges from previous experiments. Beginning with a bottom frame in the horizontal position (Figure 22), we put the outer shell inside the steel frame (Figure 23).

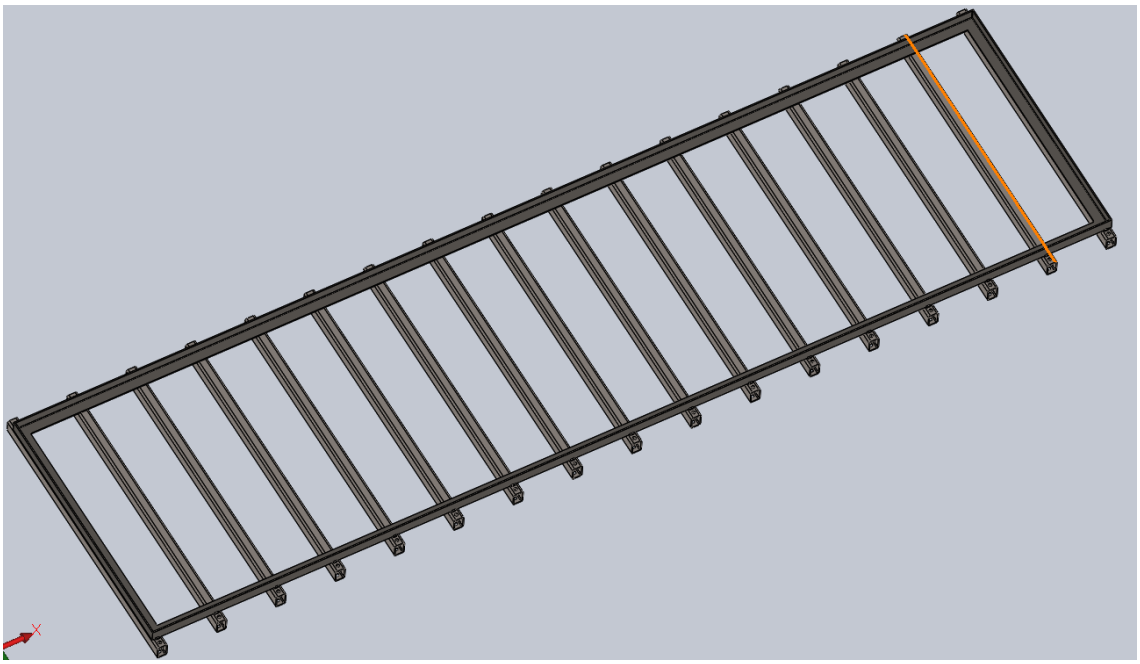

Figure 22. The Bottom Steel Bars and Frame

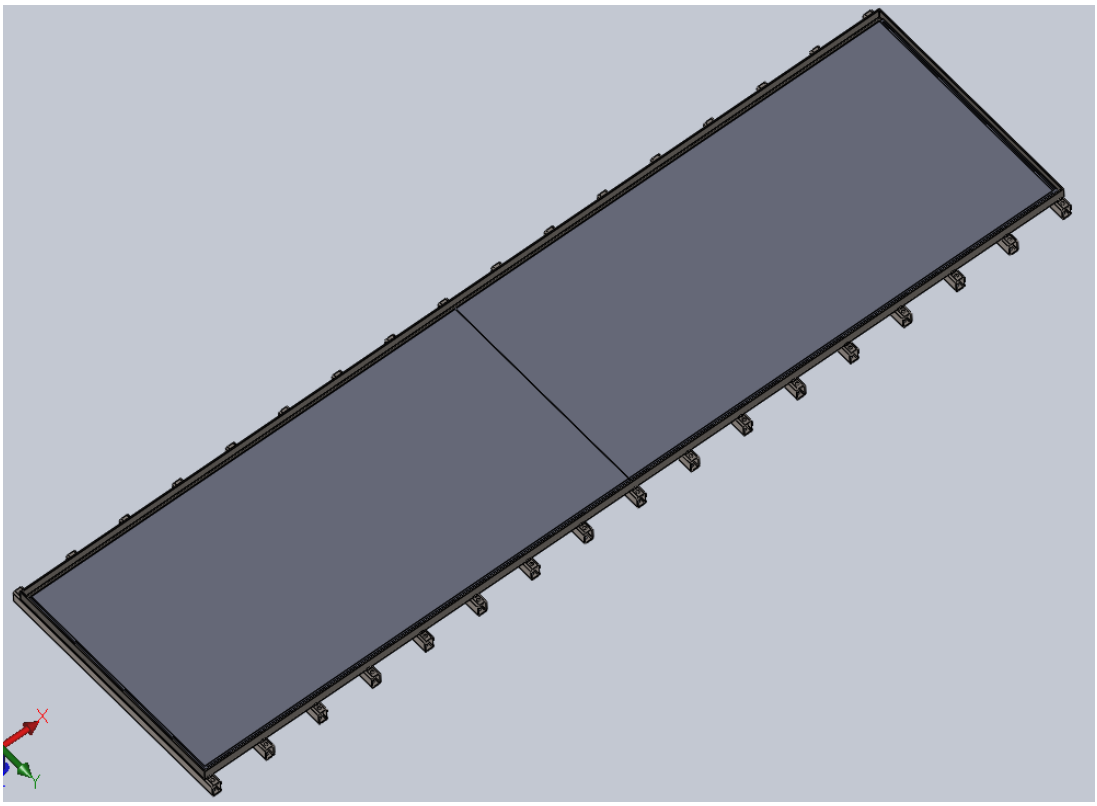

Figure 23. The Bottom Outer Shell was Inserted Into the Steel Frame

Next, we put the top and bottom cap into the steel bar (Figure 24). We then inserted rubber gaskets into the slot (Figure 25) on both pieces and secured them using silicone. Once they are in, we used a mallet to push the outer shell slightly toward the bottom of the frame to align well with the bottom cap. This is necessary to achieve a tight assembly later.

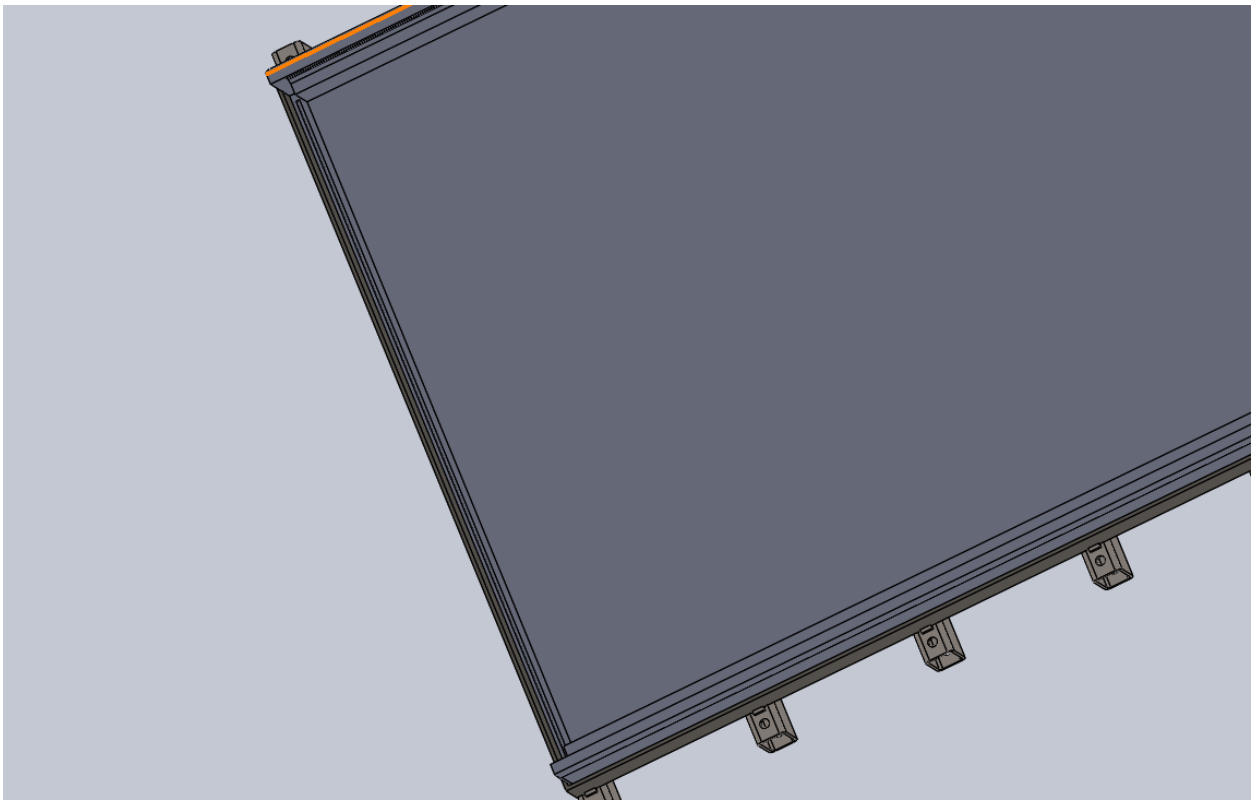

Figure 24. Steel Frame With Top and Bottom Cap Installed

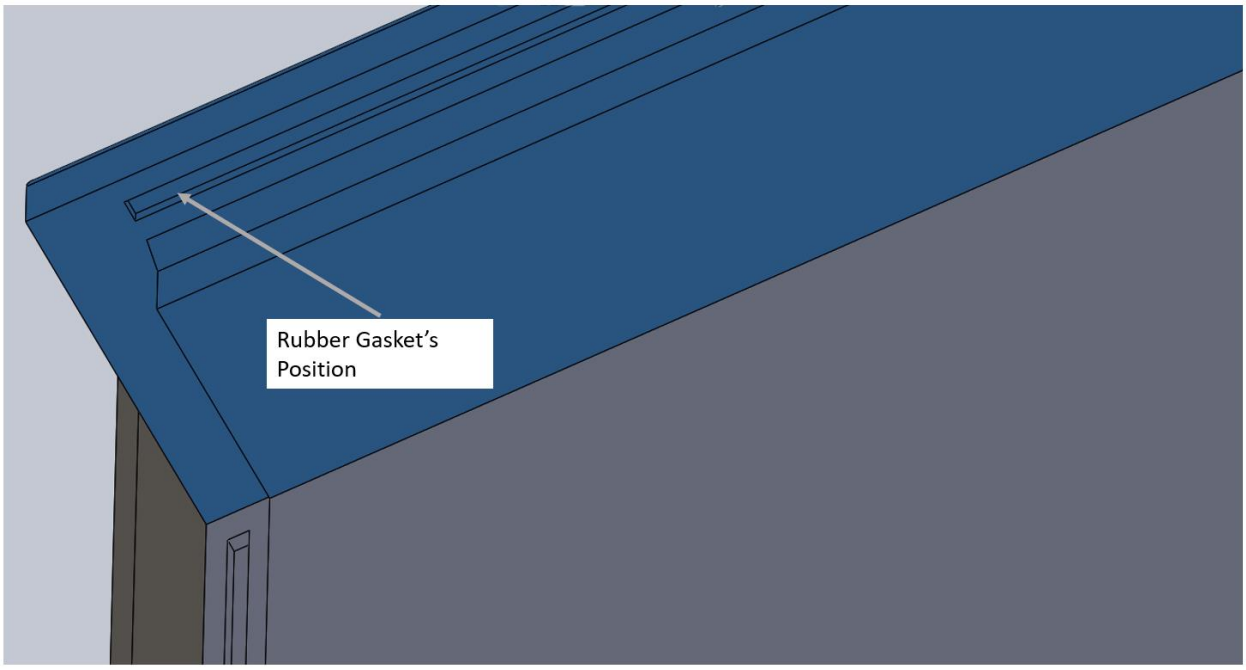

Figure 25. Position to Install Rubber Gasket

Next, we put the filler layers on top of the outer shell panels. To achieve a 0.2" fracture width, a 0.2" spacer was used; thus, a filler with 0.15" thickness was chosen. Figure 26 shows this process after putting the fillers on.

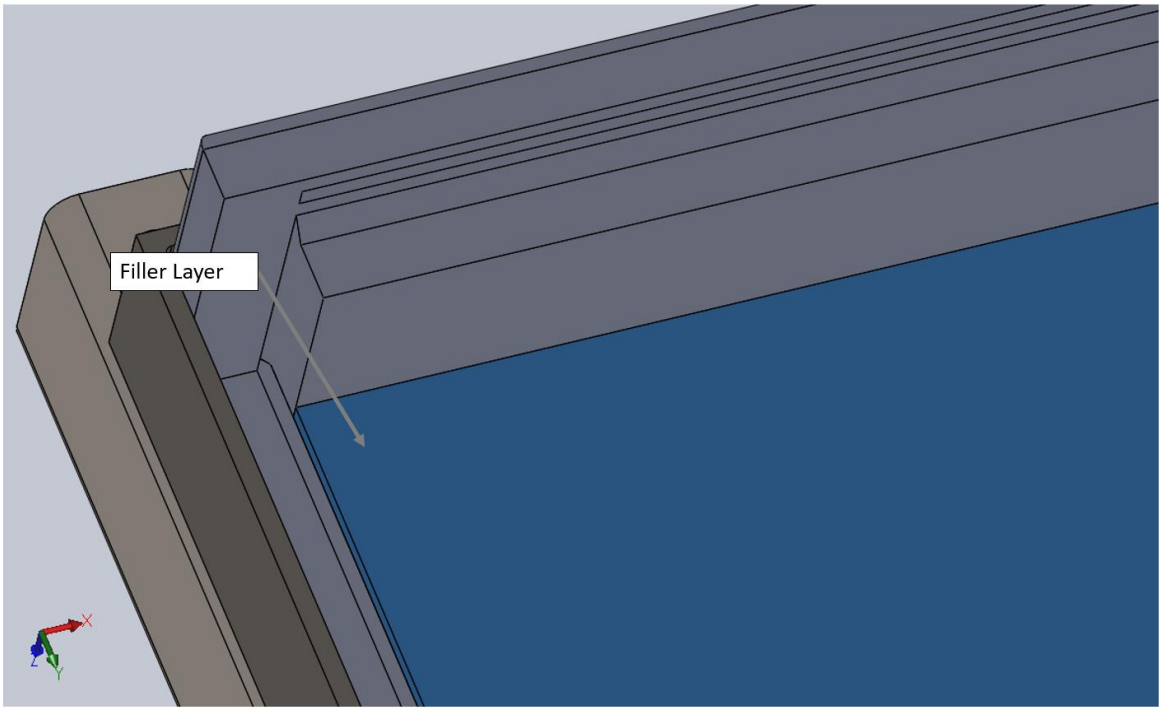

Figure 26. Outer Shell With Fillers

After Figure 26, we installed an inner shell layer. It's shown in Figure 27.

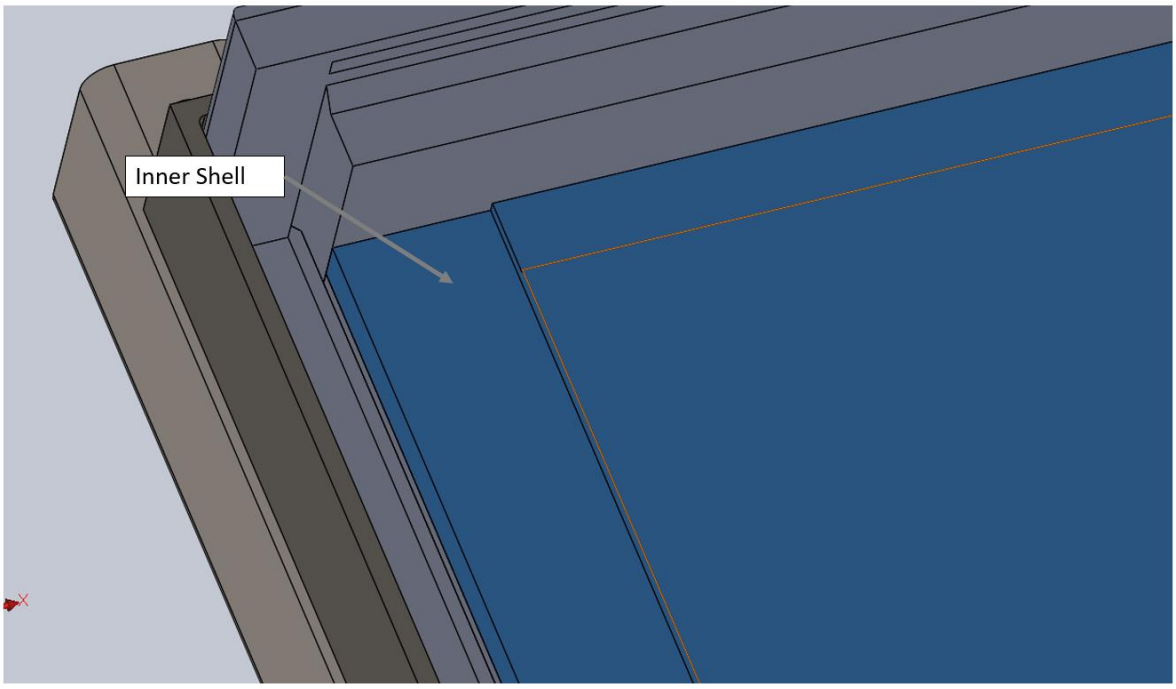

Figure 27. Inner Shell Layer Installed

A polycarbonate layer can then be added (Figure 28).

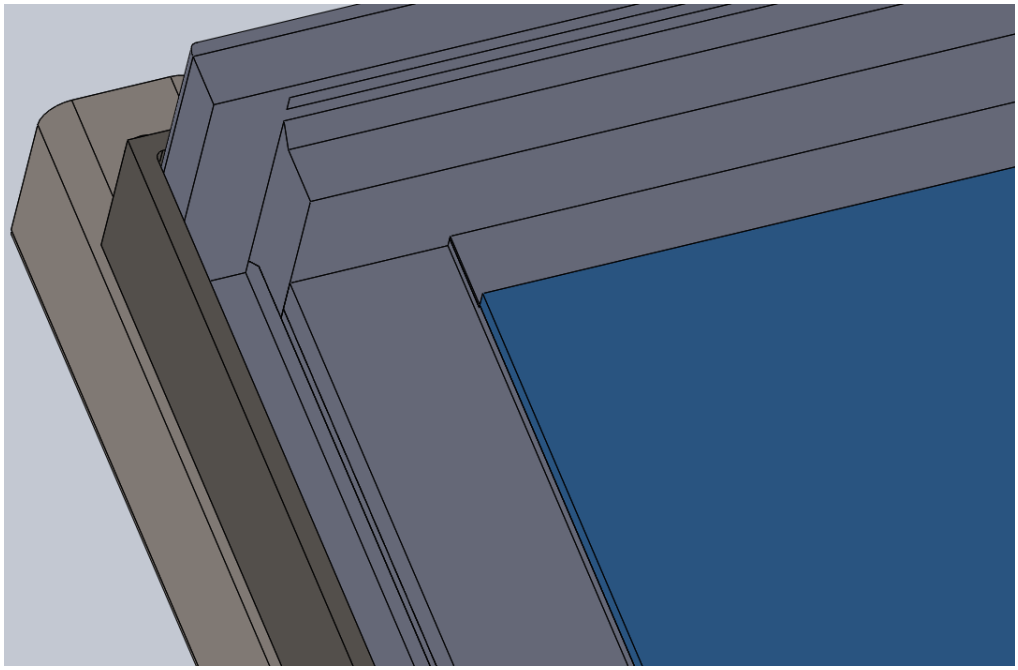

Figure 28. Inner Shell With Polycarbonate Layer

Then, we installed the top, bottom, and side spacers (Figure 29).

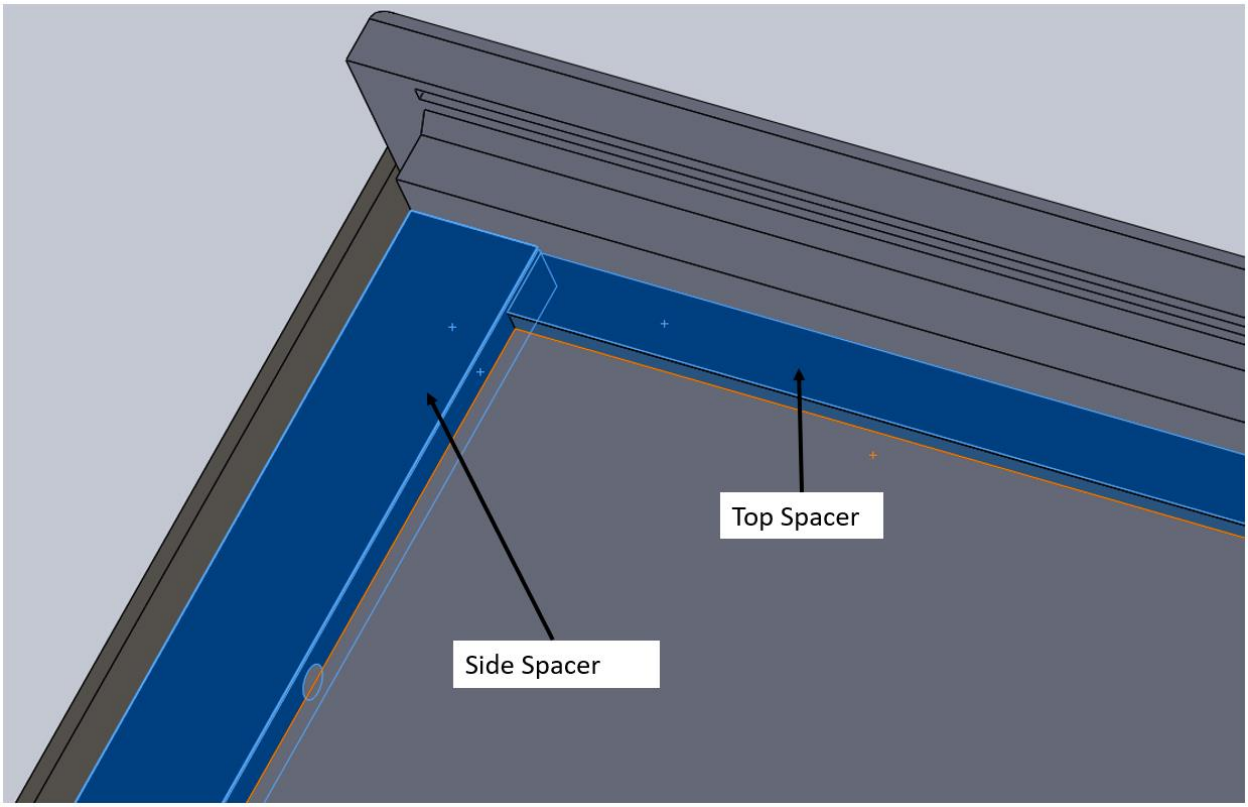

Figure 29. Inner Shell With Spacers Installed

On top of the spacer, we then installed another layer of polycarbonate (Figure 30).

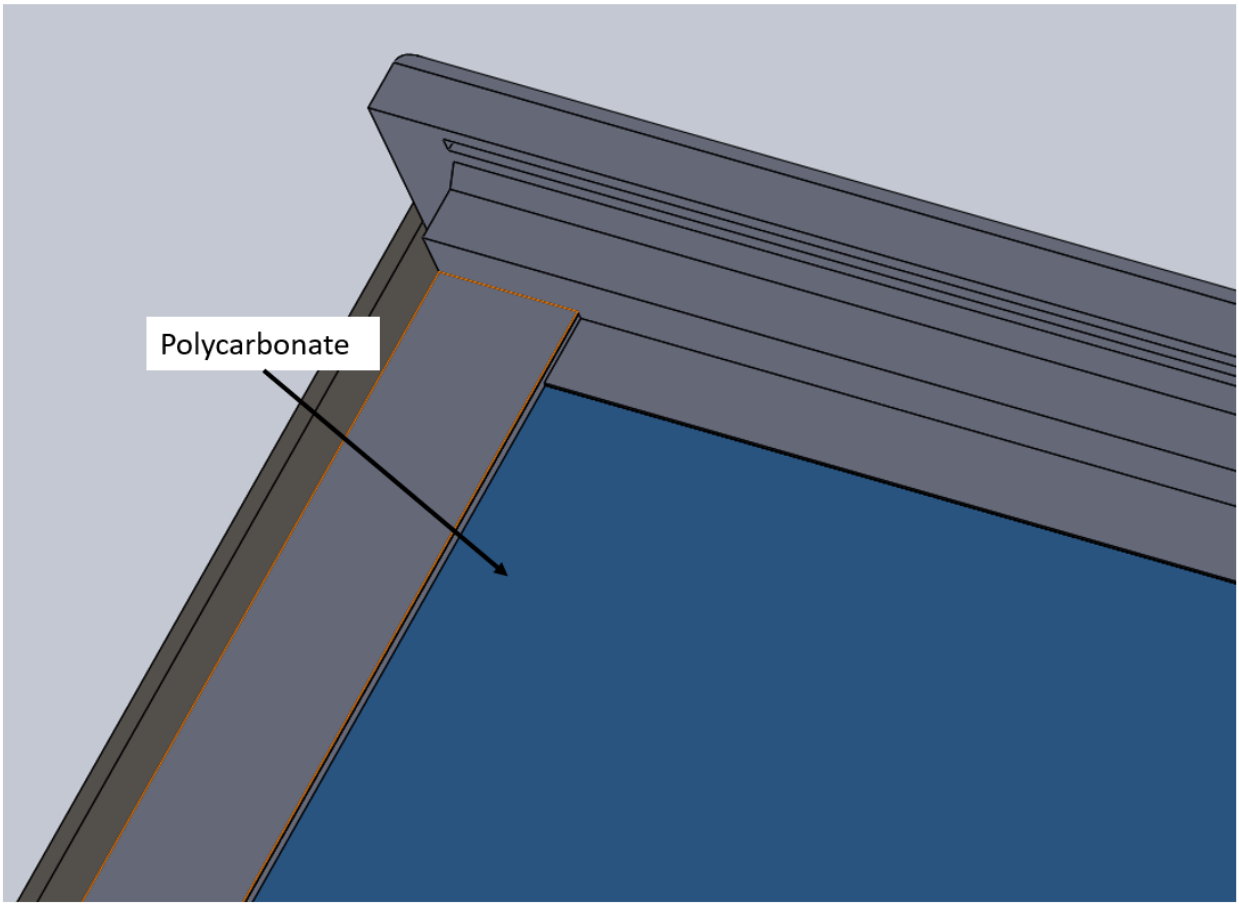

Figure 30. Polycarbonate on the Spacers

After this step, we installed the rest of the layers in order: Inner Shell and Fillers. Then, we added silicone gasket into the slot on at the inlet and outlet securing them with silicone. Then, we inserted the outer shell's inlet and outlet (Figure 31). We added extra silicone around the cone to make sure there is no leakage. Finally, we put the outer shell on top, the other steel frame (Figure 32) and bolted them all with steel bars (Figure 33). The assembly is complete (Figure 33).

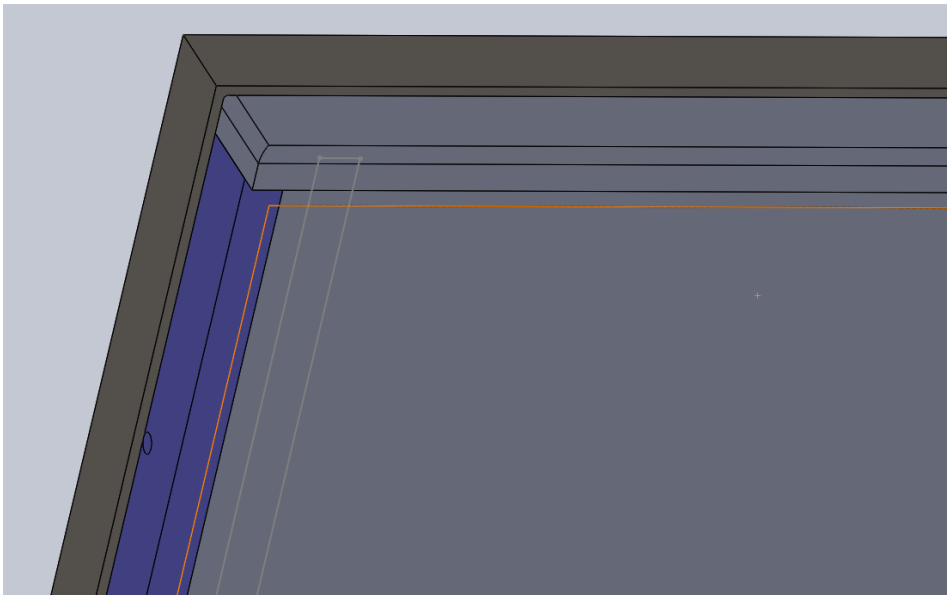

Figure 31. Outer Shell's Inlet

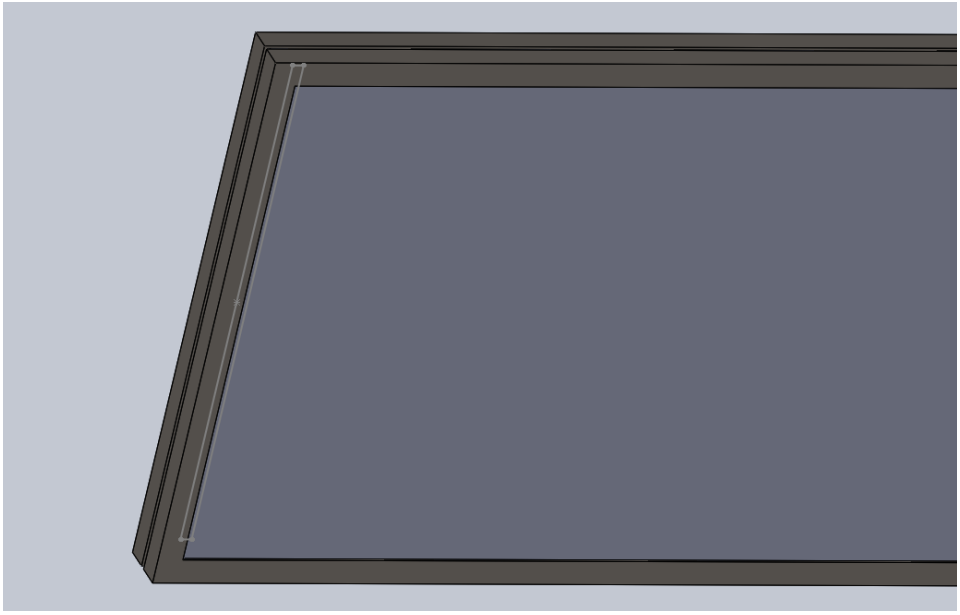

Figure 32. Assembly With Outer Shell and Steel Frame Installed

Figure 33. The Completed Panels

2.3.2 Fluid Mixing Procedure

The mixing procedure is crucial in ensuring the frac fluid in the experiment is representative of field-level frac fluid. Since we only had 50 lbm of proppant, we needed to adjust the amount of fiber according to this amount. The fluid composition is given in Table 4.

Table 4. Fracturing Fluid Composition for 60 Gallons

Fluid	60 gal (227.125 L)
Proppant	49.56 lbm (22,480.038 g)
PGA fiber	0 - 0.300 lbm (0 - 136 g)
Guar	0.300 lbm (136 g)

Guar gum cannot be added directly into the tank since there will be fish-eye, a phenomenon when only the surface of the guar portion is hydrolyzed thus preventing the rest from contacting water. Thus, we need to gradually dissolve guar in small amount. To begin, we measured out 226.8 g (0.5 lbm) of guar. We then turned on the mixer so that a vortex can be seen. Using a small spoon, we scooped up a teaspoon-sized of guar and dropped into the bucket by tapping the spoon lightly and repeatedly on the bucket's wall. The guar powder should land on the wall of the vortex. If the fluid becomes thick enough, we emptied it into the tank and repeated the process until all the guar is used.

2.3.3 Measuring the Viscosity

Measuring viscosity comes after the final fluid composition is prepared and before pumping slurry into the panels. For experiments with fibers, we take a fluid sample after adding fibers into the mixing tank. We then measured the viscosity of this fluid using a FANN rheometer (Figure 16). In both experiment 2 and 3, we got a value of 3.0 cp.

2.3.4 Fill Up and Air Bleeding Procedure

The first step in running the experiment is filling up the panels with fluid. Excessive pressure buildup can cause the panels to inflate and break; it is essential to make sure that the pressure gauge is reading less than 2.0 psi always.

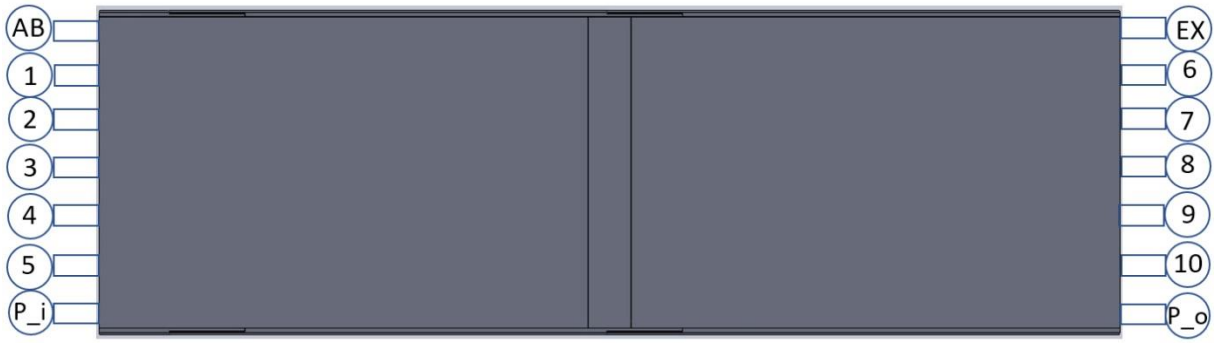

- 1 – 5: Inlet Valves
- 6 – 10: Outlet Valves
- AB: Air Bleeding Valve
- EX: Extra Valve, No Significant Usage
- P_i: Inlet Side Pressure Sensor and Pressure Relief Valve
- P_o: Outlet Side Pressure Sensor

Figure 34. Position of Valves and Sensors on the Panels

The valves' positions are shown in Figure 34. We filled the mixing tank up to 100 gallons with water or slickwater. With the pump at a stop, we closed valve 5, 8, 9, and 10. While watching the pressure valve, the VFD is set slightly above 500 RPM while the pump valve on the diverting line is adjusted to achieve 3 - 4 gpm. As the water level reached valve 6, we closed it and reduce pump rate. At this time, the EX valve should be closed, and the AB valve should be open. Once fluid escaped the AB valve, we stop the pump.

2.3.5 Slurry Pumping Procedure

Starting with valve 6-10 closed, as the first person ramped up the VFD to 10 gpm, the other opens valve 6. If the air gap at the top surface widens, we needed to increase flow rate and limit valve 6. If pressure approaches 2.00 psi, we must open valve 6 again. In experiment 2 and 3, we could pump at around 13 gpm without going above 2.00 psi.

2.3.6 Cleaning Procedure

Due to the size of the acrylic assembly, it was difficult to clean up after an experiment. Thus, we came up with a quick method to remove proppant without disassembling it. To access the middle channel, we first needed to remove the outlet pressure gauge, P_o, along with the valve and nipple. Next, we removed the inlet pressure gauge and pressure relief valve. At this point, some proppant could flow out from both inlet and outlet. To retrieve them, we inserted a bucket beneath the opening. At the outlet, we attached a garden hose to the outlet's nipple using appropriate adapter. We turned on the water until it exceeds the top proppant dune. Since water served as a transporting medium for the proppant, it would carry proppant with it along its surface. Replace the bucket at the inlet with a new one when it is full. We repeated this process until proppant out-flow rate significantly decreases.

At this point, the proppant dune should be too flat for the water to carry efficiently. We would need to directly push the proppant out of the inlet. From the outlet, we pushed the beginning of the steel wire through the port, making sure the hook and all attached pieces pass through smoothly. The wire should go all the way from the outlet to the inlet. At the end of the procedure, one should see clearly the bottom of the panels.

3. RESULTS AND DISCUSSION

3.1 Stress-Strain Analysis and Factor of Safety

For economic and safety reasons, before manufacturing the steel frames and bars, we needed to run a stress analysis on the assembly. We utilized Solidworks, a professional CAD software, on the model shown in Figure 35. Ideally, our panels should be able to endure an internal pressure of 10 psig and handle 3,600 lb of acrylic panels. 3,600 lb is the total weight of all parts of the acrylic estimated by Solidworks. Solidworks used finite element analysis to calculate stresses, strains, and displacements. To begin with, we apply fixtures on the bottom of each steel bars (Figure 35). By doing this, we are assuming that the panels will be placed on the ground.

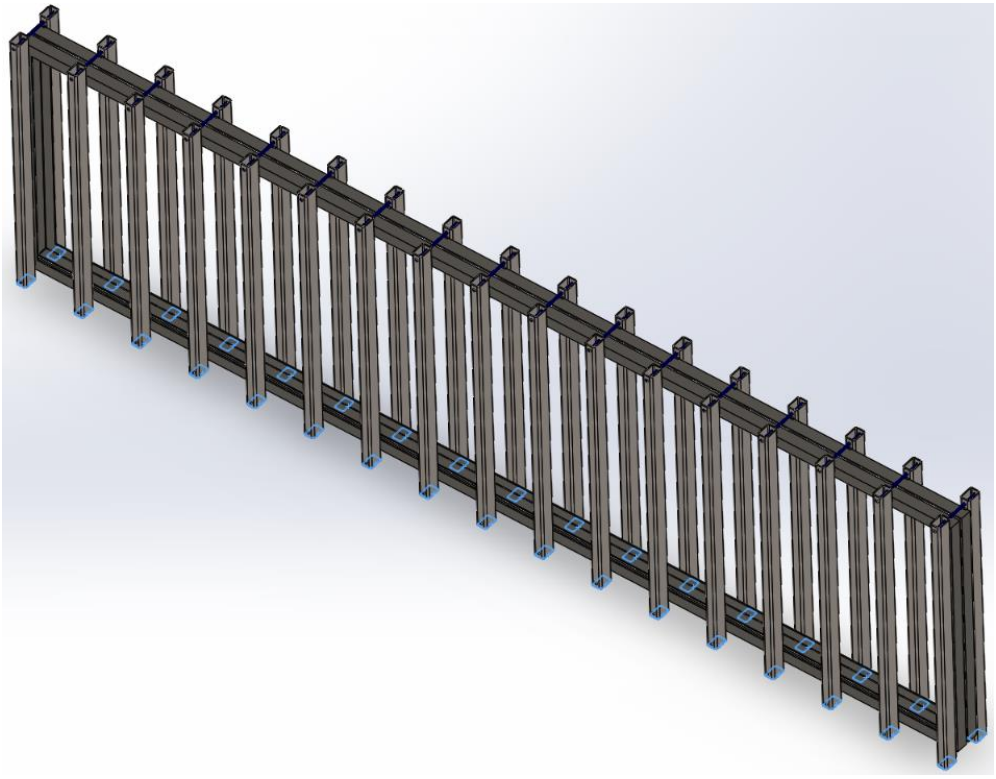

Figure 35. Fixture Location on the Panels

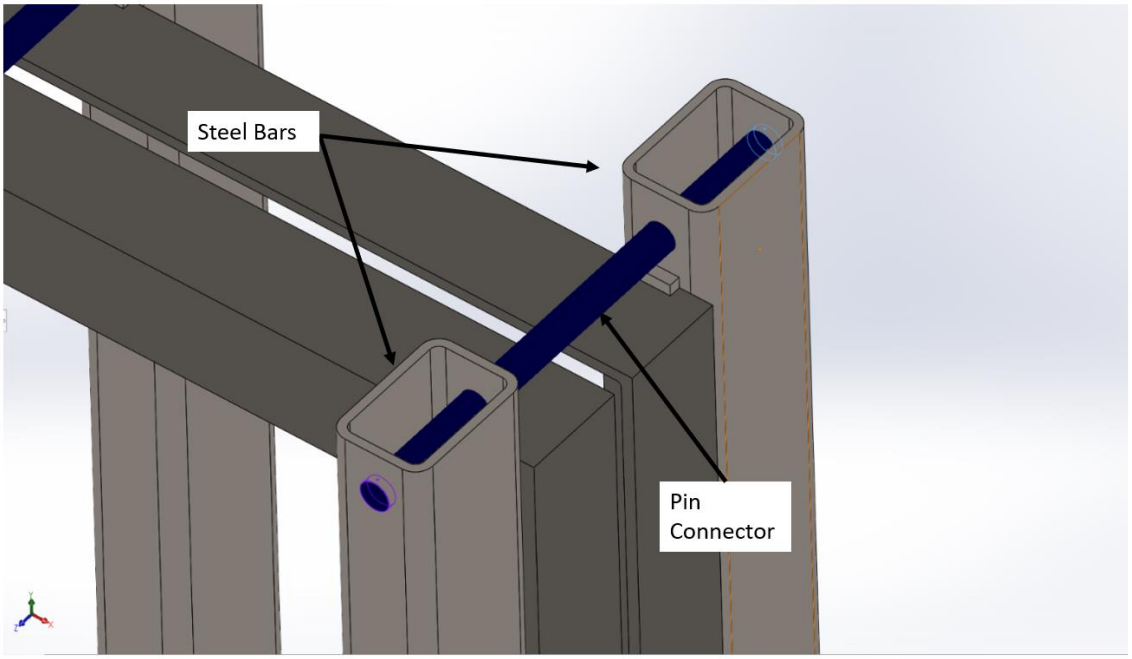

Figure 36. Pin Connector Joining Two Steel Bars

Each bar is connected to the frames by a pin connector. This is a good assumption since we used steel spacer to keep the bars apart (Figure 36). The steel spacer keeps the bars together by using nuts and bolts (Figure 37).

Figure 37. Steel Spacer for the Bars

We assumed that, in the worst case, our internal fluid pressure would be 10 psig. This pressure would expand the slot within the panels, pushing them out in all directions. In the simulator, we applied 10 psig to all faces meeting the panels (Figure 38). Also, a constant force of 3,600 lbf is applied vertically on the bottom beams (Figure 39); each beam would take on 1,800 lbf. This stands for the weight of the panels when the whole assembly is lifted vertically up.

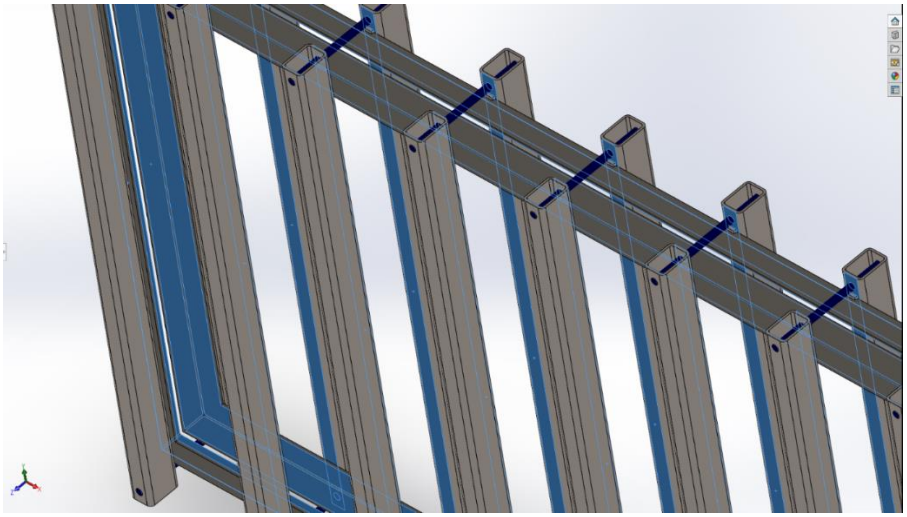

Figure 38. Faces Where Pressure is Applied

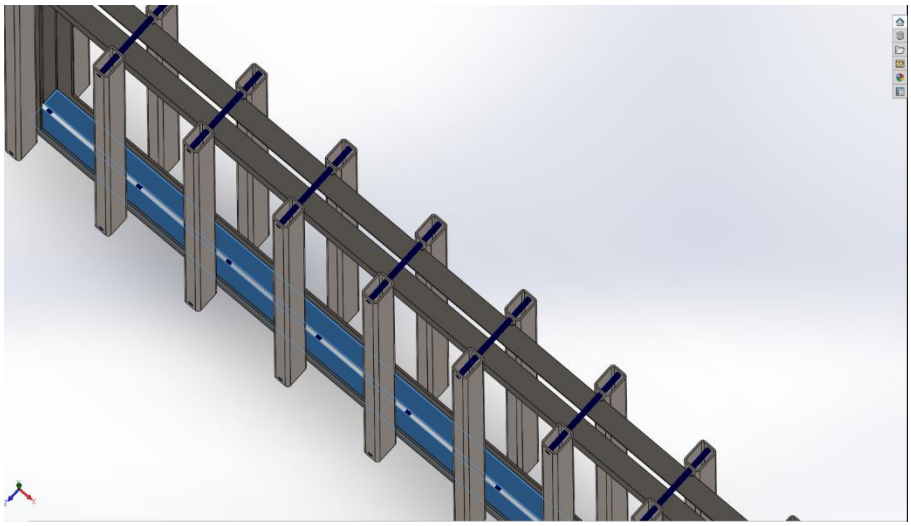

Figure 39. Faces Where Normal Forces are Applied

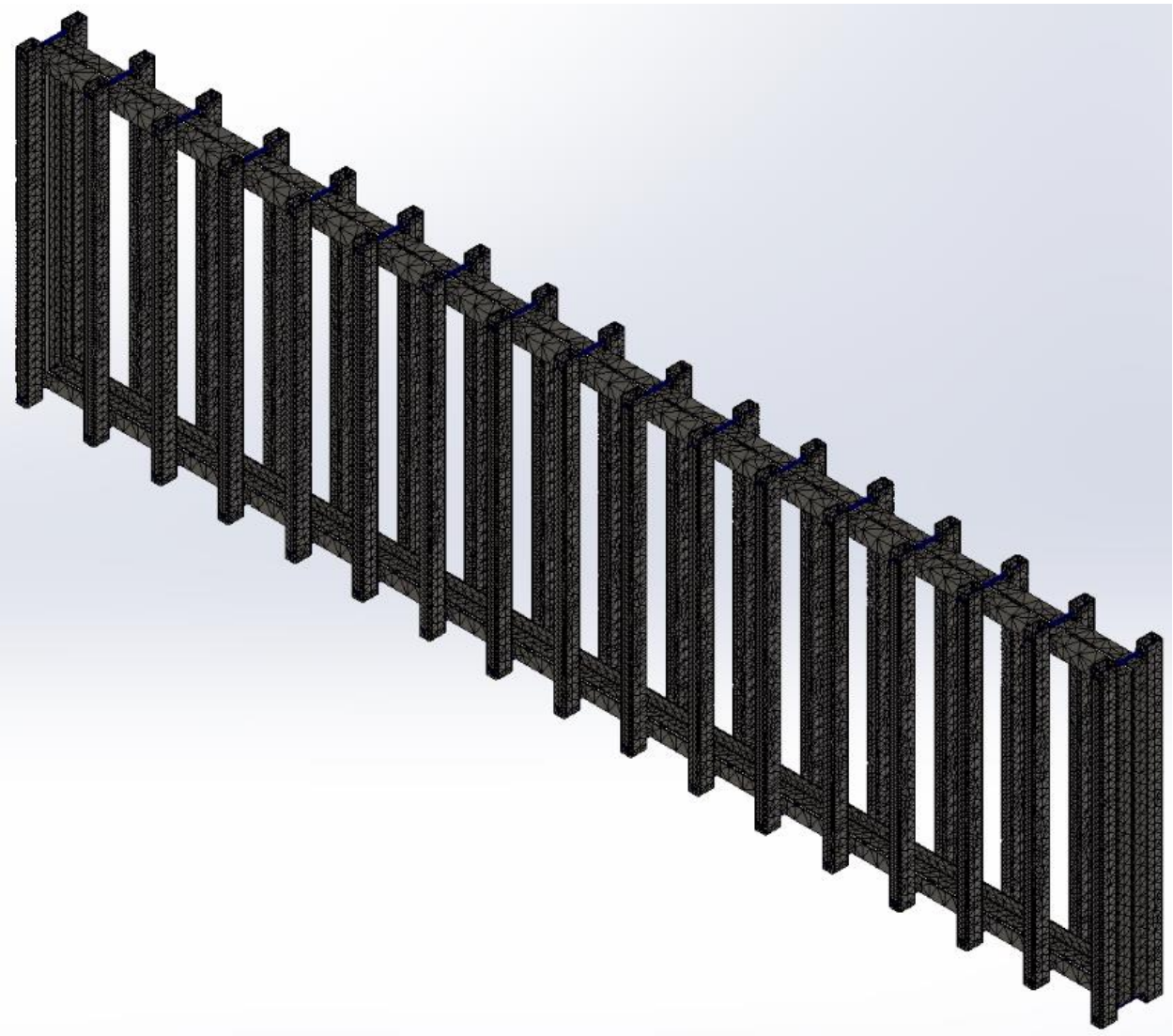

Figure 40. Mesh Generated by Solidworks

Next, we apply curvature-based mesh to the panels (Figure 40). Since our frame contacts forces at a 90^{o} angle, without accounting for curvature, the stress around a 90^{o} angle would be infinite. The analysis would then be incorrect. Curvature-based mesh is clearest in Figure 41.

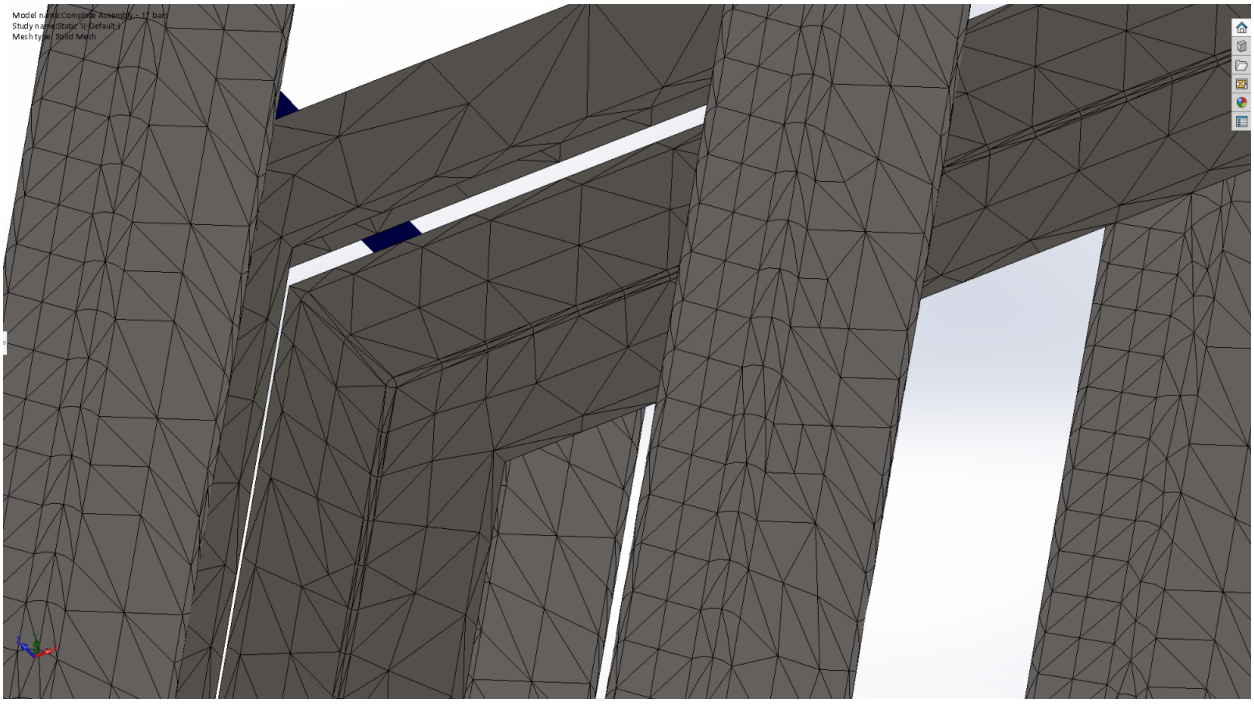

Figure 41. Effect of Curvature-Based Mesh

After running the simulation, we have the following results (Figure 42). Stresses are maximum where the steel spacer contacts of the bar, but only at the end.

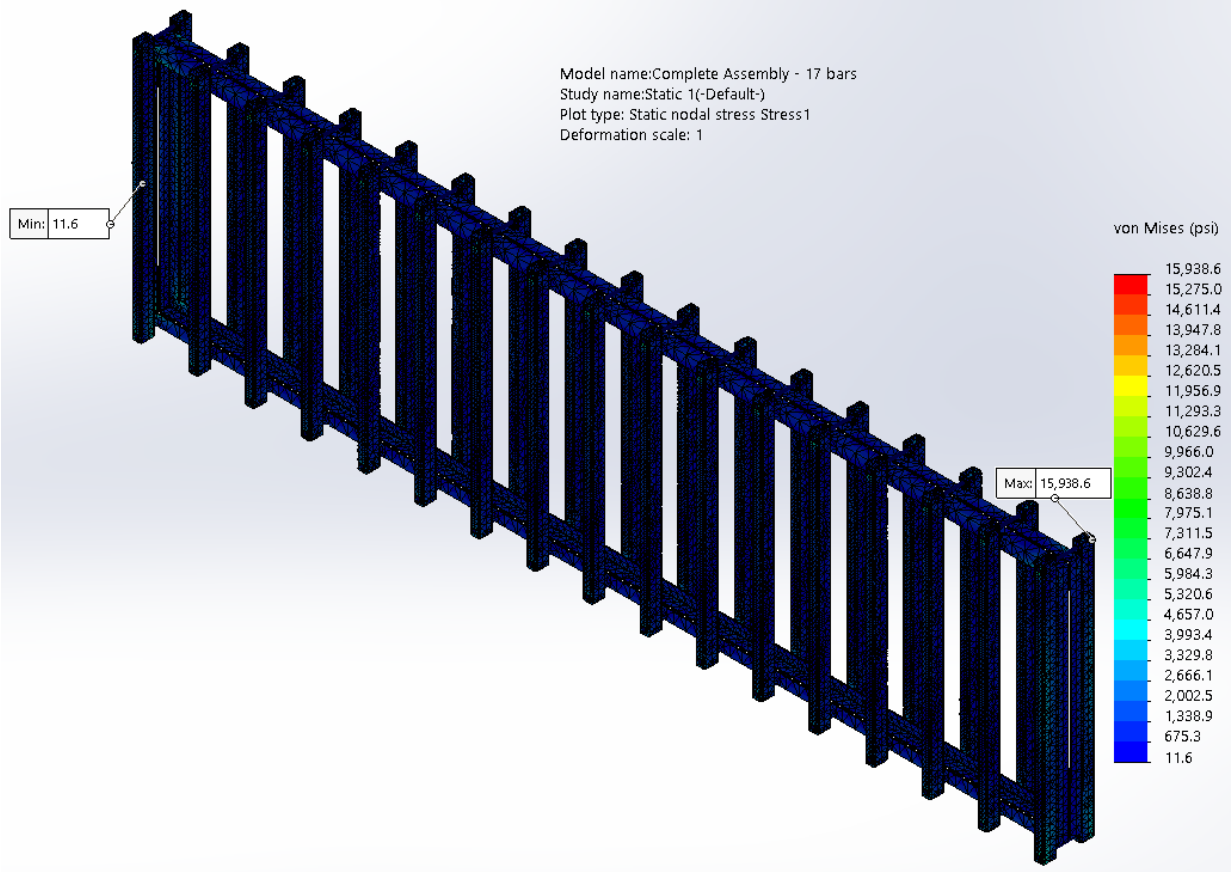

Figure 42. Estimated Stresses at Given Loads and Pressure

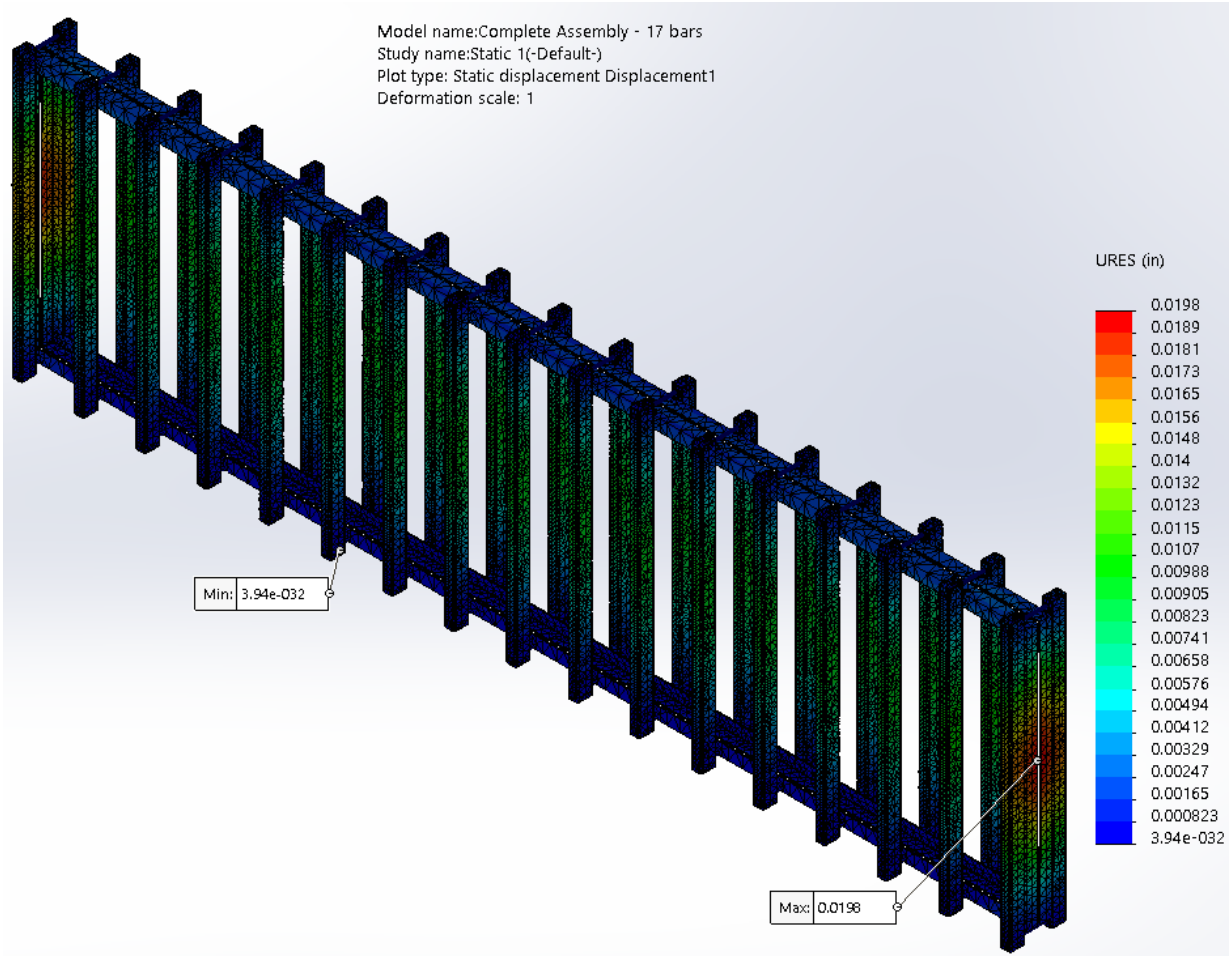

Figure 43. Displacements

Maximum displacement is 0.0198”, but it only occurs at the center of the end bar. Around other bars, the displacement is 0.01” maximum. Overall, displacements occur at the center of each steel bar, but they are at or less than 0.02”.

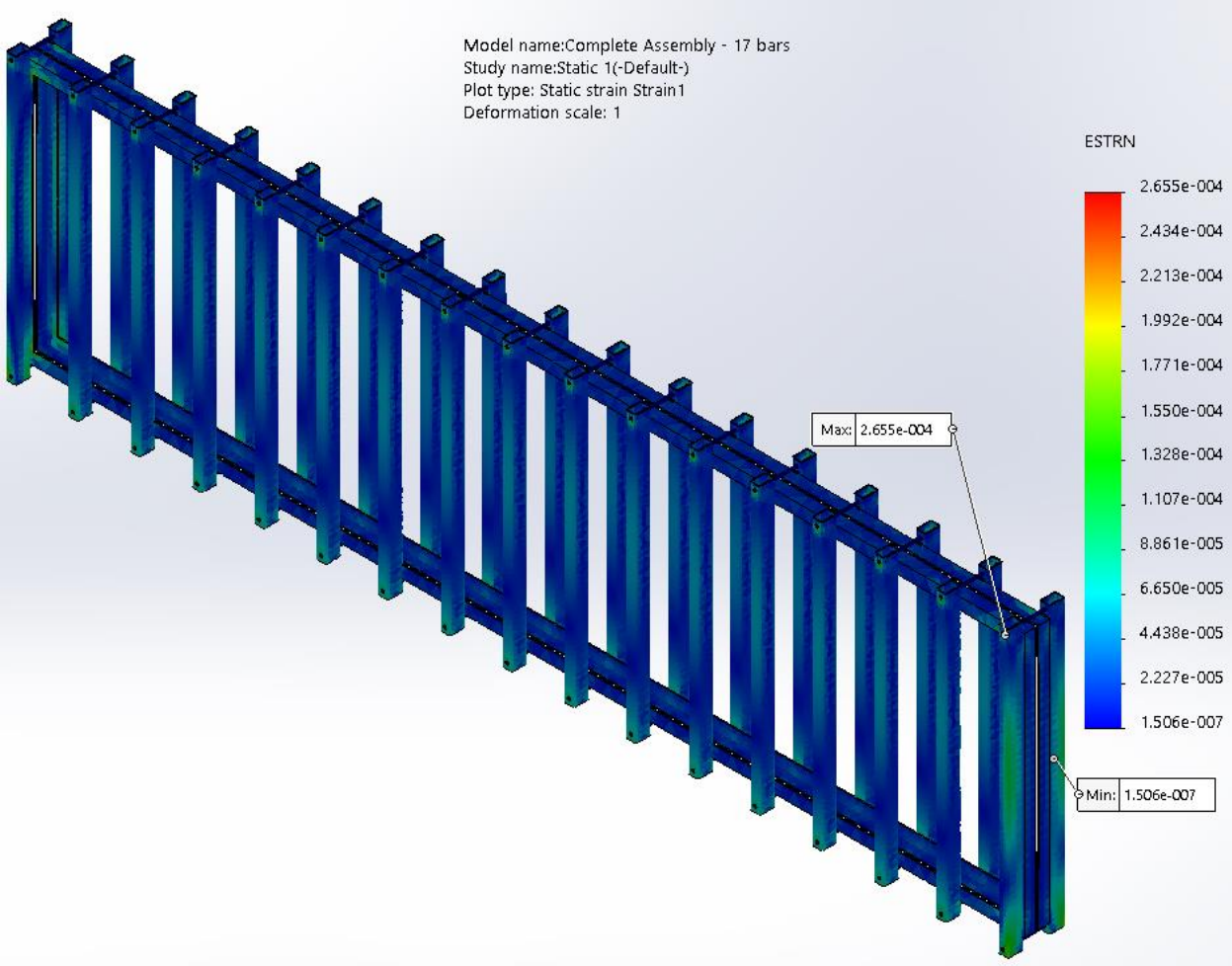

Figure 44. Strain

Figure 44 verifies stresses. The biggest value occurs where the spacer meets the steel bar, but only at the last bar. Maximum strain is 2.655×10^{-4}. Minimum strain is 1.506×10^{-7}. At other location, high strain was also observed around the contact point of bar and spacer as well.

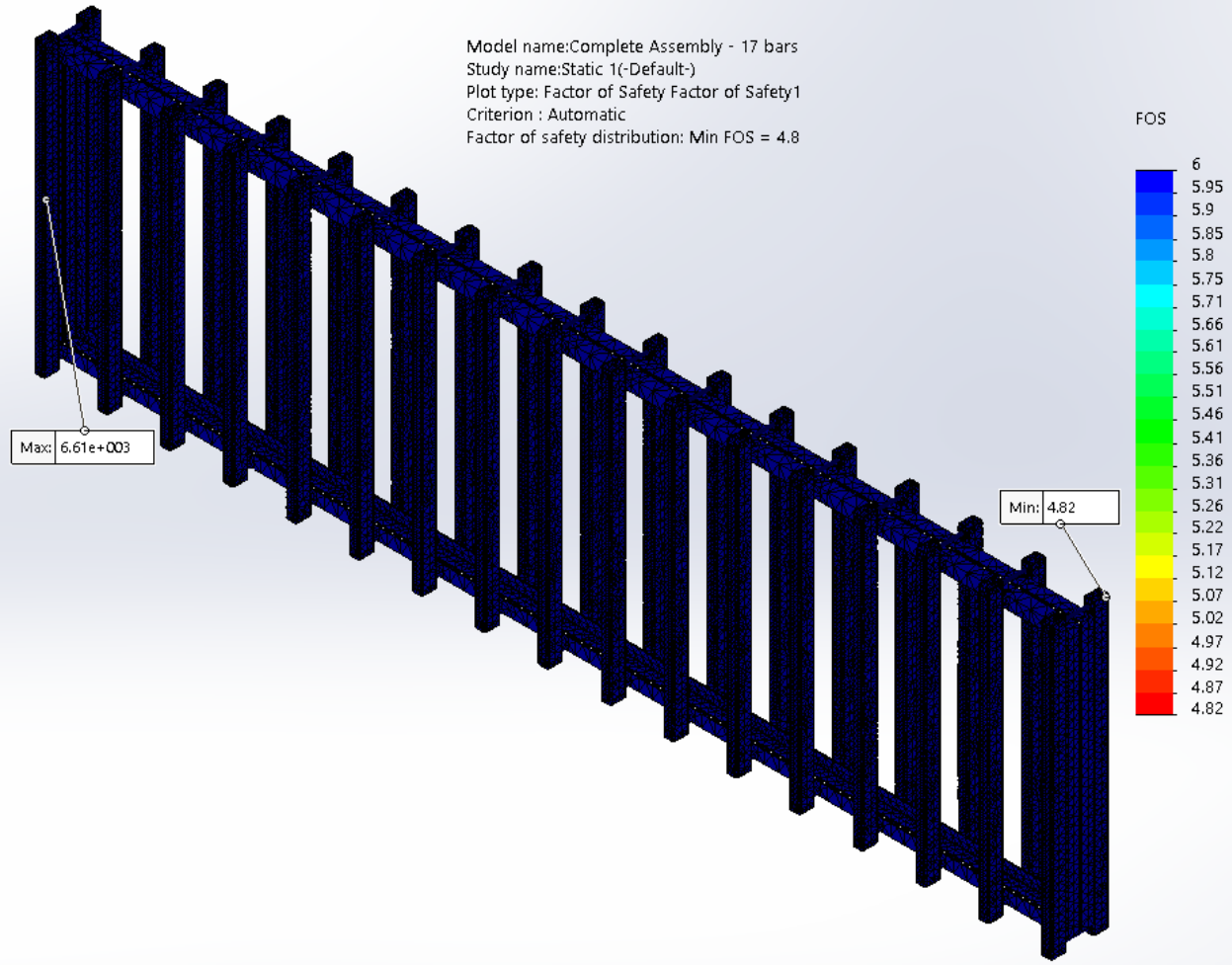

Figure 45. Factor of Safety

As shown in Figure 45, our design has a minimum factor of safety (FOS) of 4.82 around the spacer-steel bar contact (Figure 46). This means that, when we have 10 psig internal pressure, the steel frame can still perform within a safe margin. Thus, we concluded that our design was safe for the experiment.

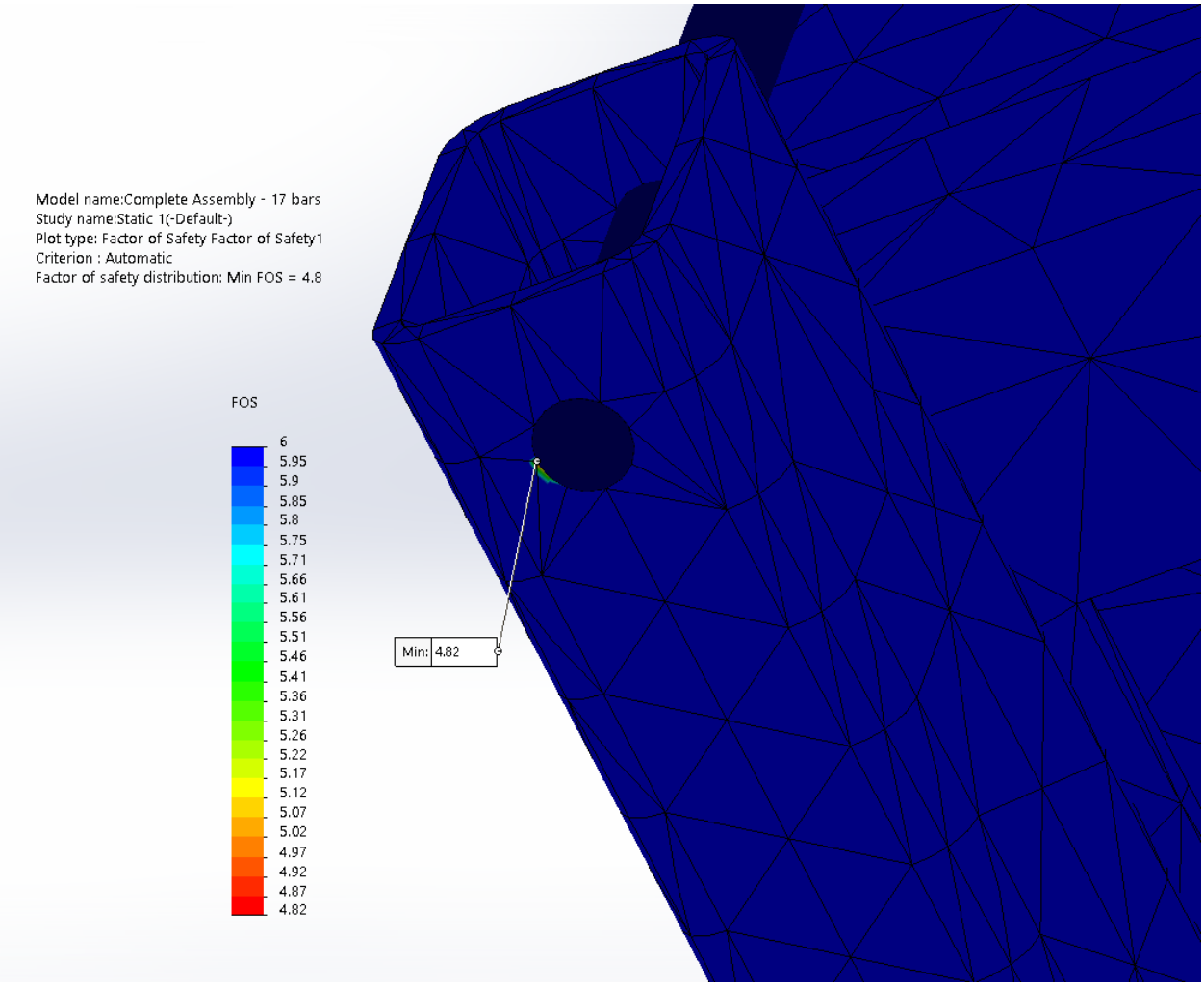

Figure 46. The Weakest Link in the Panel

With the completed panels, we ran the experiment three times. The first was with water and 20/40 proppant; the second with slickwater and 20/40 proppant; and the third with slickwater, PGA/PLA 50/50 and 20/40 proppant.

3.2 Experiment 1 – Control Study

Experiment 1 was conducted with water and 20/40 proppant at 75°F. The result is representative of a frac job that did not use a viscosifier. It is necessary to compare the result from this test with

the subsequent ones. The fluid composition and test details are shown in Table 5. Since the present study tried to replicate results in (Tran 2017) and compared the results, we would use the same proppant concentration that they used, which was 0.826 lbm/gal. We only had 50 lbm of proppant available, thus, we could only prepare 60 gal of fluid at said concentration. Flow rate was set to maximum for the best proppant transport capability. A snapshot of every 20 seconds is given from Figure 47- Figure 54.

Table 5. Fluid Composition and Pumping Scheme in Experiment 1

PGA fiber concentration	0 lbm / 1000 gal
Flow rate	24 gpm
Volume of fluid pumped	60 gal
Guar concentration	0.0 oz
Mesh size	20/40
Proppant amount	50 lbm
Proppant concentration	0.826 lbm/gal
Outlet	1, 2, 3, 4, 5
Apparent viscosity	1 cp

Figure 47. Experiment 1 - At 0 Second

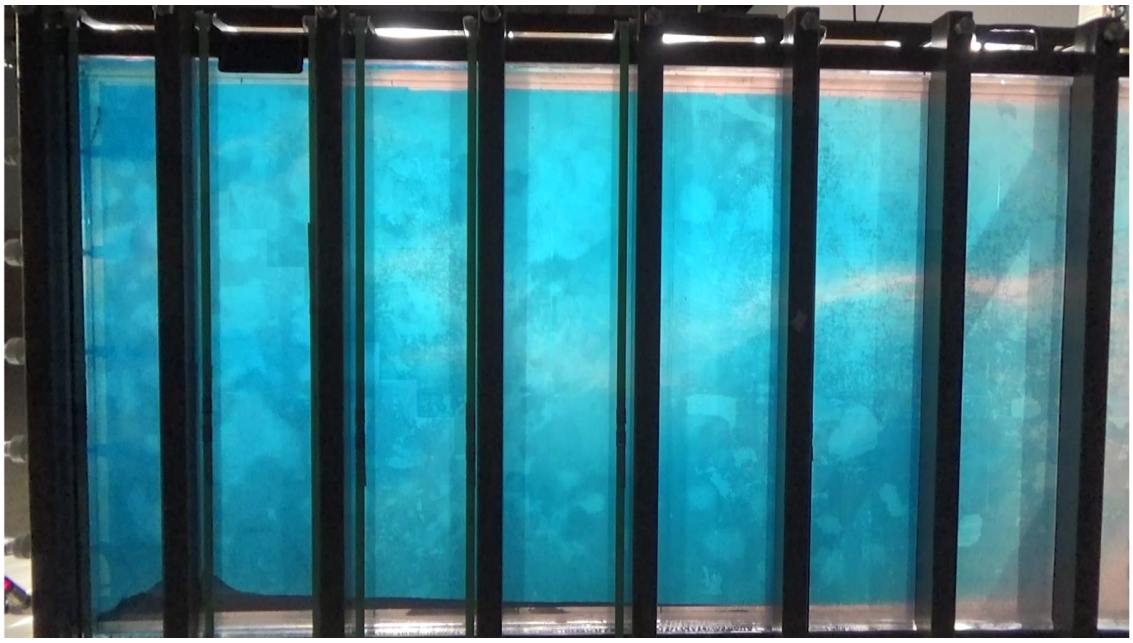

Figure 48. Experiment 1 at 20 Seconds

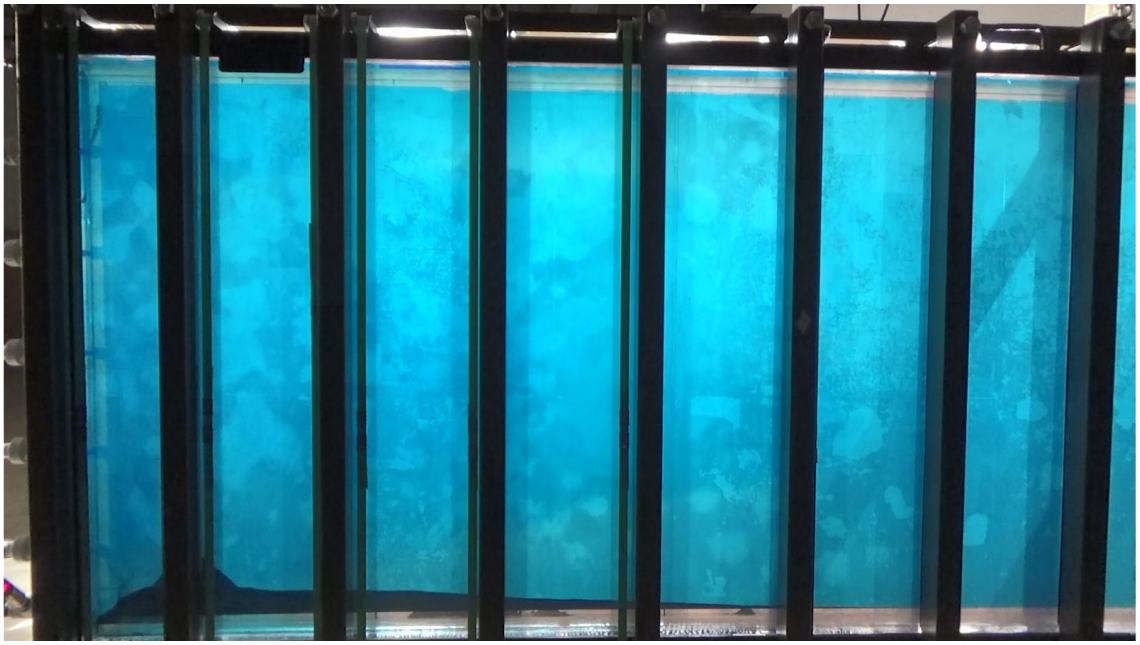

Figure 49. Experiment 1 at 40 Seconds

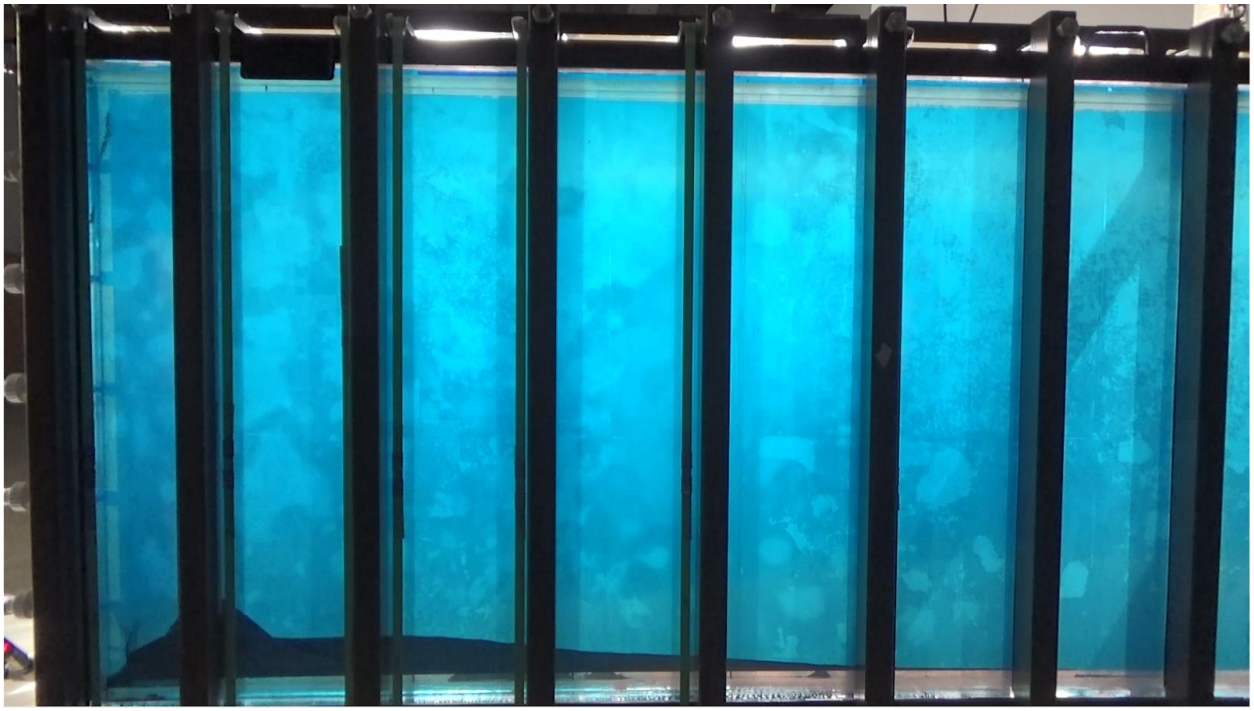

Figure 50. Experiment 1 at 1 Minute

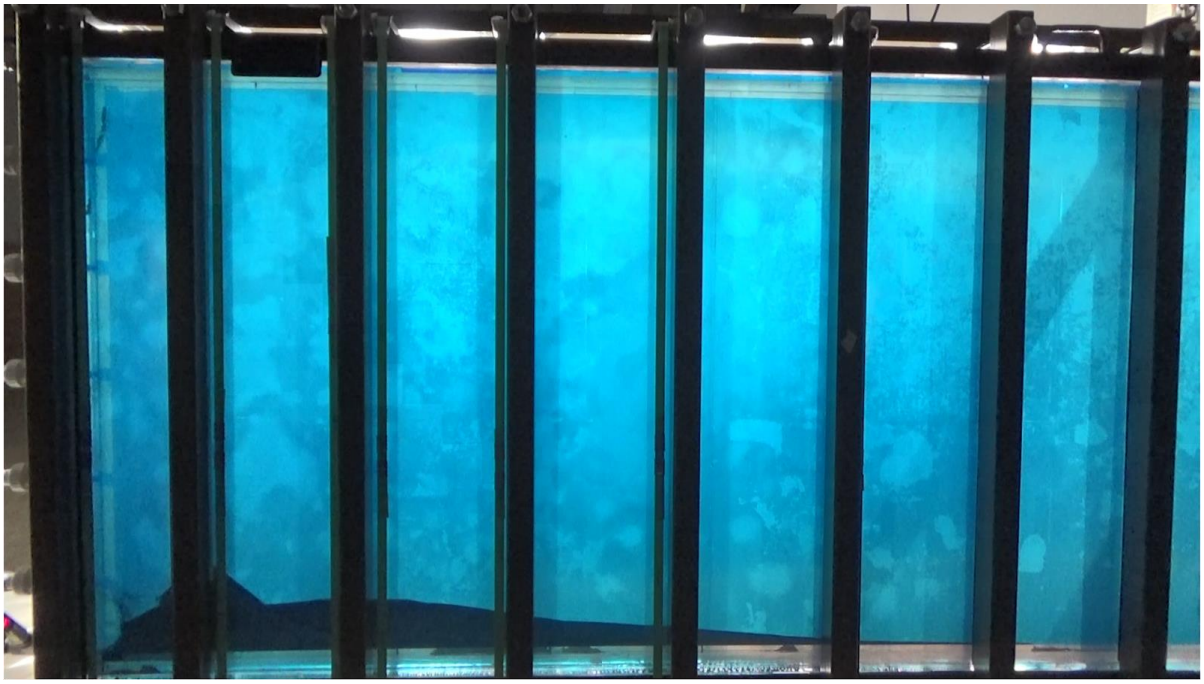

Figure 51. Experiment 1 at 1 Minute and 20 Seconds

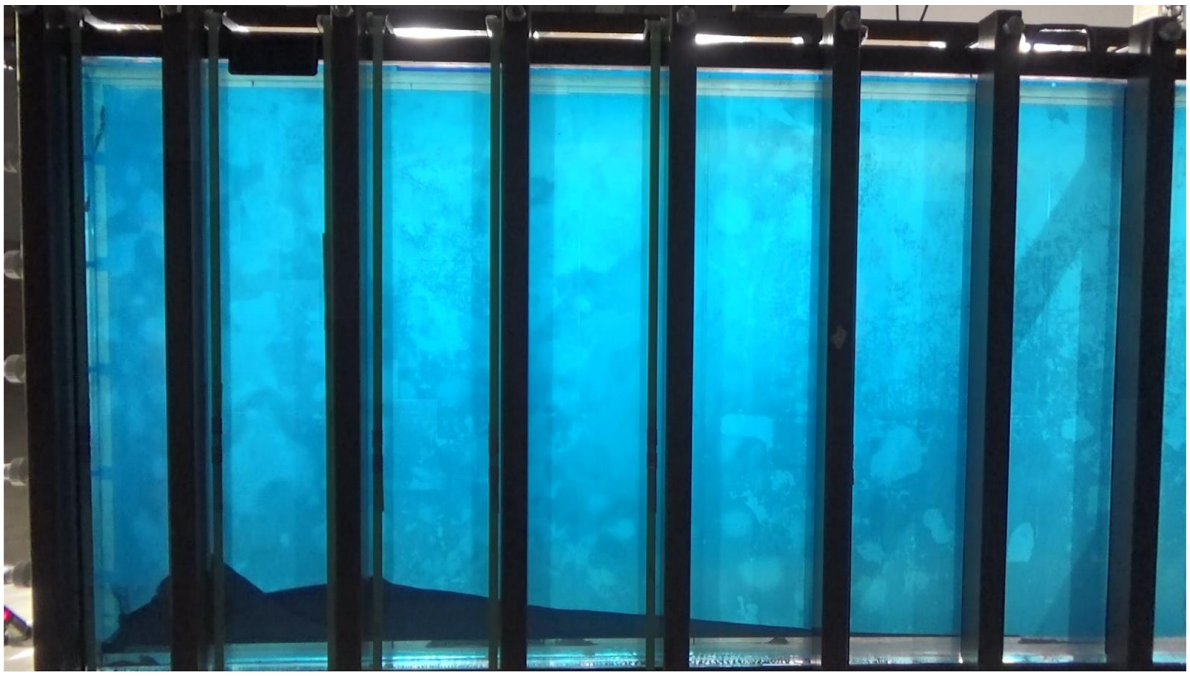

Figure 52. Experiment 1 at 1 Minute and 40 Seconds

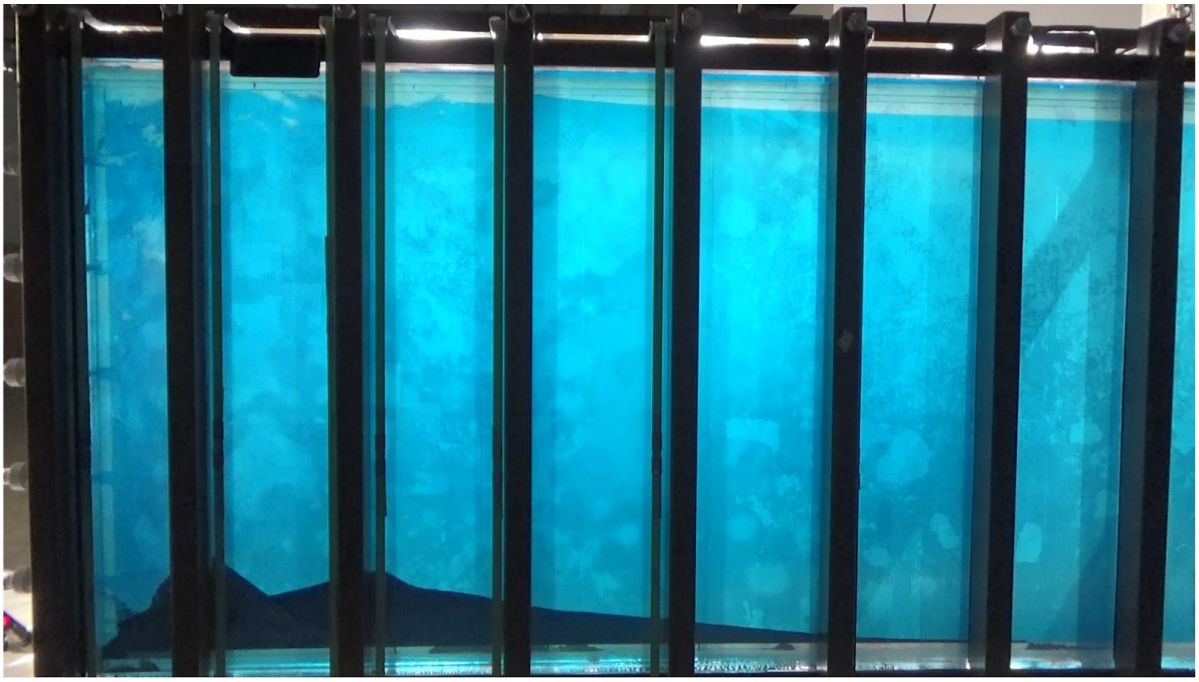

Figure 53. Experiment 1 at 2 Minutes

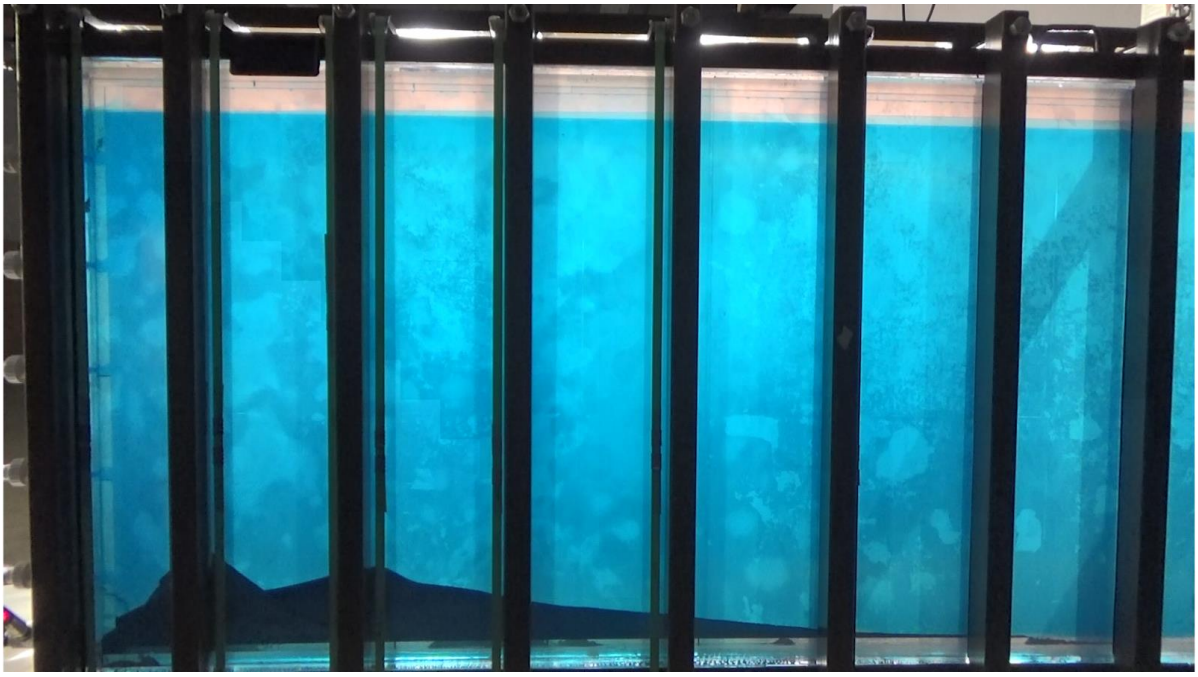

Figure 54. Experiment 1 at 2:10

Experiment 1 suggested that, without viscosity modifier and fibers, proppant will quickly accumulate on the bottom. The same results also occurred on our small-scale test (Figure 55). However, Figure 54 reveals an abnormality in experiment 1. There were 3 dunes of proppant in the assembly (Figure 56). The spacer in Figure 2 was meant to push layers on both of its sides toward the outer shell, maintaining a constant-width channel, this result showed that such spacer was not wide enough to push. We widened the acrylic spacer by adding thin rubber strips. As a result, the fracture width was 0.438" instead of 0.2" (Figure 57).

Experiment 1 showed us that, without viscosifier, there is little suspension mechanism for proppant. Once entering the fracture, proppant will settle near the wellbore, creating a proppant bank. The transport mechanism is governed by movement of the proppant bank itself (Liang 2015).

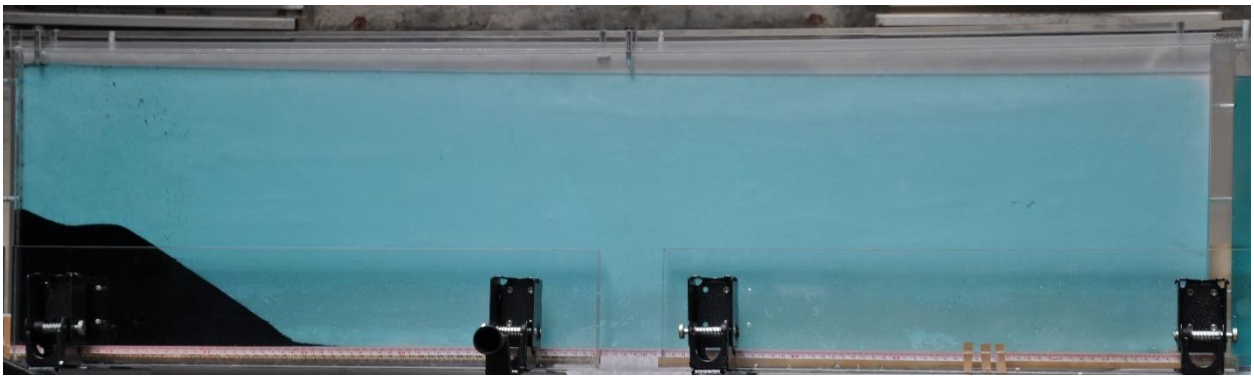

Figure 55. Water + Proppant in Small Scale Test, Reprinted From Tran (2017)

Figure 56. Dunes Between Panels

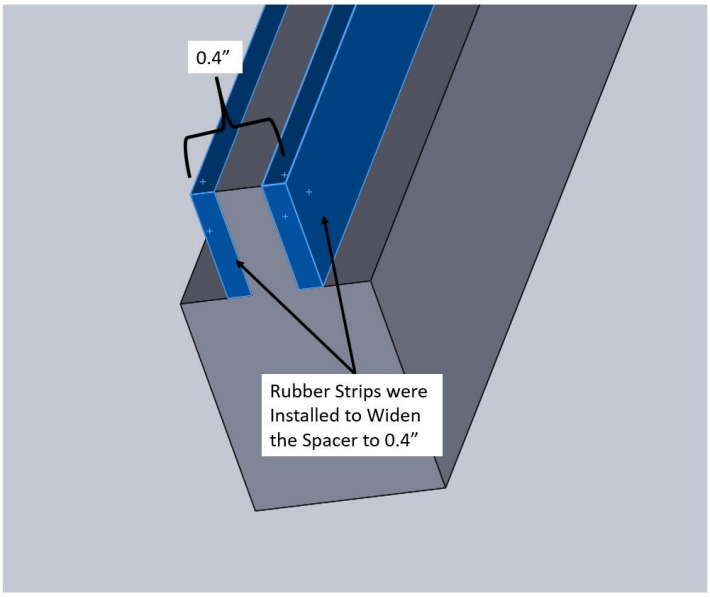

Figure 57. Width of the Spacer After Adding Rubber Strips

3.3 Experiment 2 – Control Study with Slickwater

To show the significance of slickwater fracturing without fibers, we added a small amount of guar into water at a concentration of 5 lbm / 1000 gal. The experiment was run with a fracture

width of 0.438”. Below, a snapshot of every twenty seconds is presented from Figure 58 to Figure 82. Fluid composition is shown in Table 6.

Table 6. Fluid Composition and Pumping Scheme in Experiment 2

Fiber concentration	0 lbm / 1000 gal
Flow rate	9 gpm
Volume of fluid pumped	65 gal
Guar amount	8.0 oz
Mesh size	20/40
Proppant amount	49.3 lbm
Proppant concentration	826 lbm / 1000 gal
Outlet	1, 2, 3, 4, 5
Apparent viscosity	3 cP

Figure 58. Experiment 2 at 00 Seconds

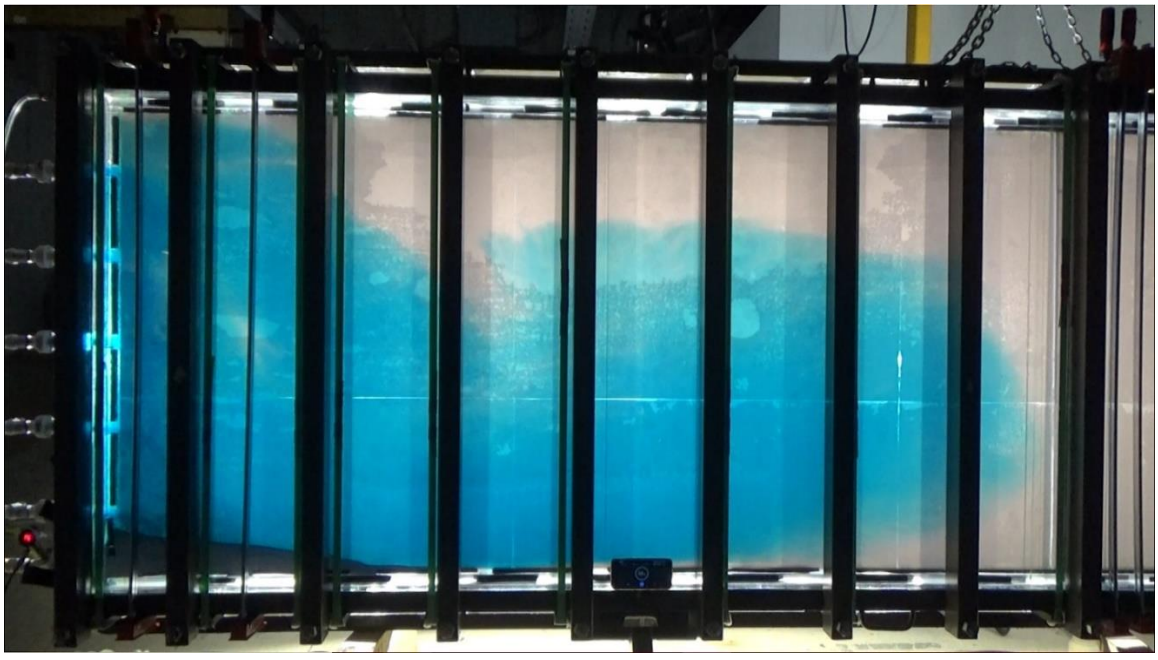

Figure 59. Experiment 2 at 20 Seconds

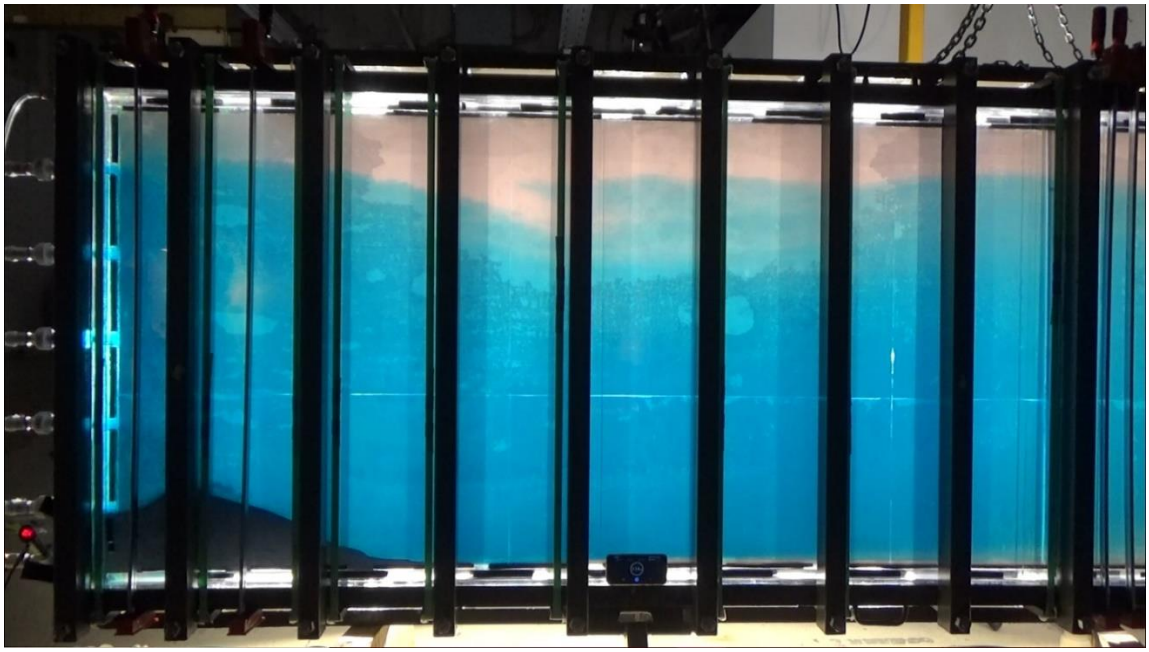

Figure 60. Experiment 2 at 40 Seconds

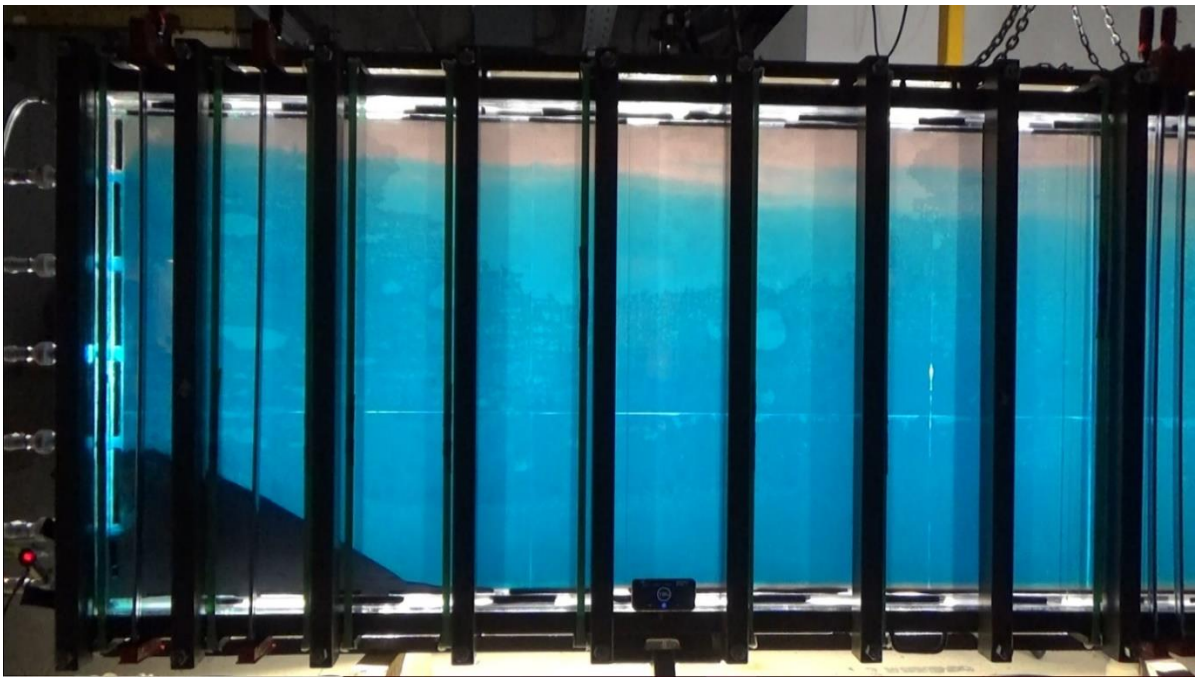

Figure 61. Experiment 2 at 1 Minute

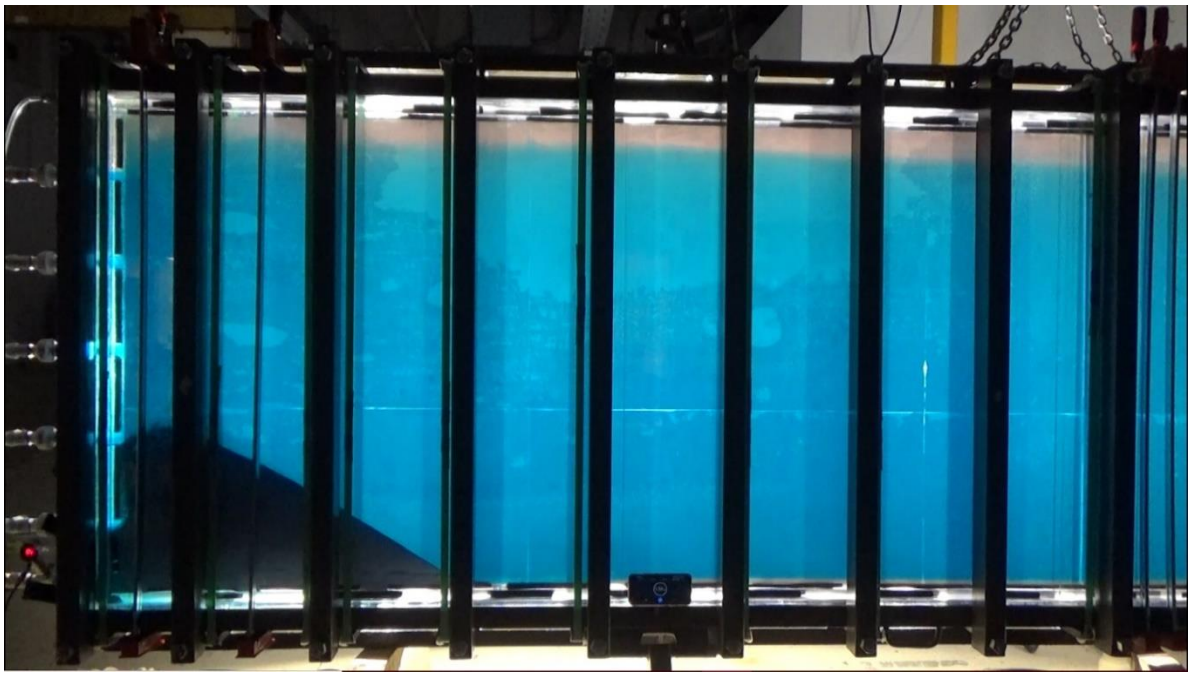

Figure 62. Experiment 2 at 1 Minute and 20 Seconds

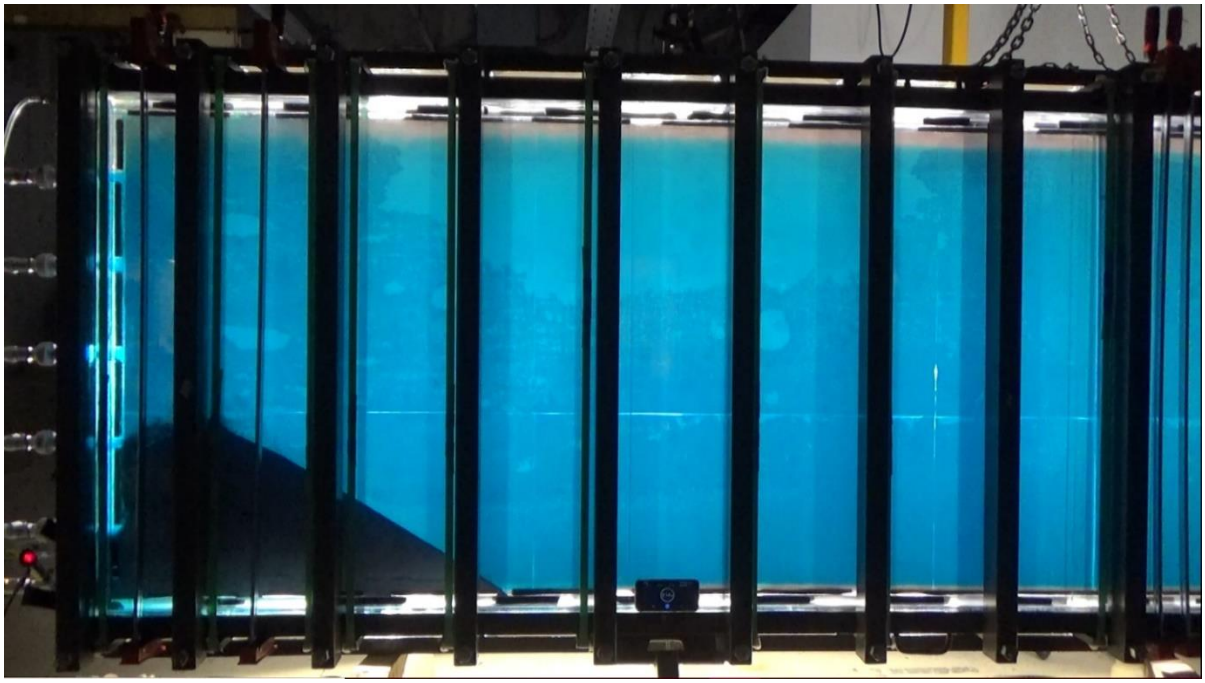

Figure 63. Experiment 2 at 1 Minute and 40 Seconds

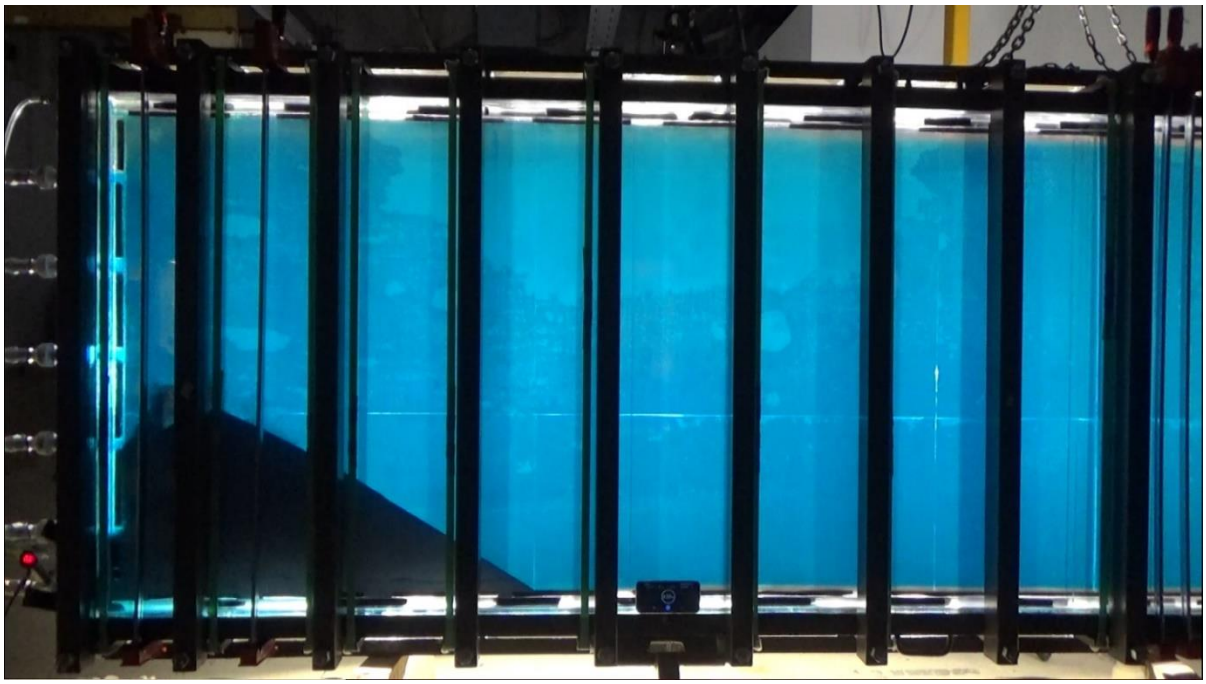

Figure 64. Experiment 2 at 2 Minutes

Figure 65. Experiment 2 at 2 Minutes and 20 Seconds

Figure 66. Experiment 2 at 2 Minutes and 40 Seconds

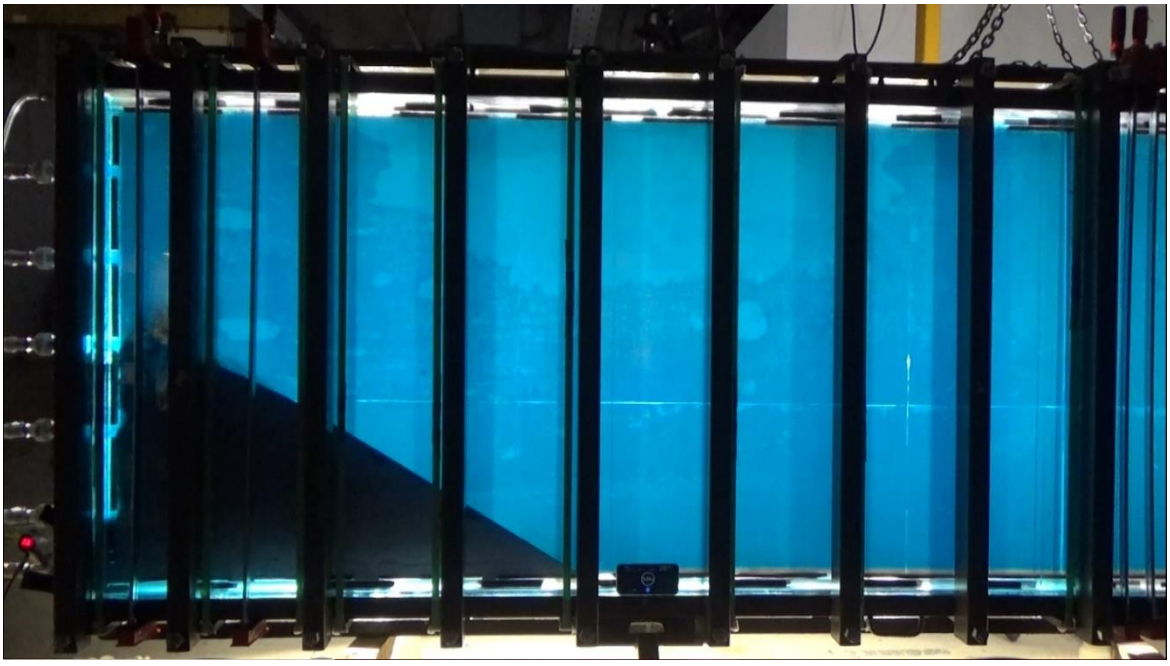

Figure 67. Experiment 2 at 3 Minutes

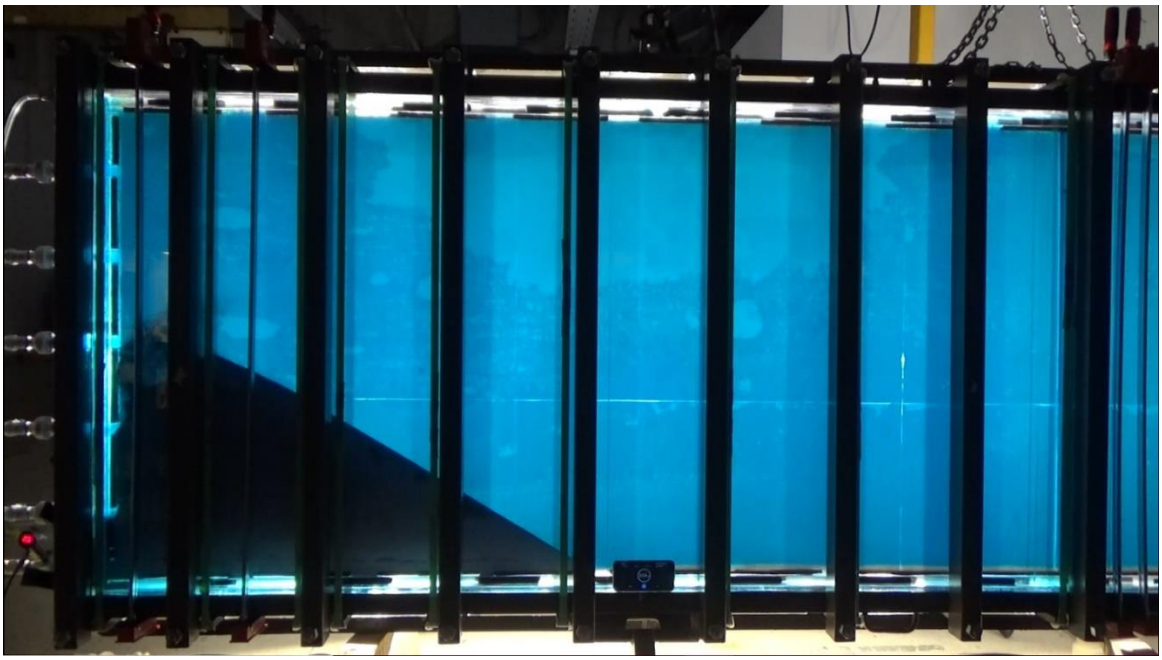

Figure 68. Experiment 2 at 3 Minutes and 20 Seconds

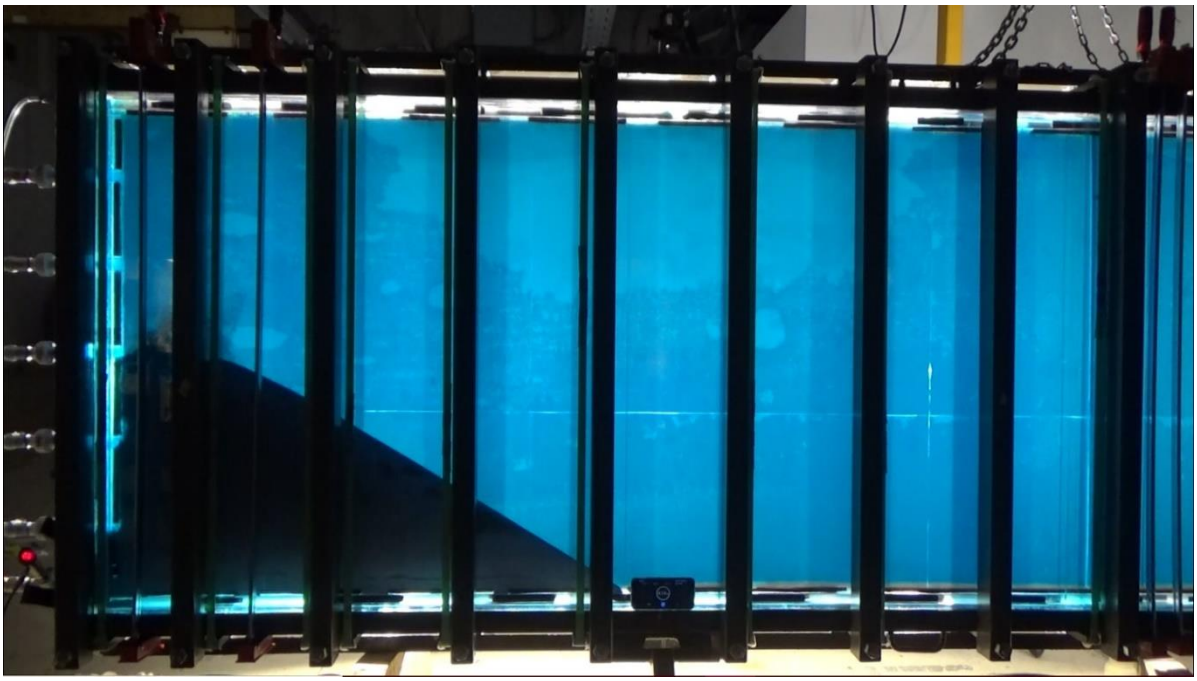

Figure 69. Experiment 2 at 3 Minutes and 40 Seconds

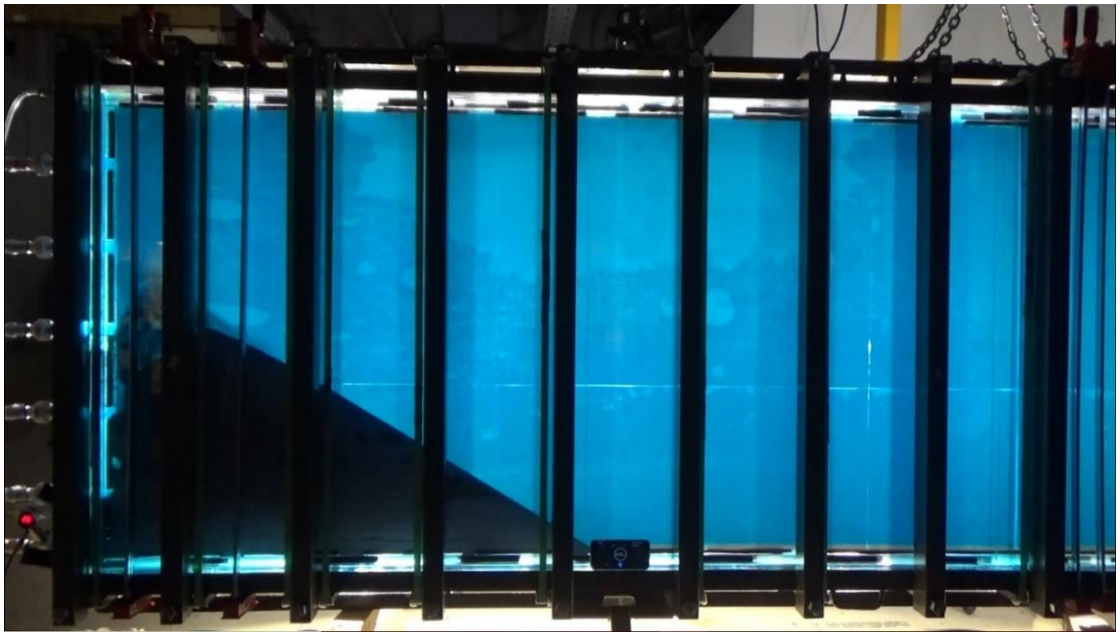

Figure 70. Experiment 2 at 4 Minutes

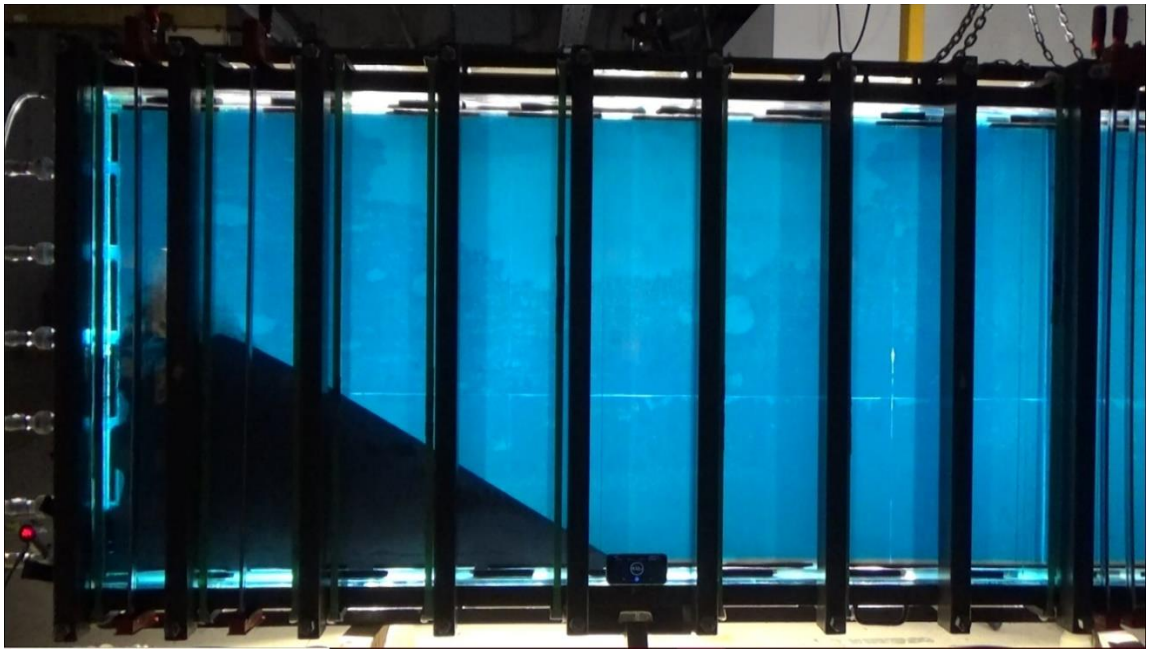

Figure 71. Experiment 2 at 4 Minutes and 20 Seconds

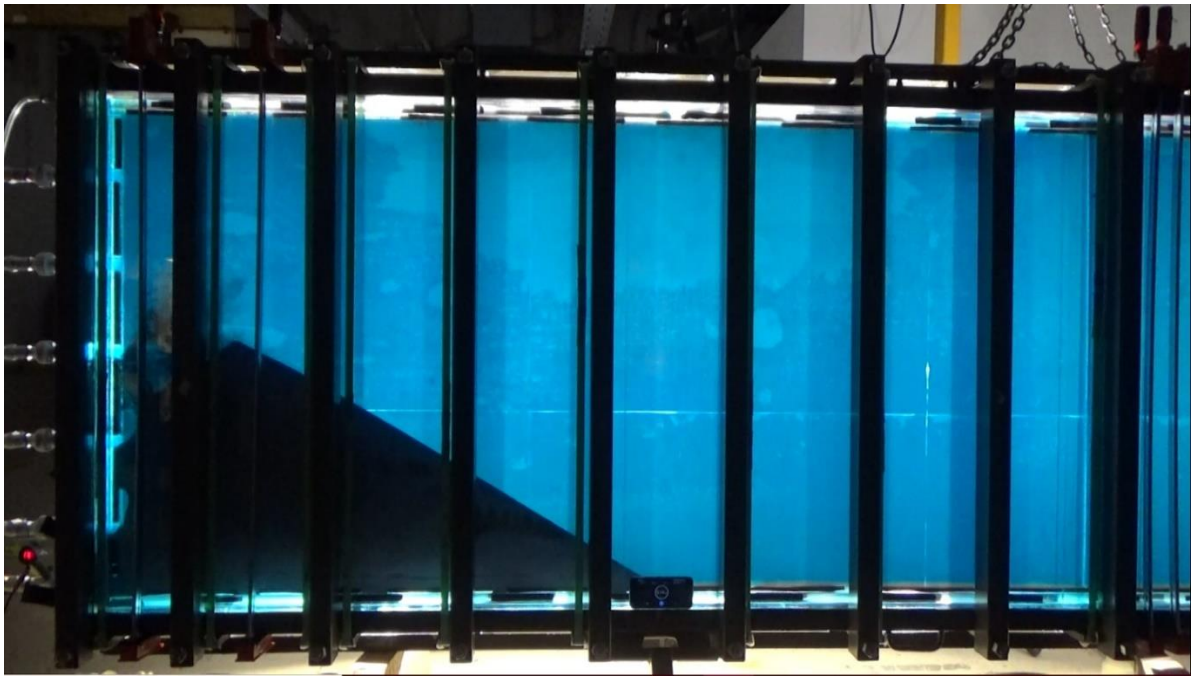

Figure 72. Experiment 2 at 4 Minutes and 40 Seconds

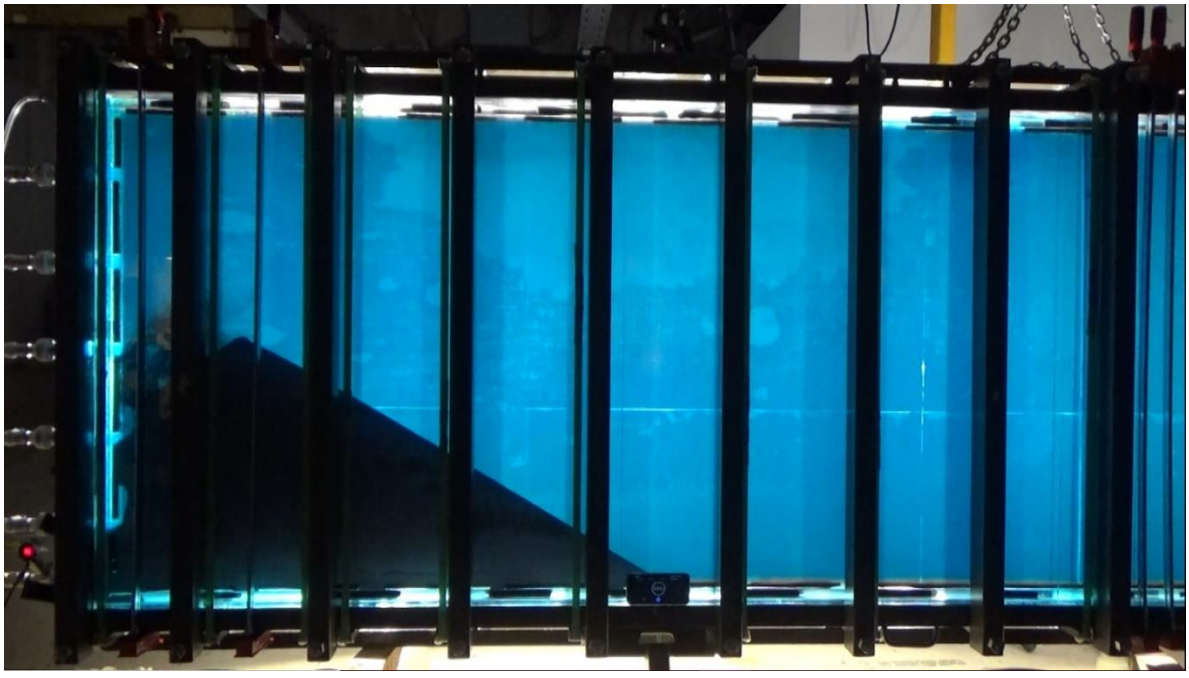

Figure 73. Experiment 2 at 5 Minutes

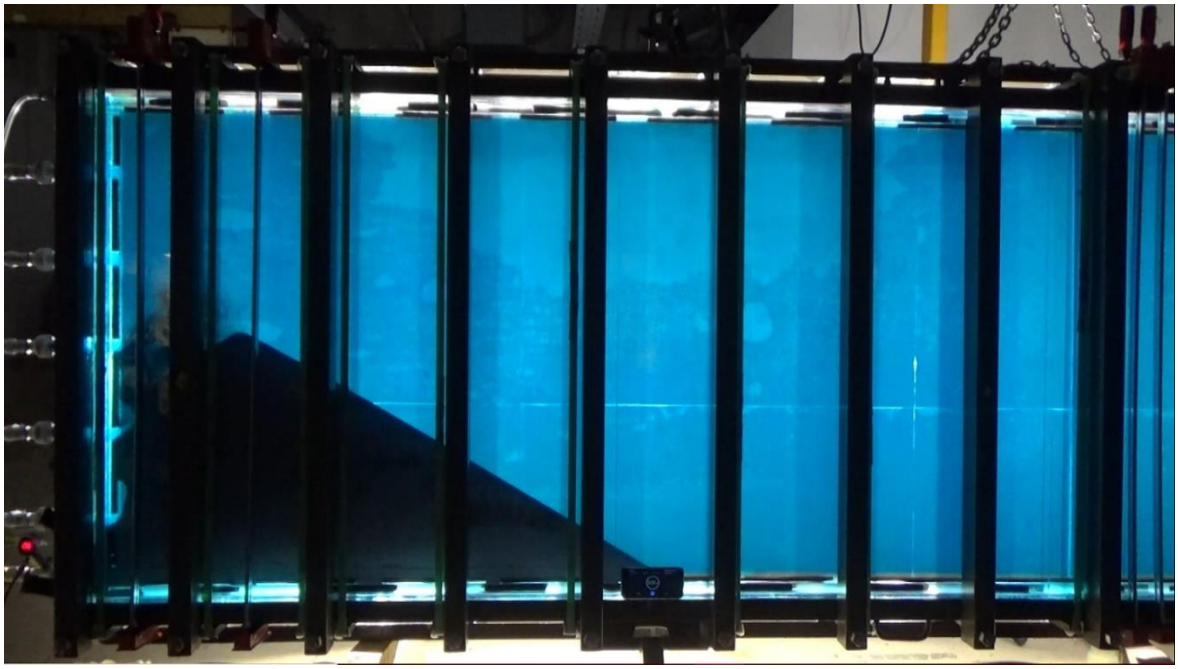

Figure 74. Experiment 2 at 5 Minutes and 20 Seconds

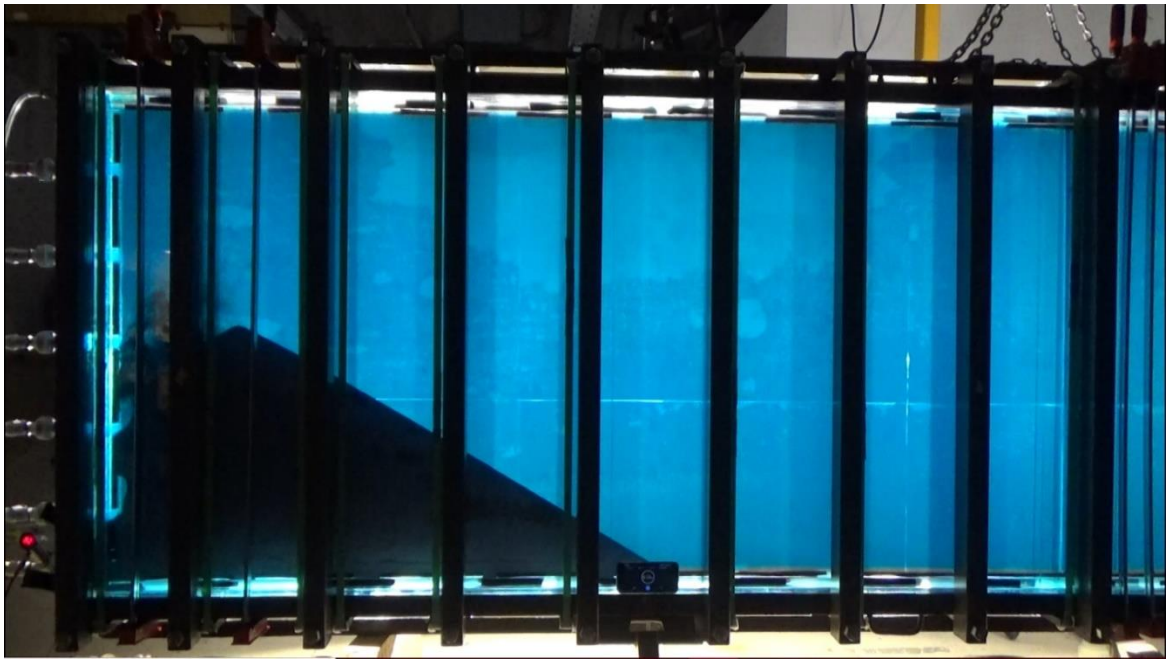

Figure 75. Experiment 2 at 5 Minutes and 40 Seconds

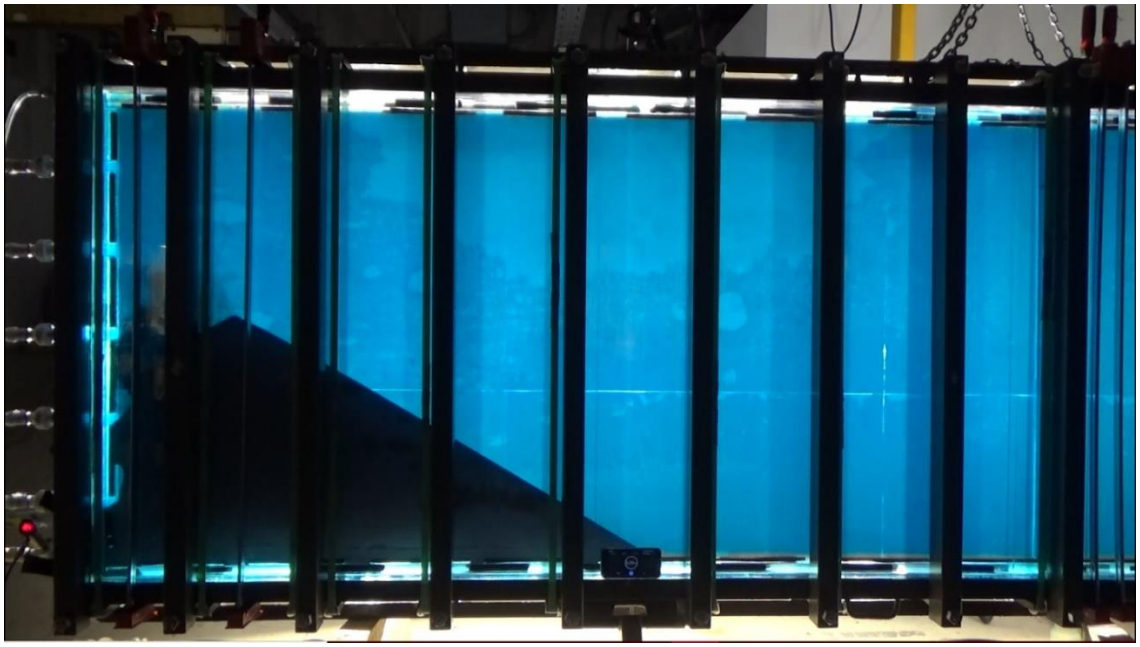

Figure 76. Experiment 2 at 6 Minutes

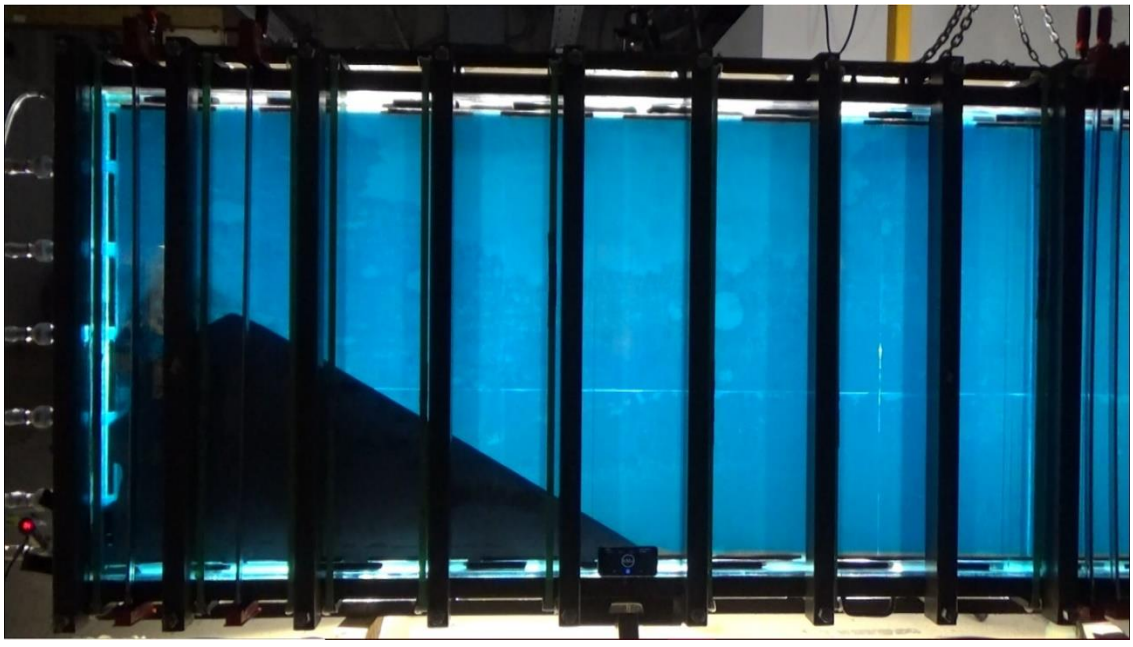

Figure 77. Experiment 2 at 6 Minutes and 20 Seconds

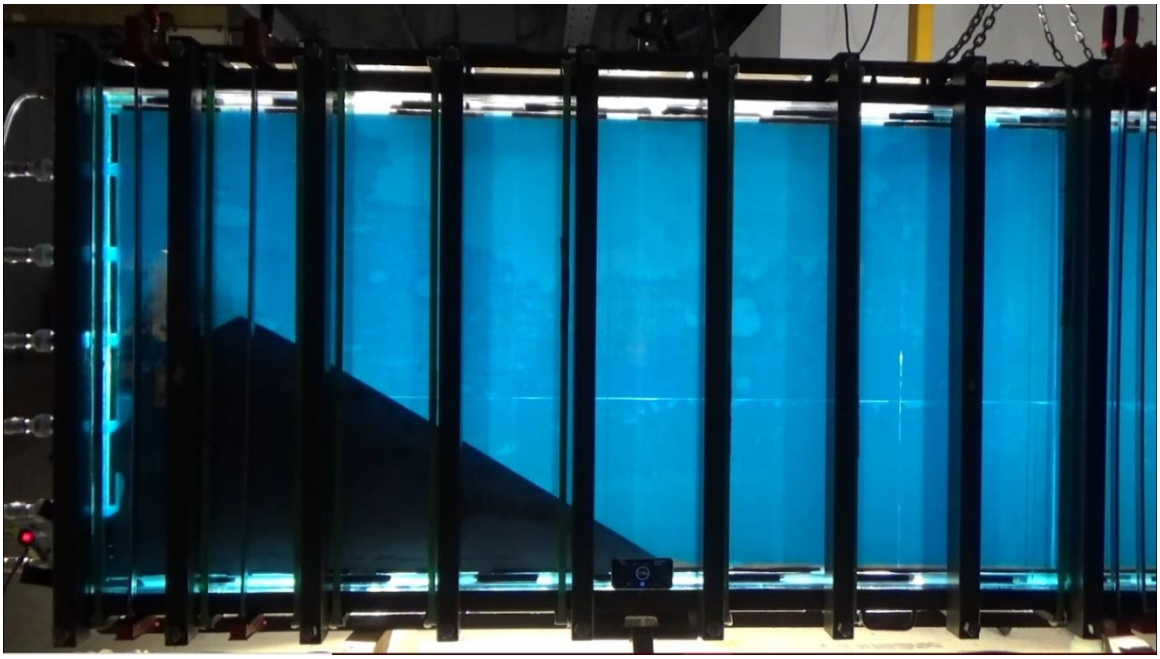

Figure 78. Experiment 2 at 6 Minutes and 40 Seconds

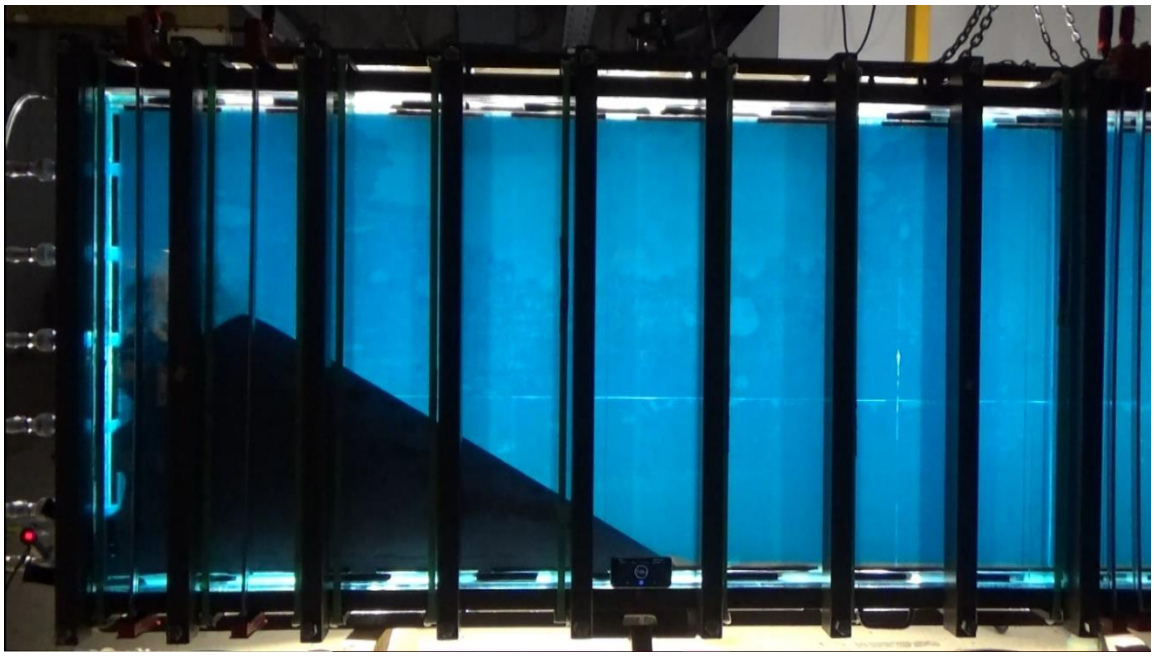

Figure 79. Experiment 2 at 7 Minutes

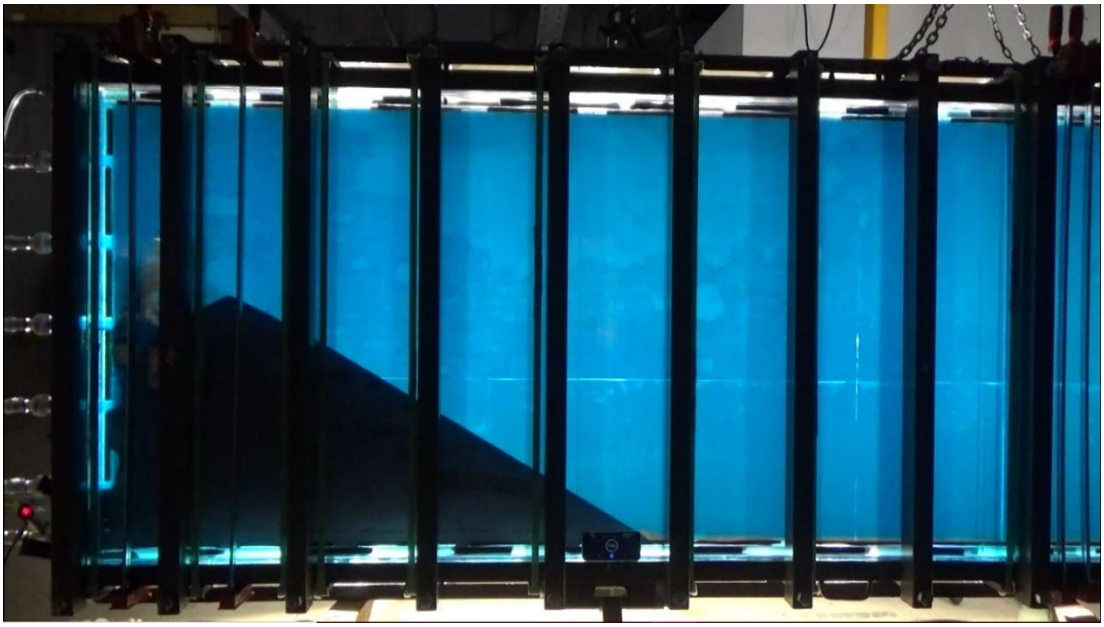

Figure 80. Experiment 2 at 7 Minutes and 20 Seconds

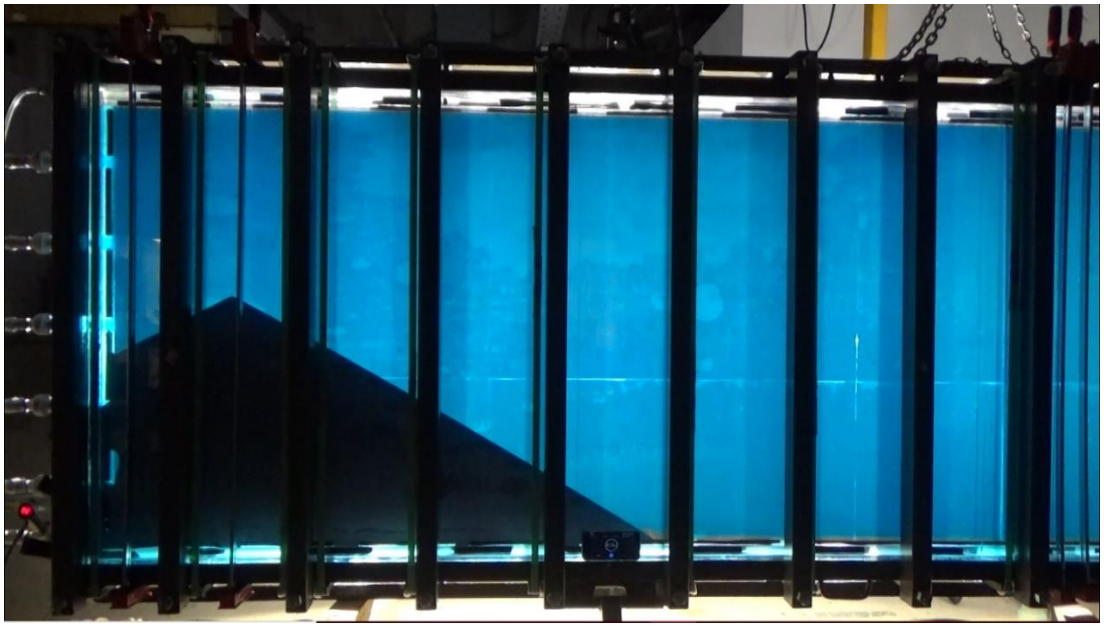

Figure 81. Experiment 2 at 7 Minutes and 40 Seconds

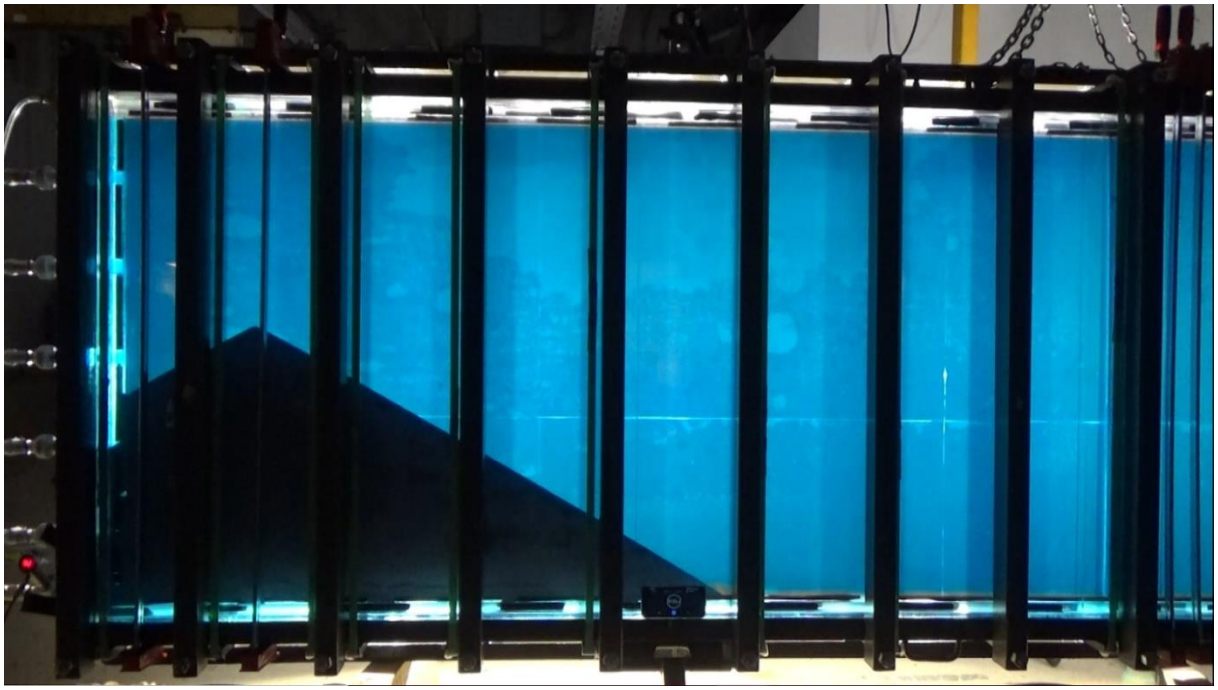

Figure 82. Experiment 2 at 8 Minutes

The shape of the proppant dune in experiment 2 properly portrays the proppant bank described in (Change 2018). Due to having low viscosity (3.0 cp), slickwater cannot suspend proppant well. As a result, the same phenomenon that occurred in experiment 1 still applies here.

After back calculating, we found that the proppant concentration we pumped into the panel was too low. Only 0.375 lbm/gal of slurry was pumped for an intended 0.826 lbm/gal. This low value suggests the proppant was not evenly distributed in the fluid as we pumped. One explanation was that our mixing scheme was insufficient. The sump pump we placed at the bottom was probably not as effective a mixing tool as a propeller-type mixer. The cone shape of the tank largely played a role since it trapped a large amount of proppant there.

Experiment 2 showed us that without fibers slickwater was not good at transporting proppant. Movement of the proppant bank is still the main driver behind proppant transport.

3.4 Experiment 3 – Study with Slickwater and Fibers

Experiment 1 and 2 showed that, on their own, both water and slickwater were not good fracturing fluid. Both could not extend fracture length due to having poor proppant suspension. To improve suspension, viscosity is viewed as the most important parameter (Liang 2015). Increasing viscosity by increasing guar concentration cannot be applied in slickwater fracturing, where guar concentration is low. However, Yoshimura (2014) proved that proppant suspension can be improved by using fibers, and Tran (2017) showed that slickwater mixed with PGA fibers were a good proppant transport material. Experiment 3 tried to replicate the results in Tran (2017).

Since PGA was not available, we used a sample containing both PGA and PLA with a ratio of 50/50 instead. In experiment 2, because of its cone-shaped geometry, the mixing tank trapped a large amount of proppant there. In experiment 3, we modified the bottom by adding a foam piece to the mixing tank (Figure 83). We believed that, as the foam piece would prevent proppant from settling to the tip of the bottom, more proppant would be pumped into the panel.

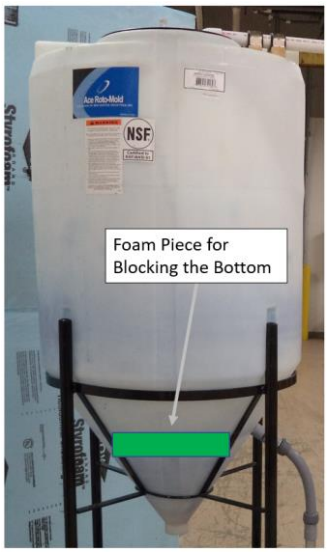

Figure 83. Location of the Foam Piece in the Mixing Tank

The fluid composition is given in Table 7. Again, a snapshot of every twenty second is presented from Figure 84 to Figure 101.

Table 7. Fluid Composition and Pumping Scheme in Experiment 3

Fiber concentration	5 lbm / 1000 gal
Fiber amount	0.325 lbm
Flow rate	12.3 gpm
Volume of fluid pumped	59.2 gal
Guar amount	8.0 oz
Mesh size	20/40

Table 7. Continue

Proppant Amount	48.3 lbm
Proppant Concentration	826 lbm/1000 gal
Inlet	1, 3, 5
Apparent Viscosity	3 cP

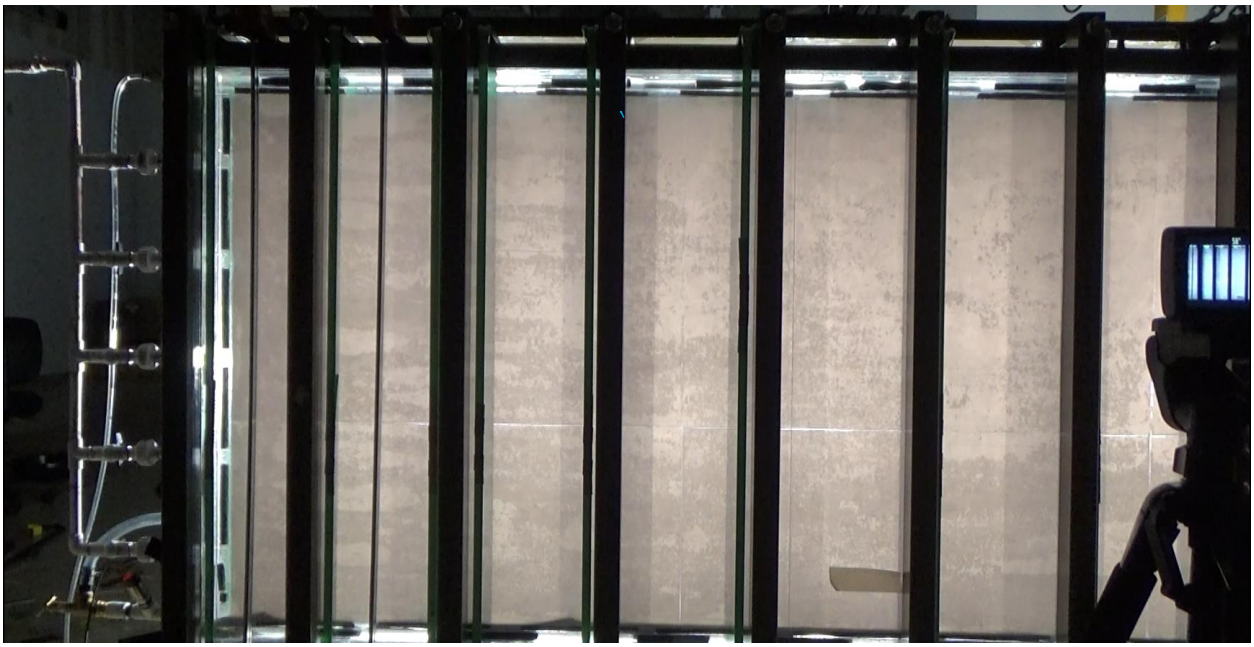

Figure 84. Experiment 3 at 0 Second

Figure 85. Experiment 3 at 20 Seconds

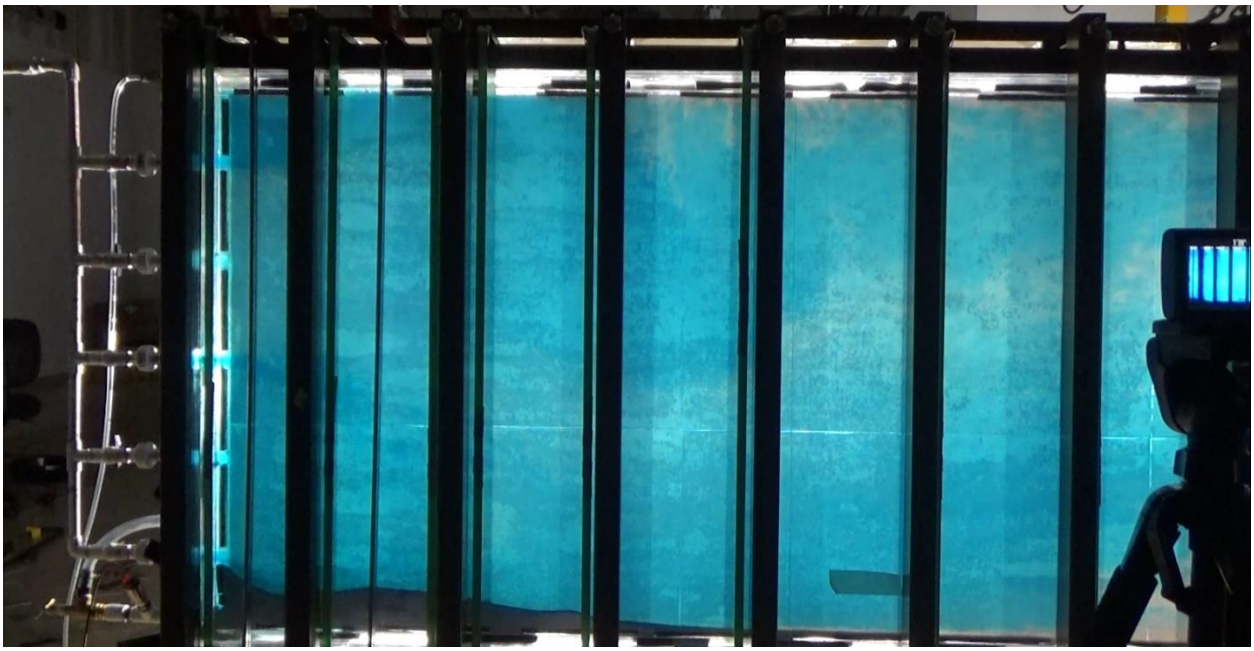

Figure 86. Experiment 3 at 40 Seconds

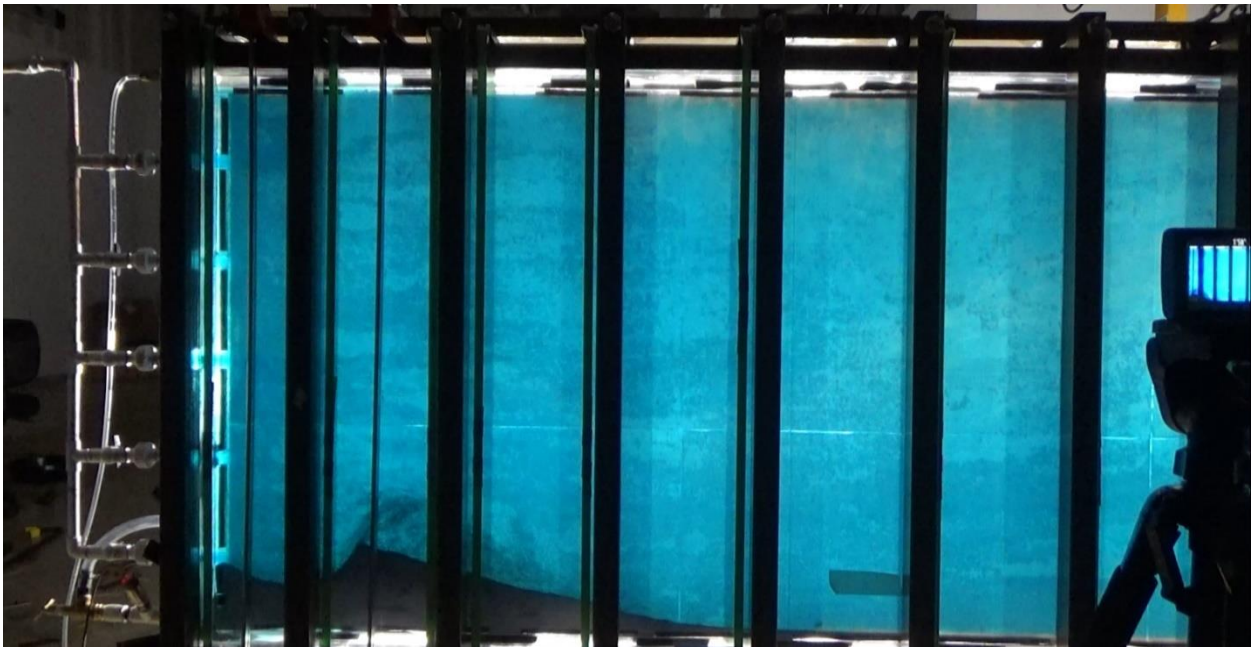

Figure 87. Experiment 3 at 1 Minute

Figure 88. Experiment 3 at 1 Minute and 20 Seconds

Figure 89. Experiment 3 at 1 Minute and 40 Seconds

Figure 90. Experiment 3 at 2 Minutes

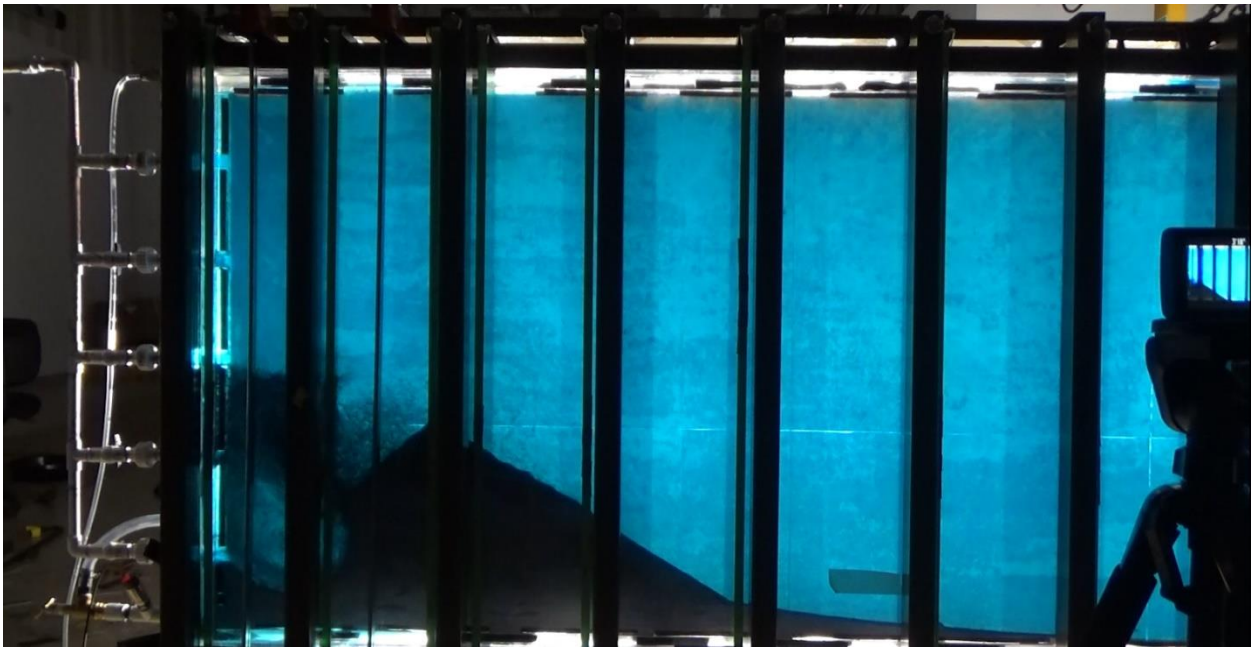

Figure 91. Experiment 3 at 2 Minutes and 20 Seconds

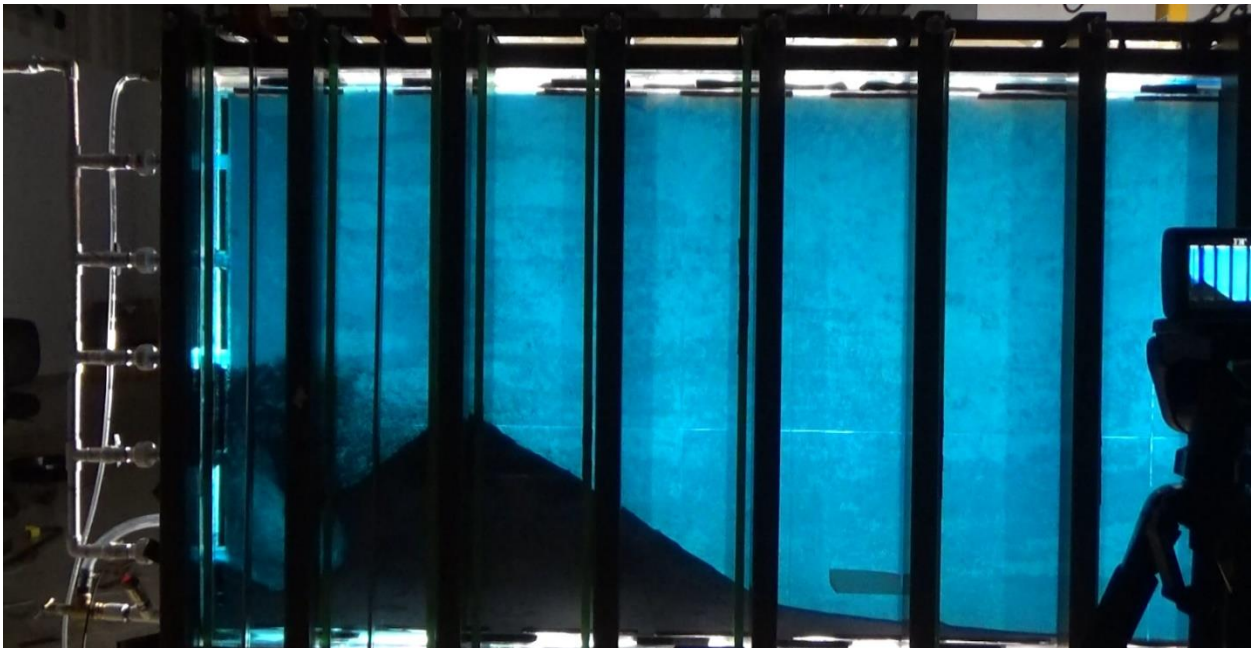

Figure 92. Experiment 3 at 2 Minutes and 40 Seconds

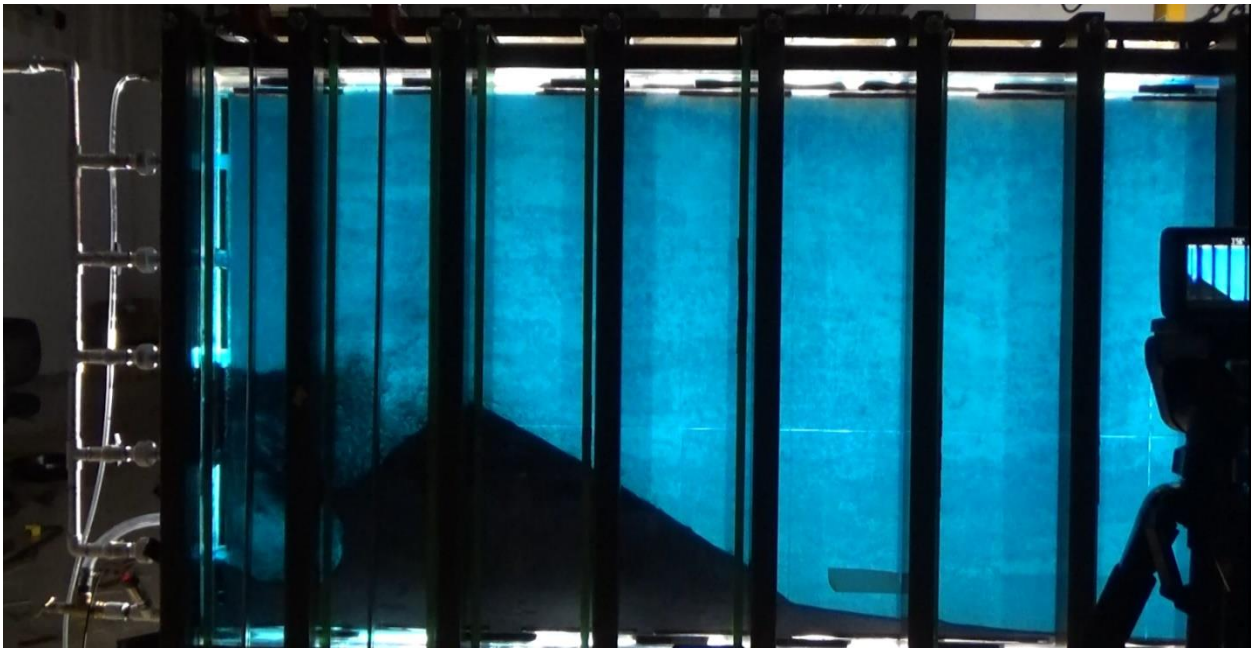

Figure 93. Experiment 3 at 3 Minutes

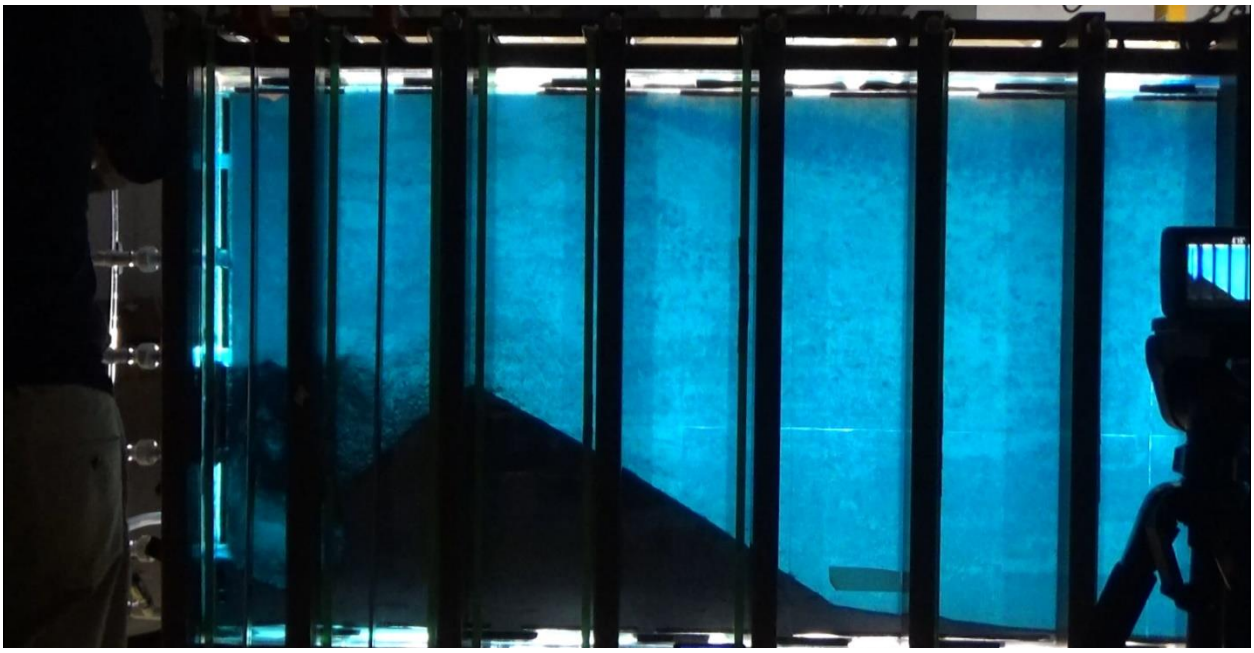

Figure 94. Experiment 3 at 3 Minutes and 20 Seconds

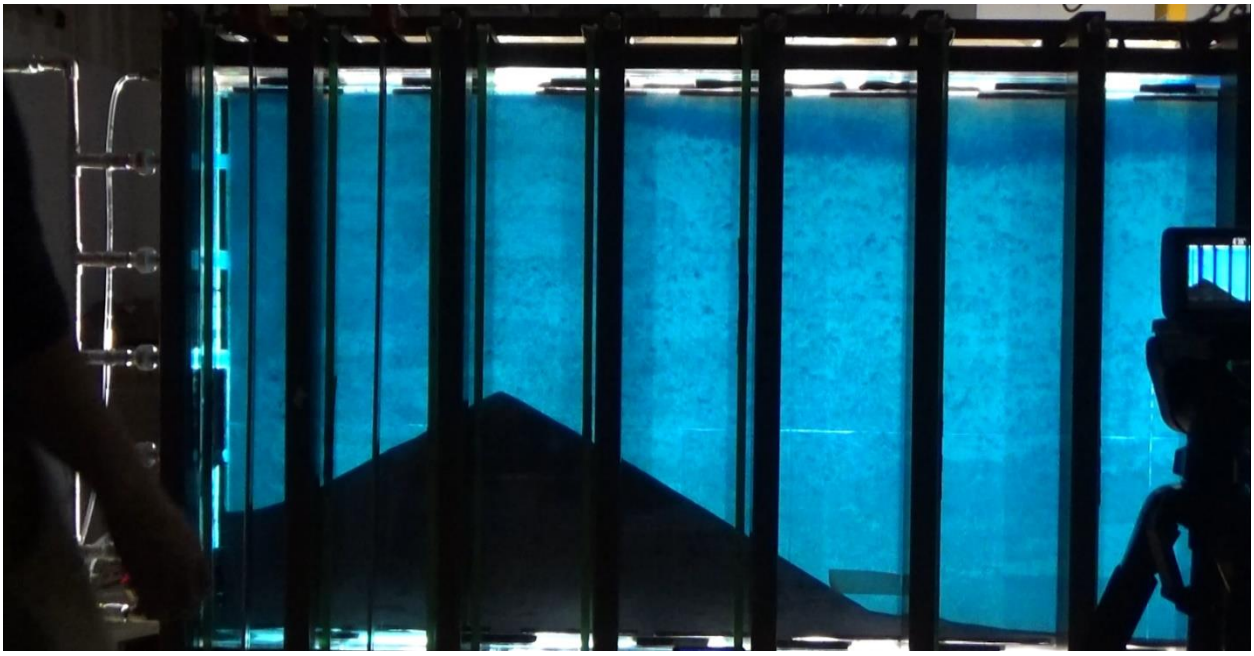

Figure 95. Experiment 3 at 3 Minutes and 40 Seconds

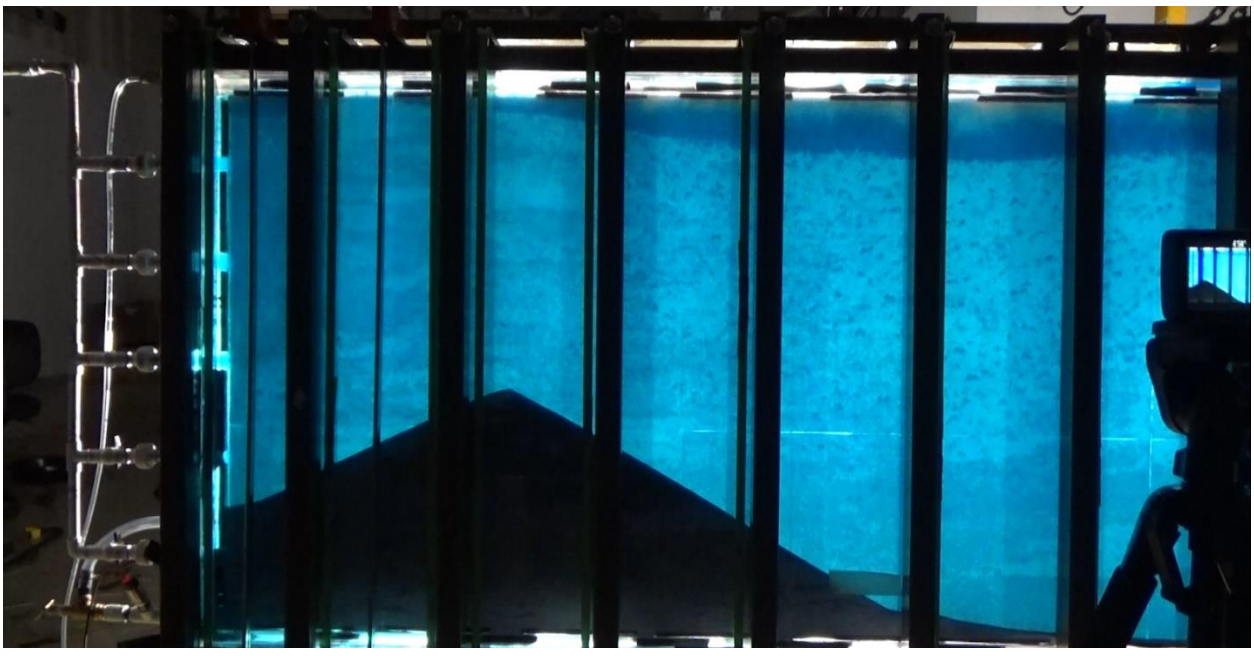

Figure 96. Experiment 3 at 4 Minutes

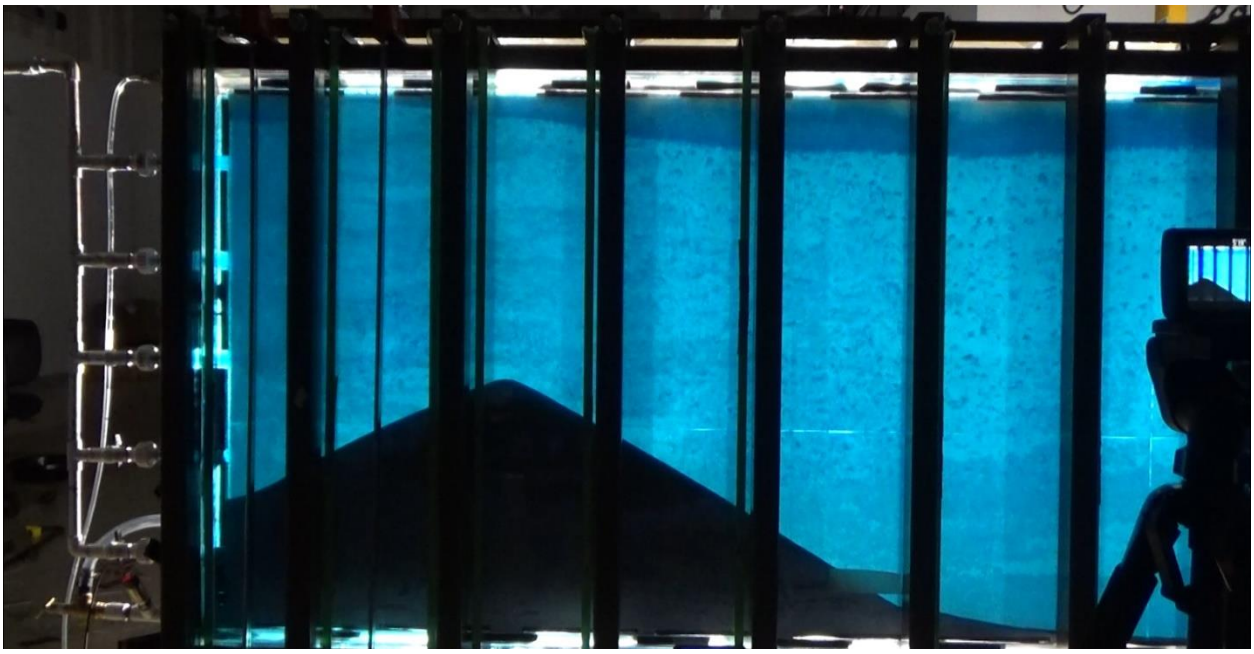

Figure 97. Experiment 3 at 4 Minutes and 20 Seconds

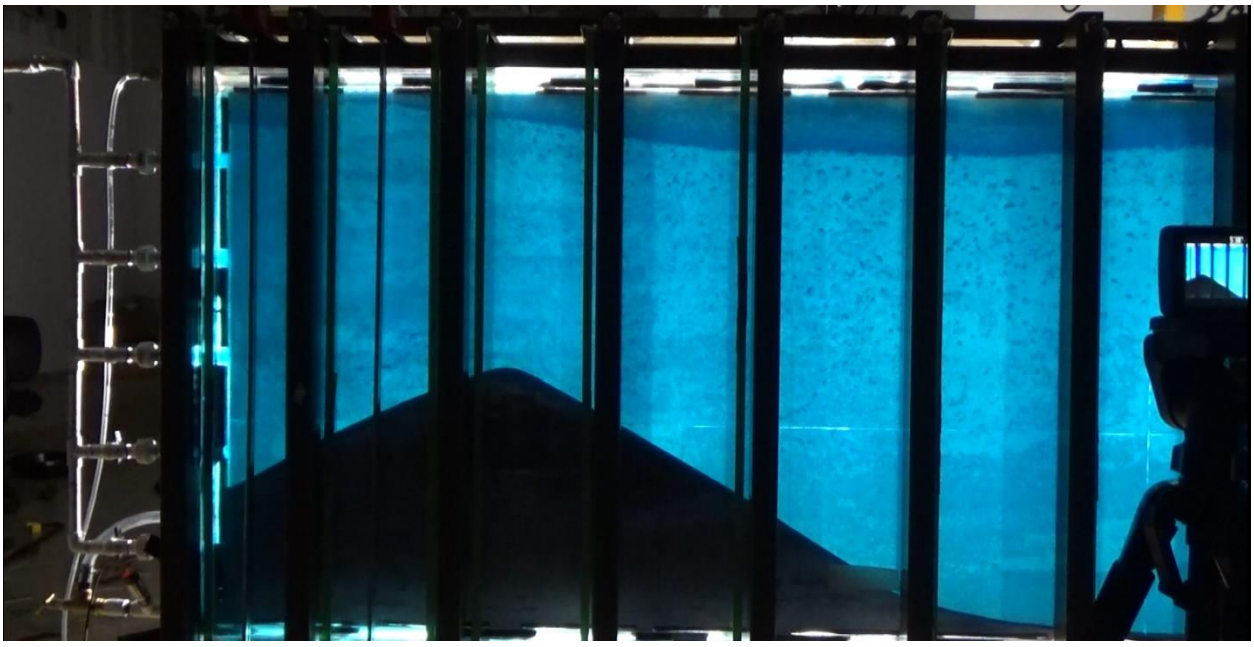

Figure 98. Experiment 3 at 4 Minutes and 40 Seconds

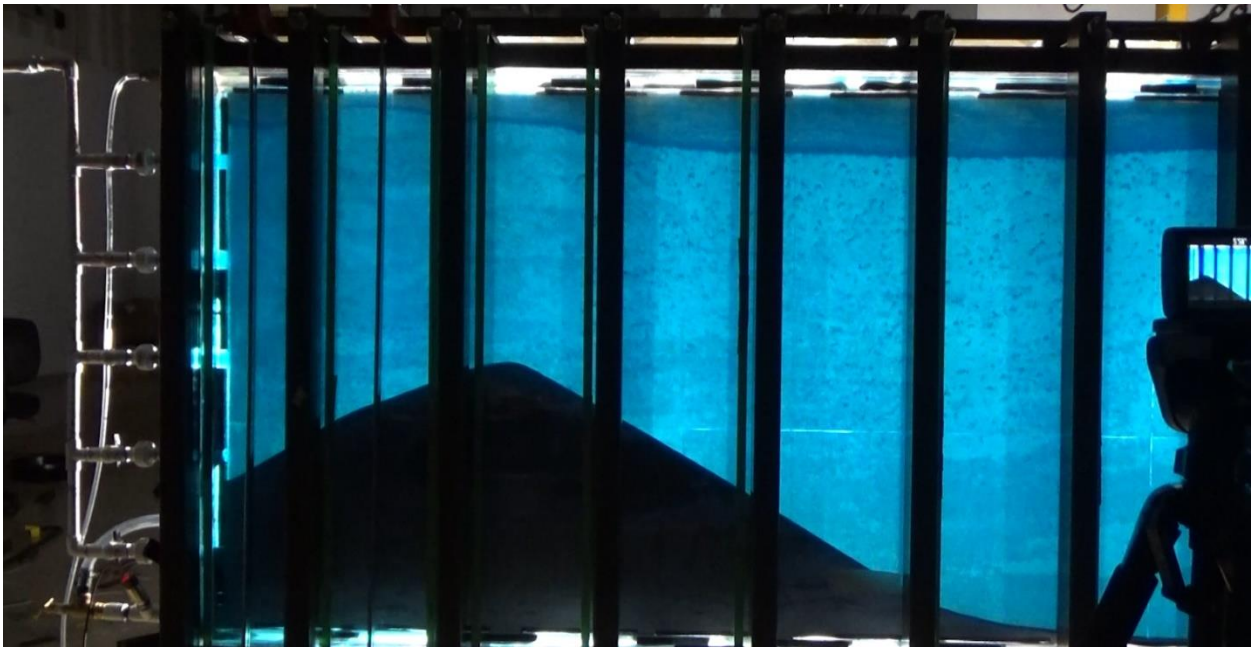

Figure 99. Experiment 3 at 5 Minutes

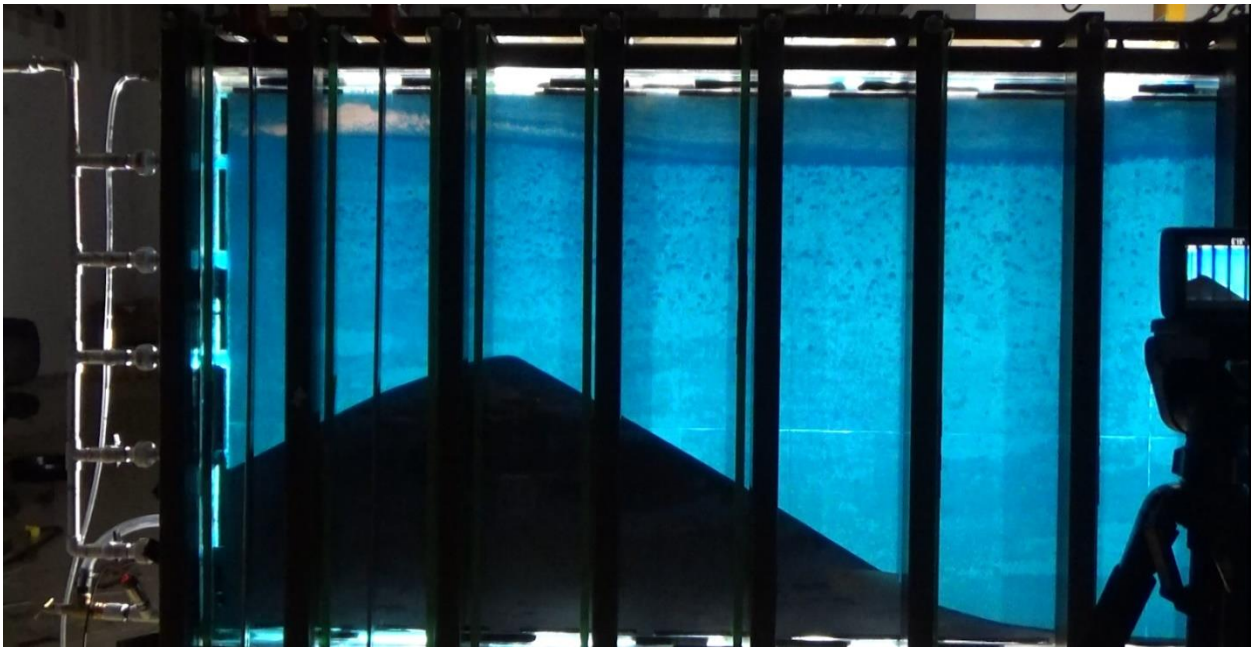

Figure 100. Experiment 3 at 5 Minutes and 20 Seconds

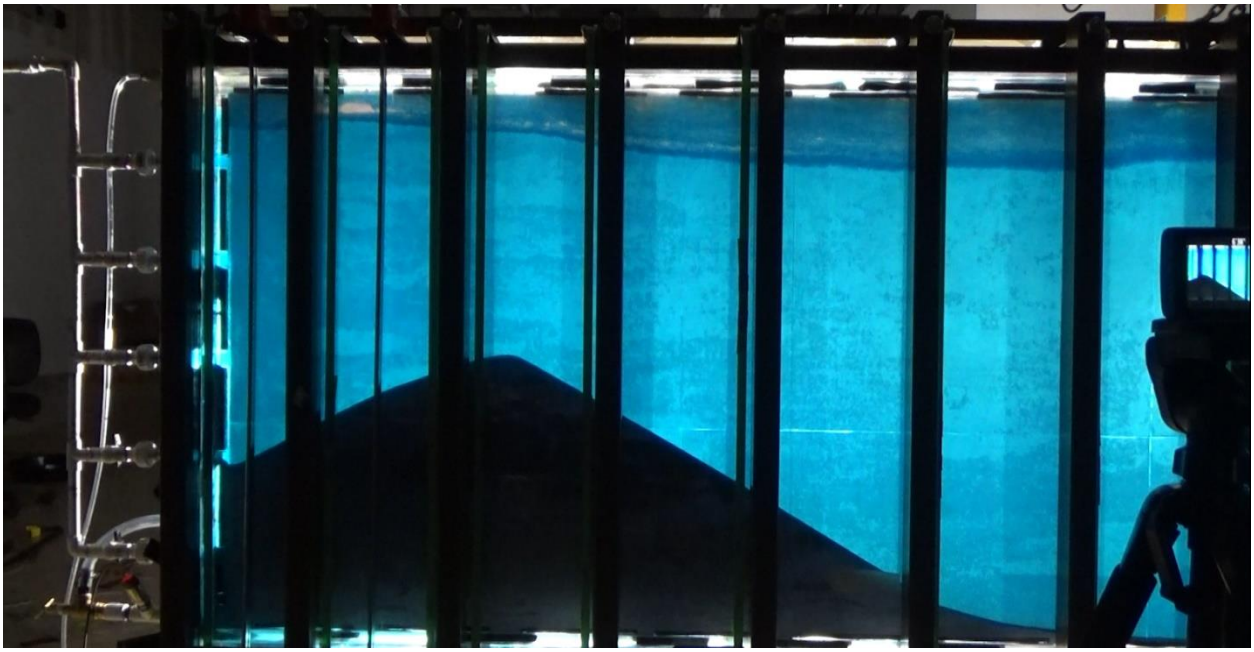

Figure 101. Experiment 3 at 5Minutes and 40 Seconds

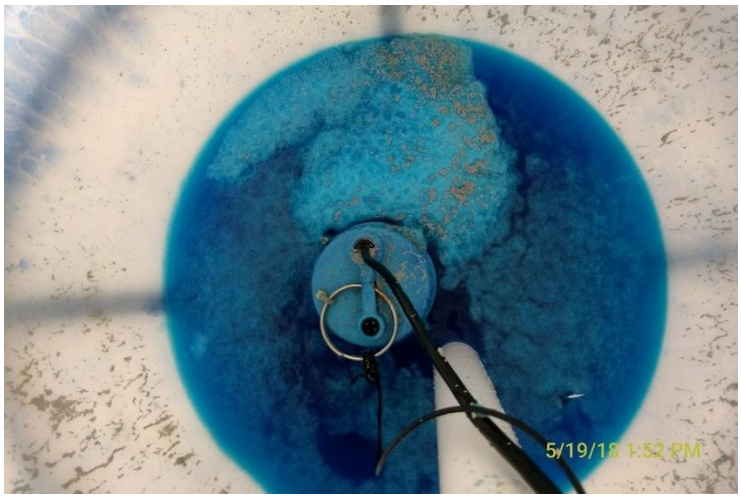

Figure 102. Inside of Mixing Tank after Experiment 3

Experiment 3 offered new observations. Firstly, fibers did not seem to have any effect on proppant suspension at all, at least when comparing to the small-scale experiment (Figure 103).

From Figure 102, which shows the inside of the mixing tank after the experiment, fibers helped little in suspending proppant in the fluid. There is a big amount of fibers and proppant at the top. Around it, fibers were flowing freely, and proppant settled to the bottom of the tank. It appeared that the fibers did not tangle with each other and trap proppants in between. The suspension of proppant in this case is, for the most part, the same as in experiment 2 (Figure 82).

Figure 103. PGA Fibers Mixed in Slickwater, Reprinted From Tran (2017)

In experiment 3, the separation of fibers and proppant displayed clearly in the panels (Figure 101). We saw a typical proppant bank near the inlet. A large amount of fibers in our fluid floated on the top of the panels. This should not be happening, considering that both PGA and PLA have a higher density than water. PGA has density in the range of 93.60 - 99.84 lbm/ft^3 while PLA 75.5-78.0 lbm/ft^3 (Tran 2017). The result suggested that fibers' quality was somehow compromised as they were in storage for almost 2 years before experiment 3.

Secondly, the fibers did not seem to hang on the panel's wall like they did in the small-scale experiment. In Figure 103, we had 0.2 inches fracture width and 0.2 inches long fibers. In experiment 3, we had 0.2 inches fibers and 0.4 inches slot. This could be the reason why the fibers were floating freely as shown from Figure 94 to Figure 101.

Thirdly, after back calculating, the proppant concentration was even less than what we had for experiment 2, which was 0.37 lbm/gal. For an intended 0.826 lbm/gal, our calculation showed 0.157 lbm/gal, which was unacceptably low. This proved that the foam piece we installed (Figure 83) before running experiment 3 did not work at all.

Tran (2017) concluded that, mixing fibers into frac fluid has two advantages. First, fibers prevent proppant from premature settling. Second, fibers help create groups of proppant, thus forming conductive channels. Figure 104 shows the proppant dune in Figure 101 at close inspection. Groups of proppant formed channels that were reminiscent of those in Figure 103. These channels proved that experiment 3 could replicate Tran (2017)'s results, though with some drawbacks. The proppant was not properly suspended. Most of the fibers and proppant were segregated (Figure 101). The channels and proppant groups were quite limited and hard to discern. Further experiment is needed to accurately reproduce the effect in Figure 103.

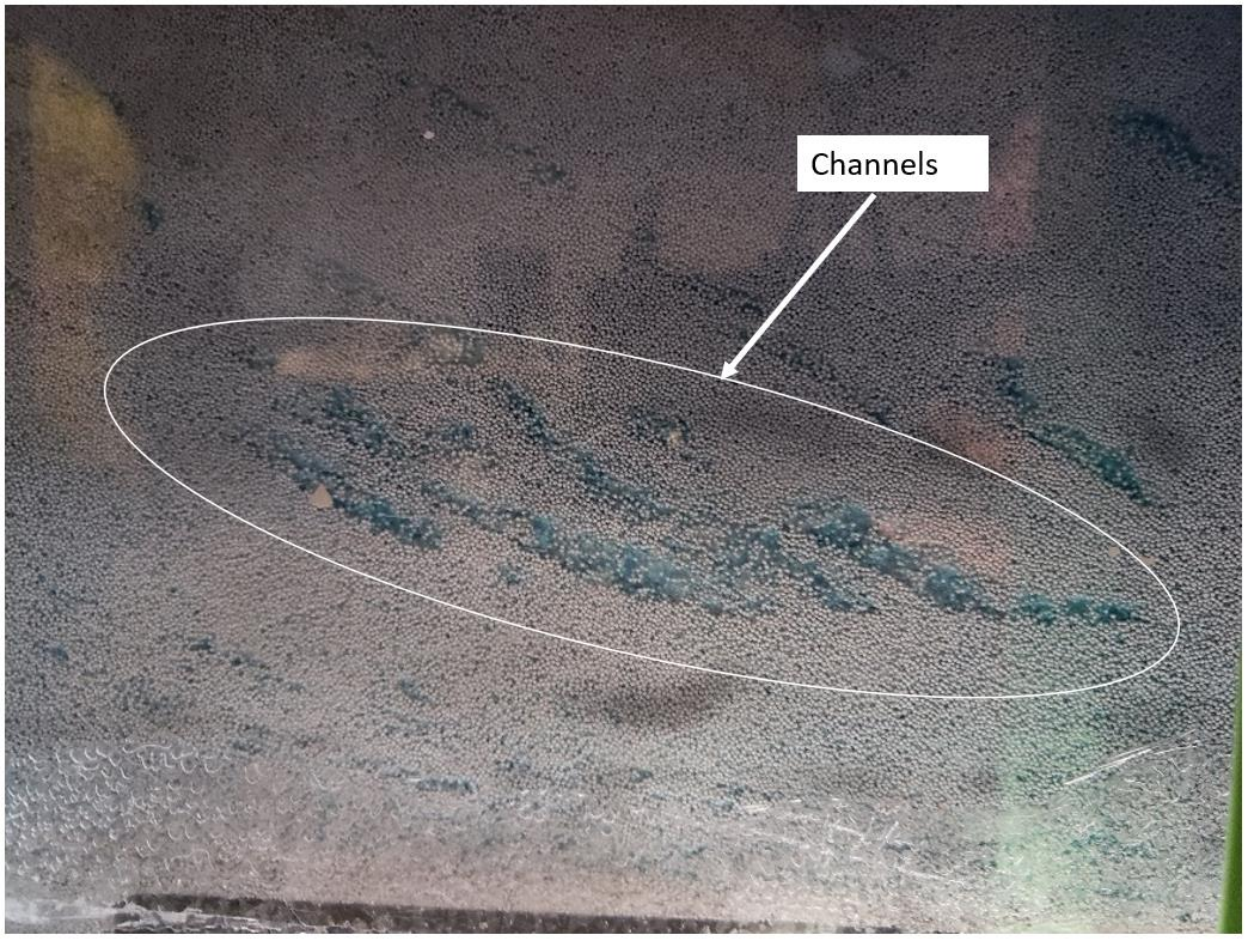

Figure 104. Channels Inside the Proppant Bank of Experiment 3

4. CONCLUSION

In this thesis, a large scale, slot flow experimental setup was designed and built. Experiments 1, 2 and 3 have shown that the large setup could successfully perform slot flow experiments.

- Experiment 1 showed a small proppant bank.
- Experiment 2 showed a large proppant bank near the inlets, a phenomenon previously observed in other research.
- Experiment 3 showed channels formed by interactions of fibers and proppant.

Unlike the small-scale setup, the large-scale setup allowed experiments to run under conditions that are more representative of field's conditions.

- The large setup's viewing area is 4' x 16', comparing to 1' x 4' in the small scale.
- The large setup could vary the fracture width from 0.1"-0.5", while the small one only had a fixed width of 0.2."
- The large setup had 5 inlets; the small setup had 3.
- The large setup could handle up to 2 psig pressure buildup; the small setup had near atmospheric pressure.
- Finally, the large setup could perform experiments with flow rate up to 24 gpm per 4 vertical foot; the small setup had low flow rate.

The mixing mechanism in the large setup still has room for improvement, especially the mixer and mixing tank.

REFERENCES

Al-Muntasheri, G. A. (2014). *A critical review of hydraulic fracturing fluids over the last decade.* Paper presented at the SPE Western North American and Rocky Mountain Joint Meeting.

Corporation, K. (2010). Kuredux Polyglicolic Acid (PGA) Resin.

Gaillard, N., Thomas, A., & Favero, C. (2013). *Novel associative acrylamide-based polymers for proppant transport in hydraulic fracturing fluids.* Paper presented at the SPE International Symposium on Oilfield Chemistry.

Handbook, A. Directory of Microbicides for the Protection of Materials.

Hou, T., Zhang, S., Yu, B., Lv, X., Zhang, J., Han, J., & Li, D. (2016). *Theoretical Analysis and Experimental Research of Channel Fracturing in Unconventional Reservoir.* Paper presented at the SPE Europec featured at 78th EAGE Conference and Exhibition.

Hu, K., Sun, J., Wong, J., & Hall, B. E. (2014). *Proppants Selection Based on Field Case Studies of Well Production Performance in the Bakken Shale Play.* Paper presented at the SPE Western North American and Rocky Mountain Joint Meeting.

Huang, F., Gundewar, R. S., Loughridge, B. W., & Steed, D. L. (2005). *Feasibility of using produced water for crosslinked gel-based hydraulic fracturing.* Paper presented at the SPE Production Operations Symposium.

Jan, B. M. (2013). Technology Focus: Drilling and Completion Fluids (November 2013). *Journal of Petroleum Technology, 65*(11), 124-124.

Jennings Jr, A. R. (1996). Fracturing Fluids-Then and Now. *Journal of Petroleum Technology, 48*(07), 604-610.

Li, L., Eliseeva, K. E., Eliseev, V., Bustos, O. A., England, K. W., Howard, P. R., . . . Ali, S. A. (2009). *Well Treatment Fluids Prepared with Oilfield Produced Water.* Paper presented at the SPE Annual Technical Conference and Exhibition.

Li, L., Ezeokonkwo, C. I., Lin, L., Eliseeva, K. E., Kallio, W., Boney, C. L., . . . Samuel, M. M. (2010). *Well Treatment Fluids Prepared With Oilfield Produced Water: Part II.* Paper presented at the SPE Annual Technical Conference and Exhibition.

Liang, F., Sayed, M., Al-Muntasheri, G. A., Chang, F. F., & Li, L. (2016). A comprehensive review on proppant technologies. *Petroleum, 2*(1), 26-39.

Medvedev, A. V., Kraemer, C. C., Pena, A. A., & Panga, M. K. R. (2013). *On the mechanisms of channel fracturing.* Paper presented at the SPE Hydraulic Fracturing Technology Conference.

Palisch, T., Vincent, M., & Handren, P. (2010). *Slickwater Fracturing: Food for Thought. SPE Prod & Oper 25 (3): 327–344*. Retrieved from

Rajagopalan, V., Awad, M., Al-Othman, M., Al-Ajmi, M., Mokhtar, A., & Sheikh, B. (2015). *Application of Flow-Channel Fracturing Technique to Unlock Potential from Reservoirs with Severe Heterogeneity and Poor Lithological Characteristics.* Paper presented at the SPE Kuwait Oil and Gas Show and Conference.

Schein, G. (2004). *The application and technology of slickwater fracturing 2004. Presented as a Distinguished Lecture During the 2004–2005 Season*. Retrieved from

Södergård, A., & Stolt, M. (2010). Industrial production of high molecular weight poly (lactic acid). *Poly (Lactic Acid): Synthesis, Structures, Properties, Processing, and Applications*, 27-41.

Tinsley, J., & Williams Jr, J. (1975). A new method for providing increased fracture conductivity and improving stimulation results. *Journal of Petroleum Technology, 27*(11), 1,319-311,325.

Tran, T., Kim, J. Y., Morita, N., & Yoshimura, K. (2017). *Application of PGA Fiber and Fluid-Loss Materials to Slick Water Fracturing.* Paper presented at the 51st US Rock Mechanics/Geomechanics Symposium.

Yoshimura, K., Matsui, H., & Morita, N. (2016). Development of Polyglycolic-and polylactic-acid fluid-loss-control materials for fracturing fluids. *SPE Drilling & Completion, 30*(04), 295-309.

APPENDIX

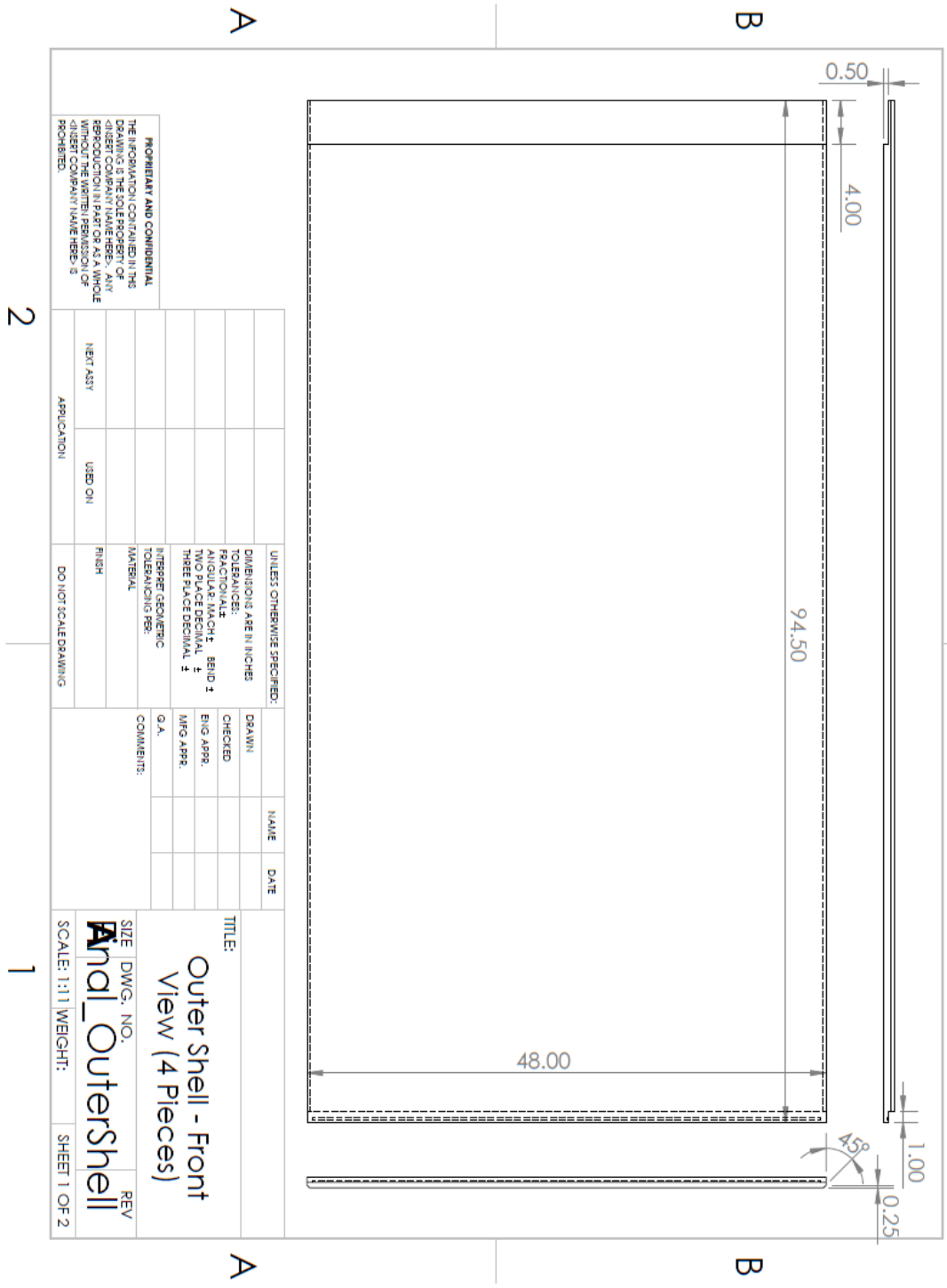
0.50
4.00
94.50
48.00
45°
1.00
0.25
A
B
2
1
UNLESS OTHERWISE SPECIFIED:
DIMENSIONS ARE IN INCHES
TOLERANCES:
FRACTIONAL ±
ANGULAR: MACH ± BEND ±
TWO PLACE DECIMAL ±
THREE PLACE DECIMAL ±
INTERPRET GEOMETRIC TOLERANCING PER:
MATERIAL
FINISH
DO NOT SCALE DRAWING
NEXT ASSY
USED ON
APPLICATION
DRAWN
CHECKED
ENG APPR.
MFG APPR.
Q.A.
COMMENTS:
NAME
DATE
PROPRIETARY AND CONFIDENTIAL
THE INFORMATION CONTAINED IN THIS DRAWING IS THE SOLE PROPERTY OF <INSERT COMPANY NAME HERE>. ANY REPRODUCTION IN PART OR AS A WHOLE WITHOUT THE WRITTEN PERMISSION OF <INSERT COMPANY NAME HERE> IS PROHIBITED.
TITLE:
Outer Shell - Front View (4 Pieces)
SIZE
A
DWG. NO.
Anal_OuterShell
REV
SCALE: 1:11
WEIGHT:
SHEET 1 OF 2

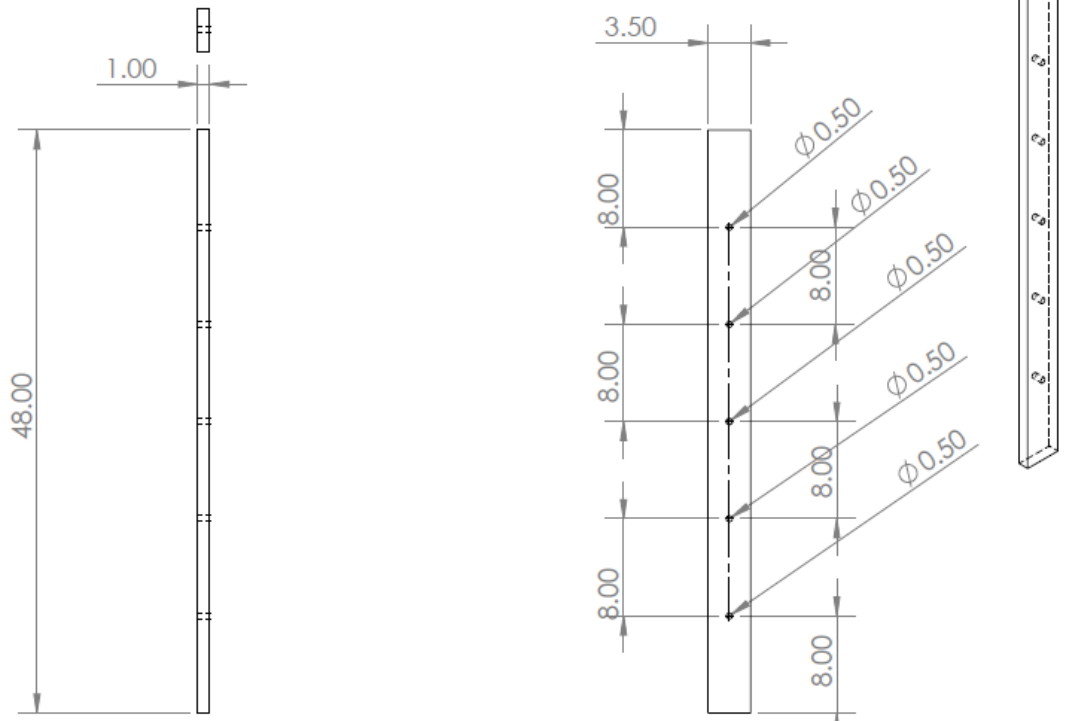

		UNLESS OTHERWISE SPECIFIED:		NAME	DATE
		DIMENSIONS ARE IN INCHES TOLERANCES: FRACTIONAL ± ANGULAR: MACH ± BEND ± TWO PLACE DECIMAL ± THREE PLACE DECIMAL ±	DRAWN		
			CHECKED		
			ENG APPR.		
			MFG APPR.		
		INTERPRET GEOMETRIC TOLERANCING PER:	Q.A.		
		MATERIAL	COMMENTS:		
NEXT ASSY	USED ON	FINISH			
APPLICATION		DO NOT SCALE DRAWING			

TITLE: Outer Shell - Inlet (2 Pieces)

SIZE	DWG. NO.	REV
A	Final_OuterShell_Inlet 5 hole p	
SCALE: 1:12	WEIGHT:	SHEET 1 OF 1

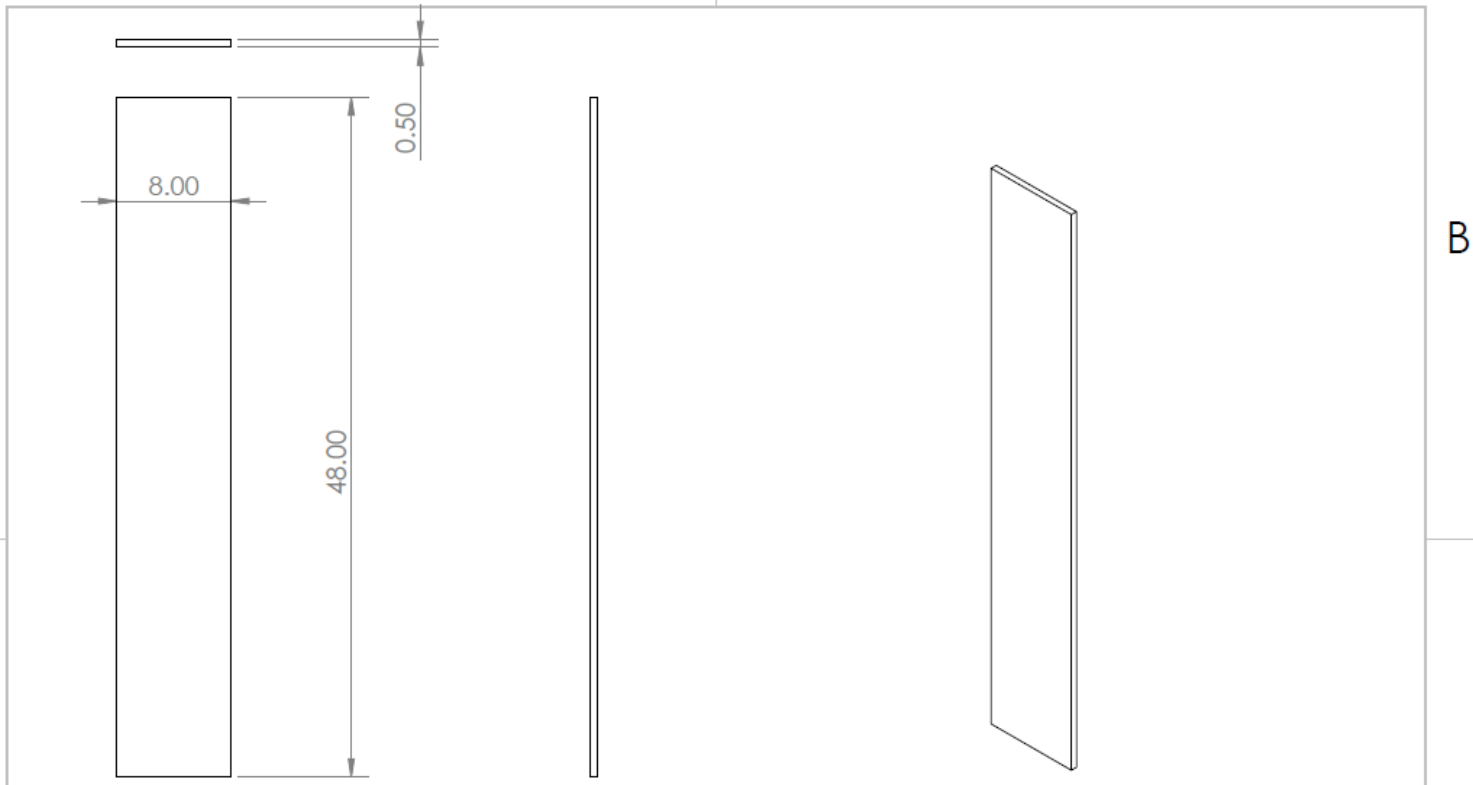

		UNLESS OTHERWISE SPECIFIED:		NAME	DATE
		DIMENSIONS ARE IN INCHES TOLERANCES: FRACTIONAL ± ANGULAR: MACH ± BEND ± TWO PLACE DECIMAL ± THREE PLACE DECIMAL ±	DRAWN		
			CHECKED		
			ENG APPR.		
			MFG APPR.		
		INTERPRET GEOMETRIC TOLERANCING PER:	Q.A.		
		MATERIAL	COMMENTS:		
NEXT ASSY	USED ON	FINISH			
APPLICATION		DO NOT SCALE DRAWING			

TITLE:
Outer Shell Patch
(2 Pieces)

SIZE	DWG. NO.	REV
A	OuterShell_Patch	
SCALE: 1:10	WEIGHT:	SHEET 1 OF 1

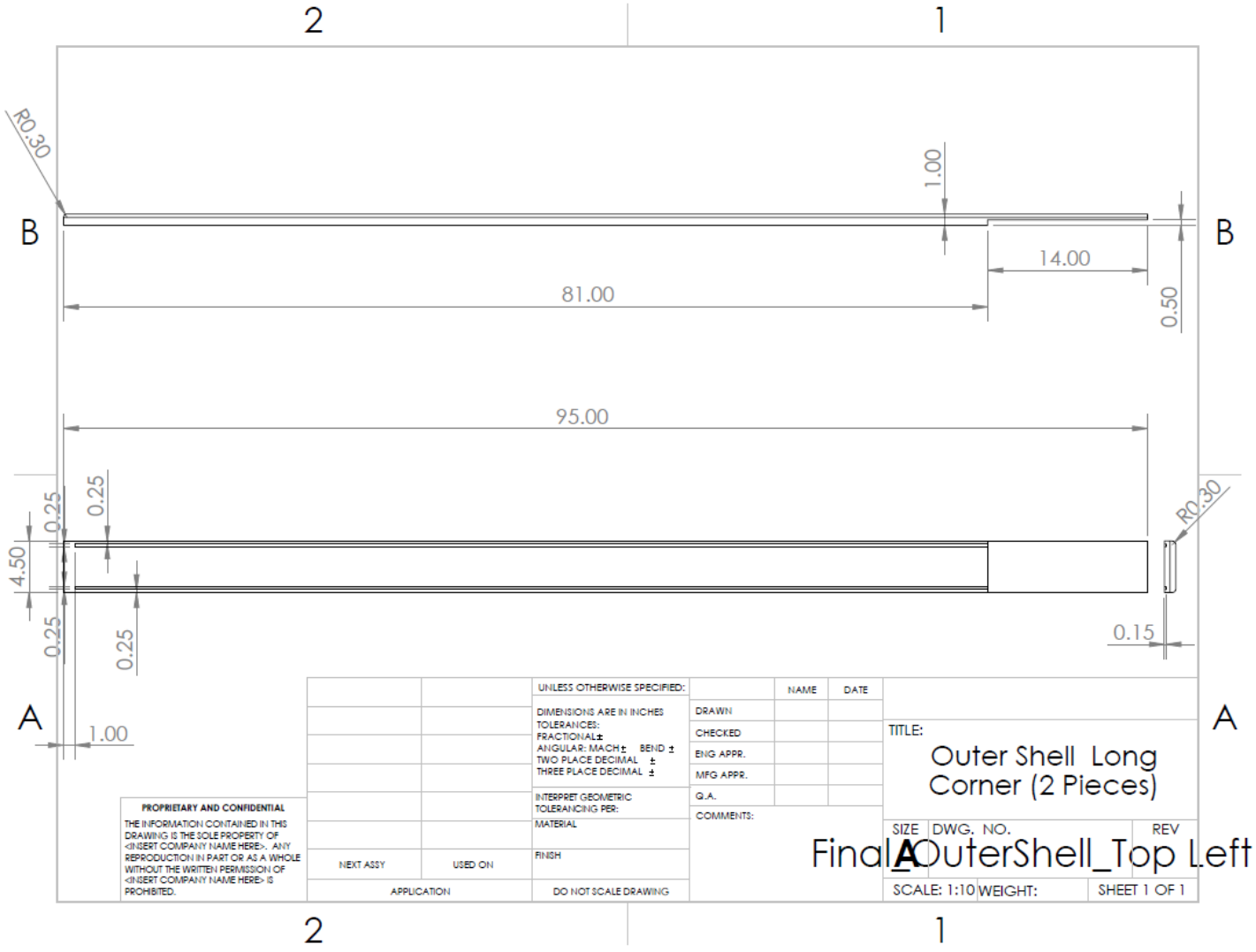

		UNLESS OTHERWISE SPECIFIED:		NAME	DATE
		DIMENSIONS ARE IN INCHES TOLERANCES: FRACTIONAL ± ANGULAR: MACH ± BEND ± TWO PLACE DECIMAL ± THREE PLACE DECIMAL ±	DRAWN		
			CHECKED		
			ENG APPR.		
			MFG APPR.		
		INTERPRET GEOMETRIC TOLERANCING PER:	Q.A.		
		MATERIAL	COMMENTS:		
NEXT ASSY	USED ON	FINISH			
APPLICATION		DO NOT SCALE DRAWING			

TITLE:
Outer Shell Long Corner (2 Pieces)

SIZE	DWG. NO.	REV
A	Final_OuterShell_Top Left	
SCALE: 1:10	WEIGHT:	SHEET 1 OF 1

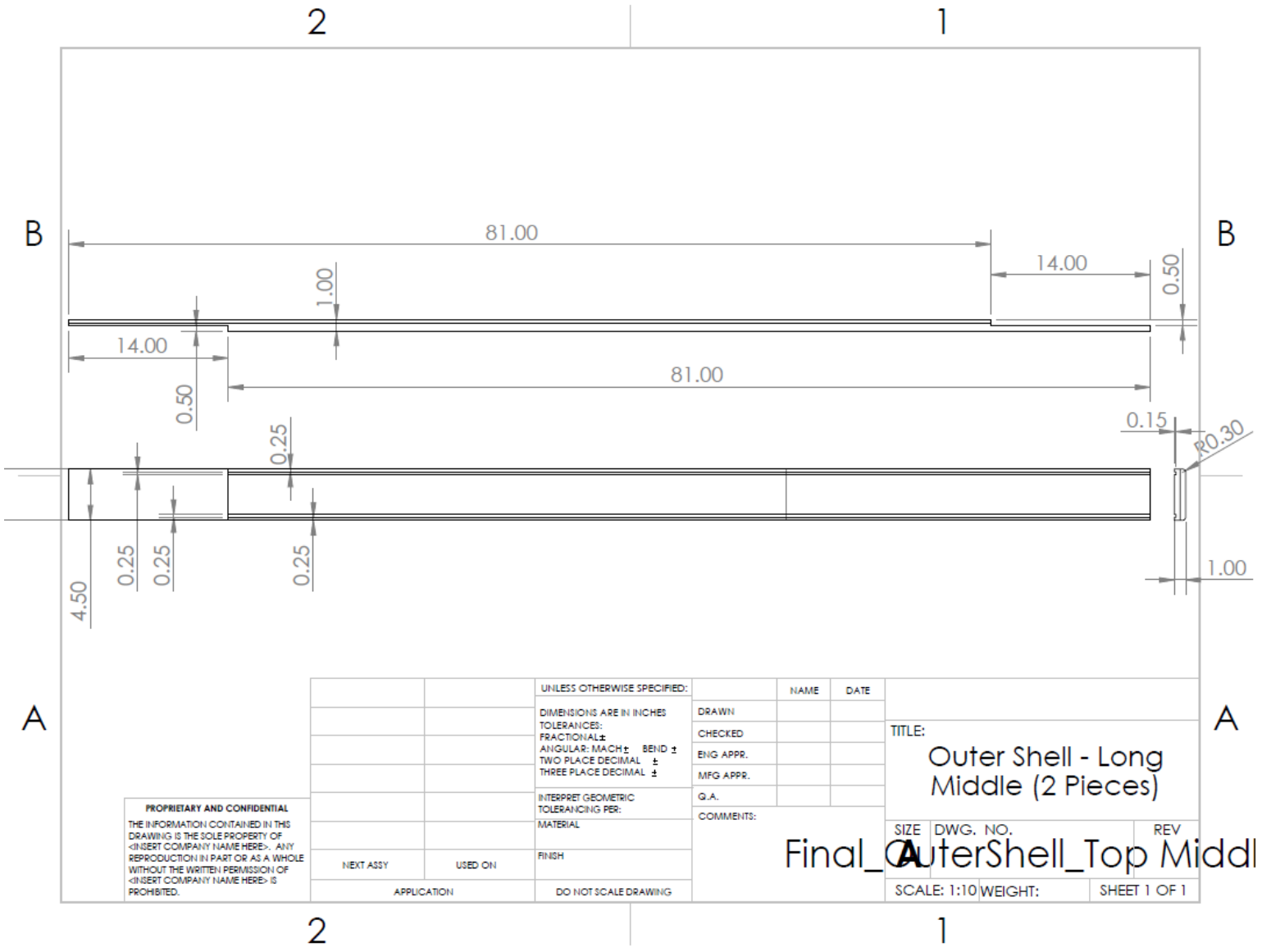

		UNLESS OTHERWISE SPECIFIED:		NAME	DATE
		DIMENSIONS ARE IN INCHES TOLERANCES: FRACTIONAL ± ANGULAR: MACH ± BEND ± TWO PLACE DECIMAL ± THREE PLACE DECIMAL ±	DRAWN		
			CHECKED		
			ENG APPR.		
			MFG APPR.		
		INTERPRET GEOMETRIC TOLERANCING PER:	Q.A.		
		MATERIAL	COMMENTS:		
NEXT ASSY	USED ON	FINISH			
APPLICATION		DO NOT SCALE DRAWING			

PROPRIETARY AND CONFIDENTIAL

THE INFORMATION CONTAINED IN THIS DRAWING IS THE SOLE PROPERTY OF <INSERT COMPANY NAME HERE>. ANY REPRODUCTION IN PART OR AS A WHOLE WITHOUT THE WRITTEN PERMISSION OF <INSERT COMPANY NAME HERE> IS PROHIBITED.

TITLE:

Outer Shell - Long Middle (2 Pieces)

SIZE	DWG. NO.	REV
A	Final_OuterShell_Top Middl	
SCALE: 1:10	WEIGHT:	SHEET 1 OF 1

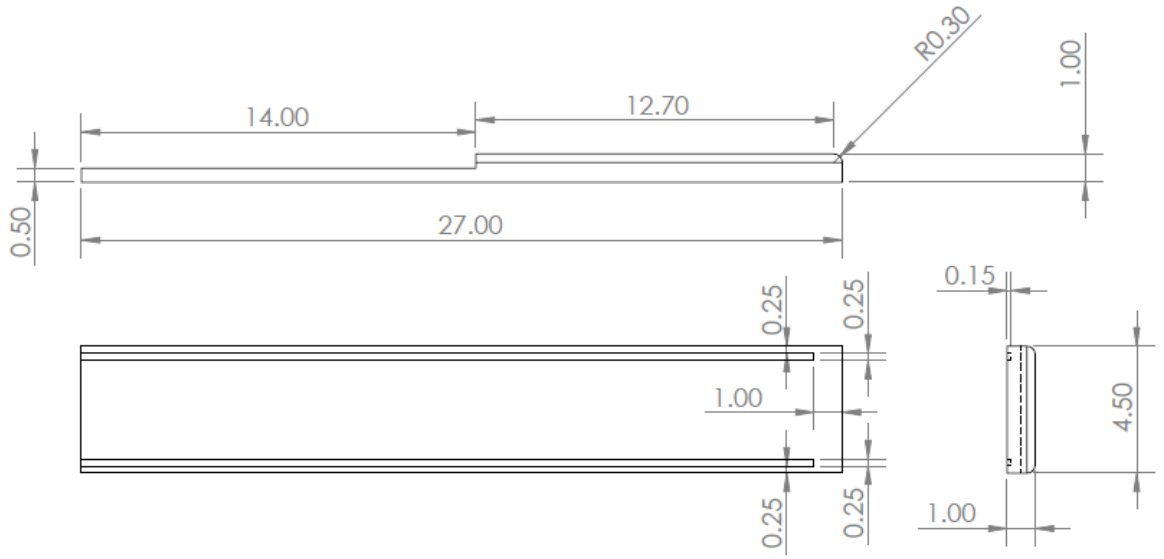

		UNLESS OTHERWISE SPECIFIED:		NAME	DATE
		DIMENSIONS ARE IN INCHES TOLERANCES: FRACTIONAL ± ANGULAR: MACH ± BEND ± TWO PLACE DECIMAL ± THREE PLACE DECIMAL ±	DRAWN		
			CHECKED		
			ENG APPR.		
			MFG APPR.		
		INTERPRET GEOMETRIC TOLERANCING PER:	Q.A.		
		MATERIAL	COMMENTS:		
NEXT ASSY	USED ON	FINISH			
APPLICATION		DO NOT SCALE DRAWING			

TITLE:

Outer Shell - Short Corner (2 Pieces)

SIZE	DWG. NO.	REV
A	Final_OuterShell_Top Right Panel E	
SCALE: 1:5	WEIGHT:	SHEET 1 OF 1

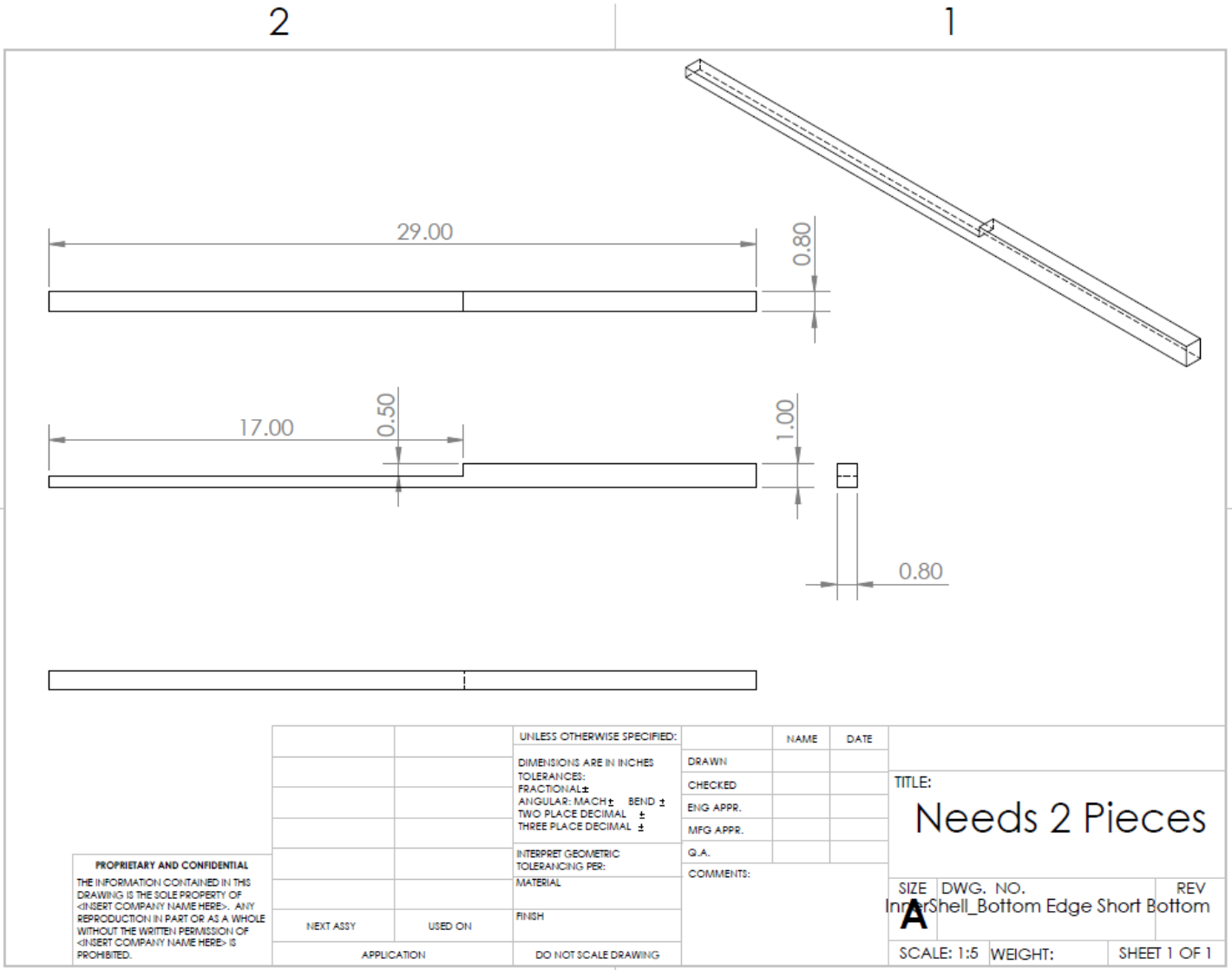
2
1
B
B
A
A
29.00
0.80
17.00
0.50
1.00
0.80
UNLESS OTHERWISE SPECIFIED:
DIMENSIONS ARE IN INCHES
TOLERANCES:
FRACTIONAL ±
ANGULAR: MACH ± BEND ±
TWO PLACE DECIMAL ±
THREE PLACE DECIMAL ±
INTERPRET GEOMETRIC TOLERANCING PER:
MATERIAL
FINISH
NEXT ASSY
USED ON
APPLICATION
DO NOT SCALE DRAWING
NAME
DATE
DRAWN
CHECKED
ENG APPR.
MFG APPR.
Q.A.
COMMENTS:
PROPRIETARY AND CONFIDENTIAL
THE INFORMATION CONTAINED IN THIS DRAWING IS THE SOLE PROPERTY OF <INSERT COMPANY NAME HERE>. ANY REPRODUCTION IN PART OR AS A WHOLE WITHOUT THE WRITTEN PERMISSION OF <INSERT COMPANY NAME HERE> IS PROHIBITED.
TITLE:
Needs 2 Pieces
SIZE
A
DWG. NO.
InnerShell_Bottom Edge Short Bottom
REV
SCALE: 1:5
WEIGHT:
SHEET 1 OF 1

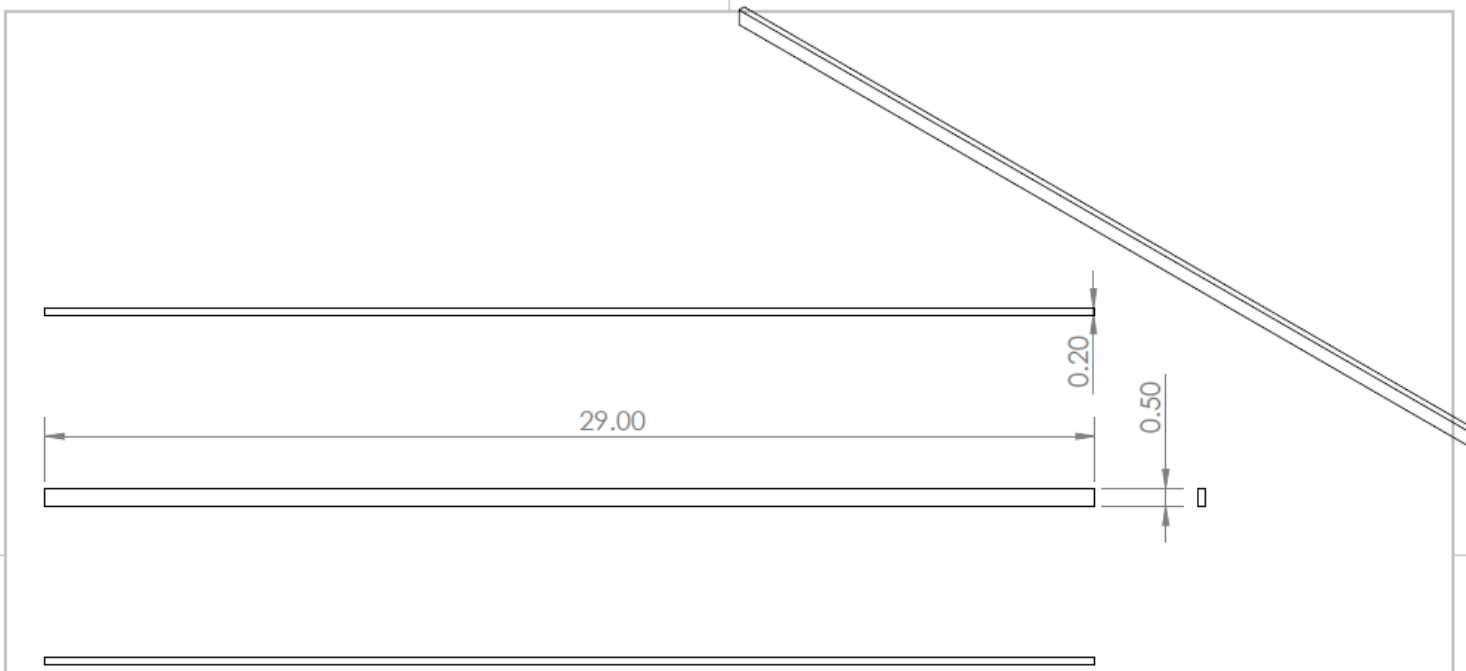

		UNLESS OTHERWISE SPECIFIED:		NAME	DATE
		DIMENSIONS ARE IN INCHES TOLERANCES: FRACTIONAL ± ANGULAR: MACH ± BEND ± TWO PLACE DECIMAL ± THREE PLACE DECIMAL ±	DRAWN		
			CHECKED		
			ENG APPR.		
			MFG APPR.		
		INTERPRET GEOMETRIC TOLERANCING PER:	Q.A.		
		MATERIAL	COMMENTS:		
NEXT ASSY	USED ON	FINISH			
APPLICATION		DO NOT SCALE DRAWING			

TITLE:

InnerShellABottom Edge Short

SIZE	DWG. NO.	REV
SCALE: 1:4	WEIGHT:	SHEET 1 OF 1

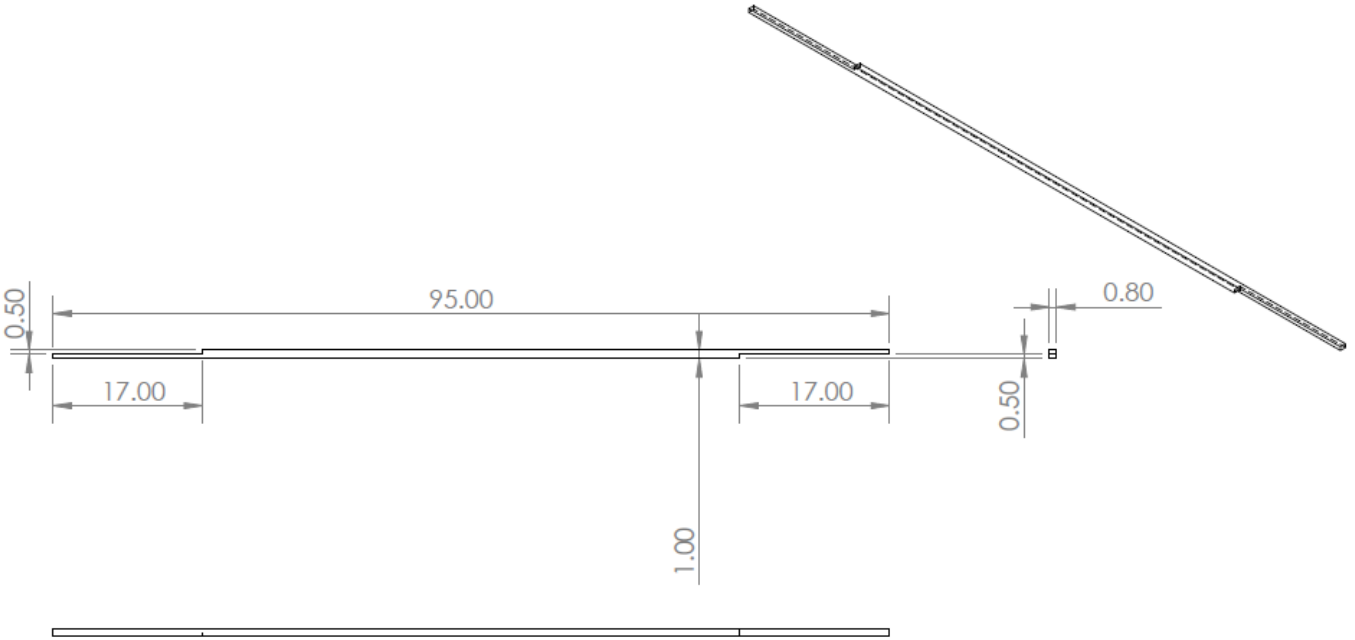

		UNLESS OTHERWISE SPECIFIED:		NAME	DATE
		DIMENSIONS ARE IN INCHES TOLERANCES: FRACTIONAL ± ANGULAR: MACH ± BEND ± TWO PLACE DECIMAL ± THREE PLACE DECIMAL ±	DRAWN		
			CHECKED		
			ENG APPR.		
			MFG APPR.		
		INTERPRET GEOMETRIC TOLERANCING PER:	Q.A.		
		MATERIAL	COMMENTS:		
NEXT ASSY	USED ON	FINISH			
APPLICATION		DO NOT SCALE DRAWING			

TITLE:

Needs 2 Pieces

SIZE	DWG. NO.	REV
A	Inner Shell_Bottom Middle Long Bottom	
SCALE: 1:16	WEIGHT:	SHEET 1 OF 1

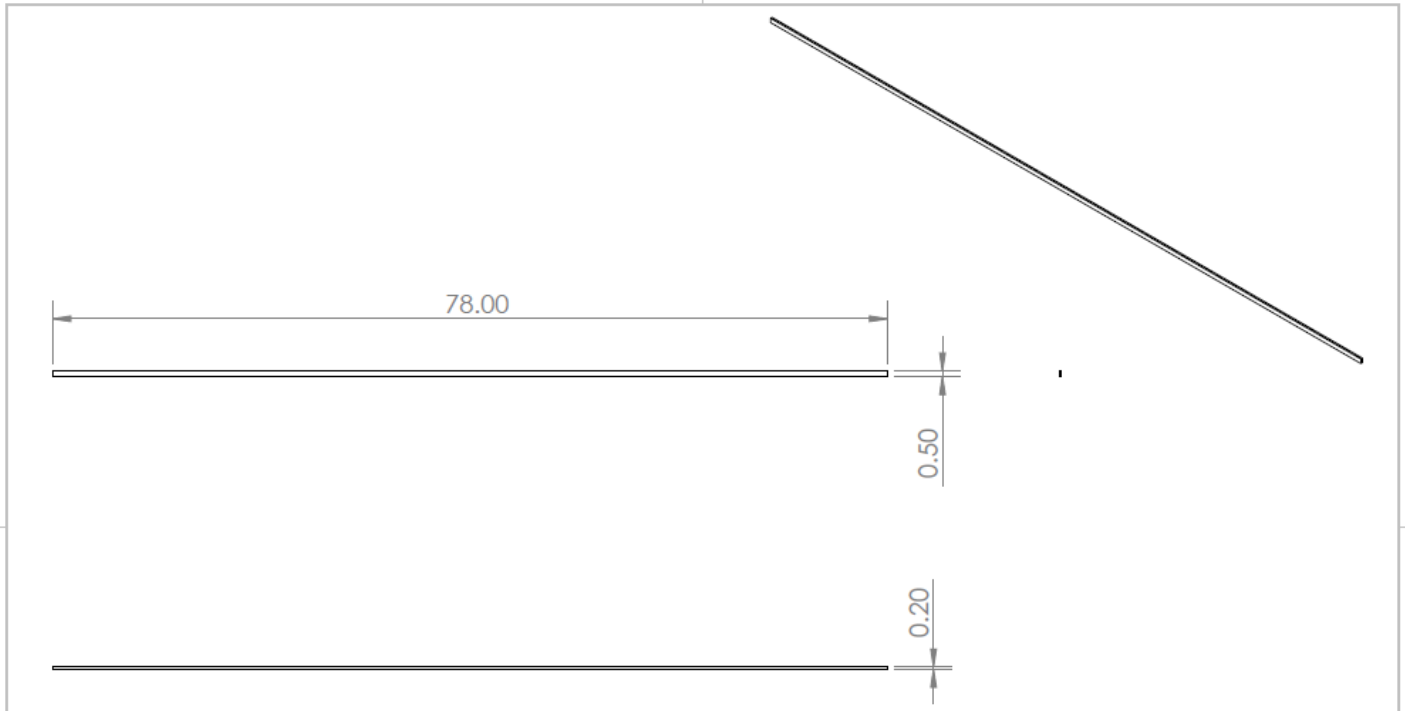

		UNLESS OTHERWISE SPECIFIED:		NAME	DATE
		DIMENSIONS ARE IN INCHES TOLERANCES: FRACTIONAL ± ANGULAR: MACH ± BEND ± TWO PLACE DECIMAL ± THREE PLACE DECIMAL ±	DRAWN		
			CHECKED		
			ENG APPR.		
			MFG APPR.		
		INTERPRET GEOMETRIC TOLERANCING PER:	Q.A.		
		MATERIAL	COMMENTS:		
NEXT ASSY	USED ON	FINISH			
APPLICATION		DO NOT SCALE DRAWING			

TITLE:

Needs 2 Pieces

SIZE	DWG. NO.	REV
A	InnerShell_Bottom Middle Long Top	
SCALE: 1:13	WEIGHT:	SHEET 1 OF 1

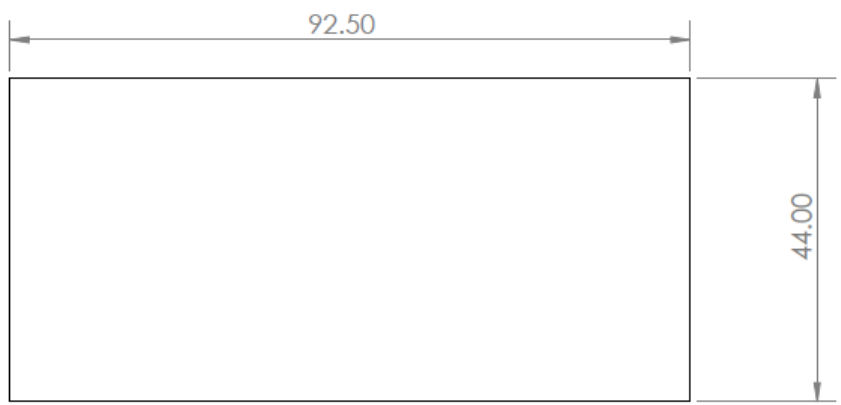

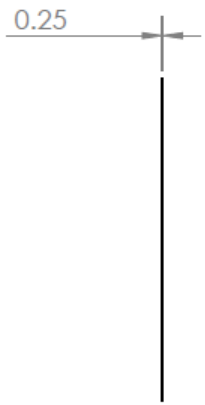

		UNLESS OTHERWISE SPECIFIED:		NAME	DATE
		DIMENSIONS ARE IN INCHES TOLERANCES: FRACTIONAL± ANGULAR: MACH ± BEND ± TWO PLACE DECIMAL ± THREE PLACE DECIMAL ±	DRAWN		
			CHECKED		
			ENG APPR.		
			MFG APPR.		
		INTERPRET GEOMETRIC TOLERANCING PER:	Q.A.		
		MATERIAL Plycarbonate	COMMENTS:		
NEXT ASSY	USED ON	FINISH			
APPLICATION		DO NOT SCALE DRAWING			

TITLE:
Polycarbonate Needs 4 Pieces

SIZE	DWG. NO.	REV
A	Polycarbonate	
SCALE: 1:20	WEIGHT:	SHEET 1 OF 1

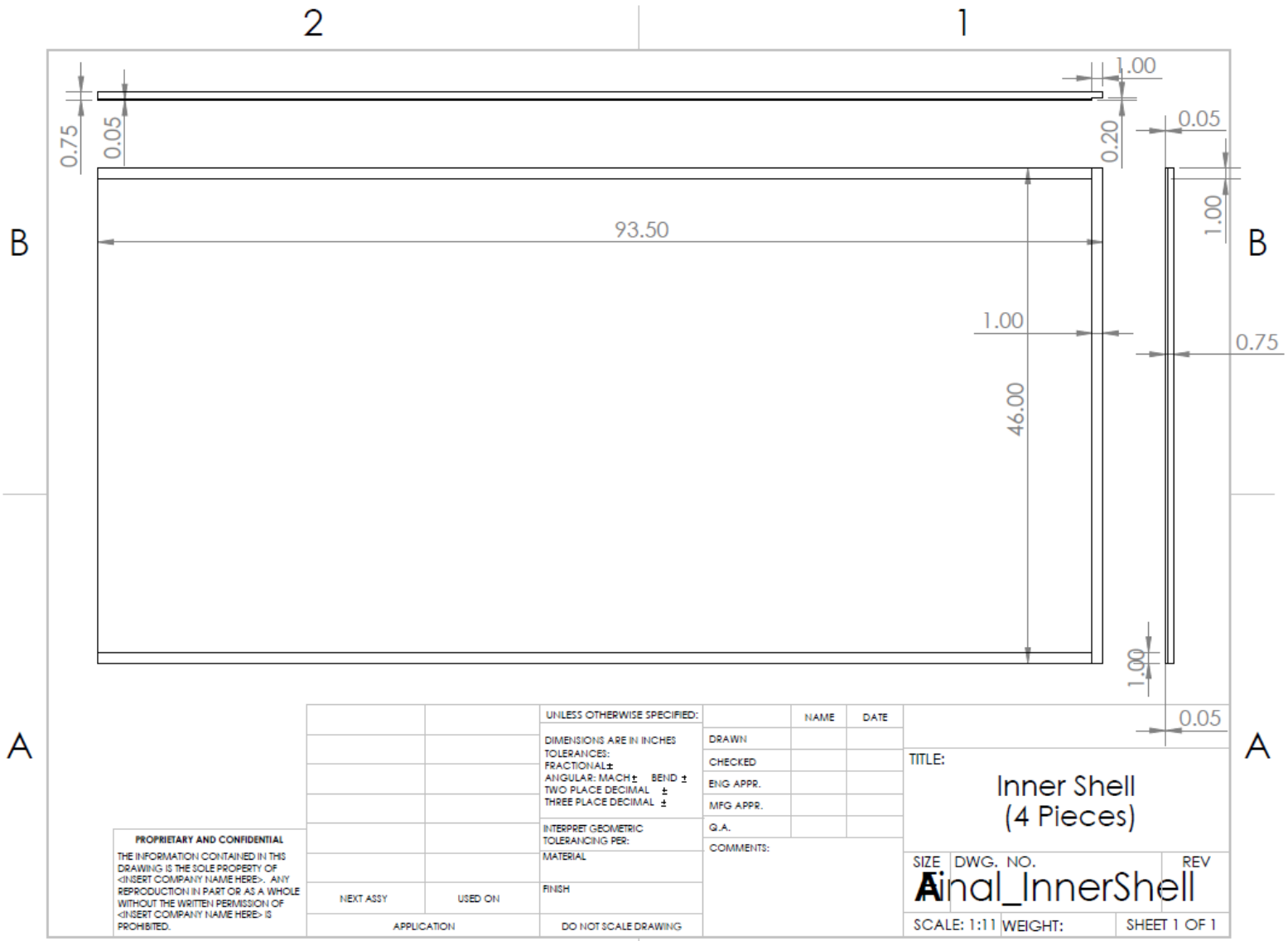

		UNLESS OTHERWISE SPECIFIED:		NAME	DATE
		DIMENSIONS ARE IN INCHES TOLERANCES: FRACTIONAL ± ANGULAR: MACH ± BEND ± TWO PLACE DECIMAL ± THREE PLACE DECIMAL ±	DRAWN		
			CHECKED		
			ENG APPR.		
			MFG APPR.		
		INTERPRET GEOMETRIC TOLERANCING PER:	Q.A.		
		MATERIAL	COMMENTS:		
NEXT ASSY	USED ON	FINISH			
APPLICATION		DO NOT SCALE DRAWING			

TITLE:

Inner Shell
(4 Pieces)

SIZE	DWG. NO.	REV
A	Final_InnerShell	
SCALE: 1:11	WEIGHT:	SHEET 1 OF 1

100

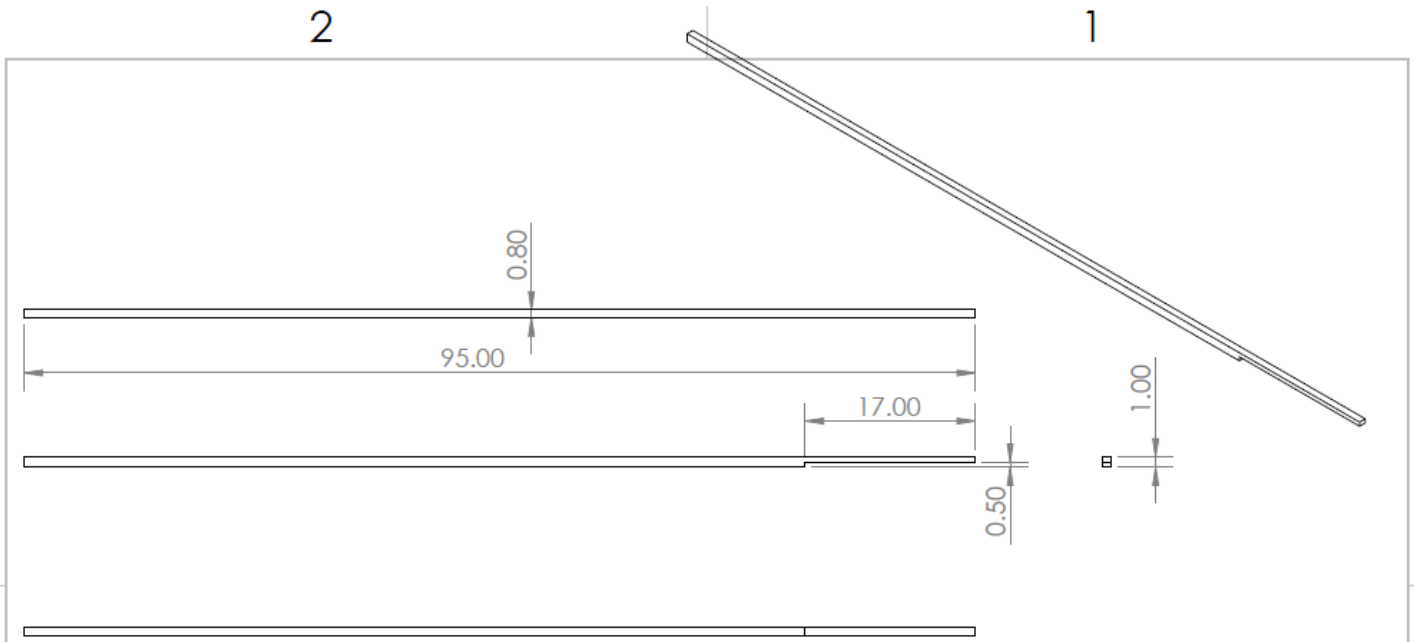

		UNLESS OTHERWISE SPECIFIED:		NAME	DATE
		DIMENSIONS ARE IN INCHES TOLERANCES: FRACTIONAL ± ANGULAR: MACH ± BEND ± TWO PLACE DECIMAL ± THREE PLACE DECIMAL ±	DRAWN		
			CHECKED		
			ENG APPR.		
			MFG APPR.		
		INTERPRET GEOMETRIC TOLERANCING PER:	Q.A.		
		MATERIAL	COMMENTS:		
NEXT ASSY	USED ON	FINISH			
APPLICATION		DO NOT SCALE DRAWING			

TITLE:
Needs 2 Pieces

SIZE	DWG. NO.	REV
A	Final_InnerShell_Bottom Left Bottom	
SCALE: 1:14	WEIGHT:	SHEET 1 OF 1

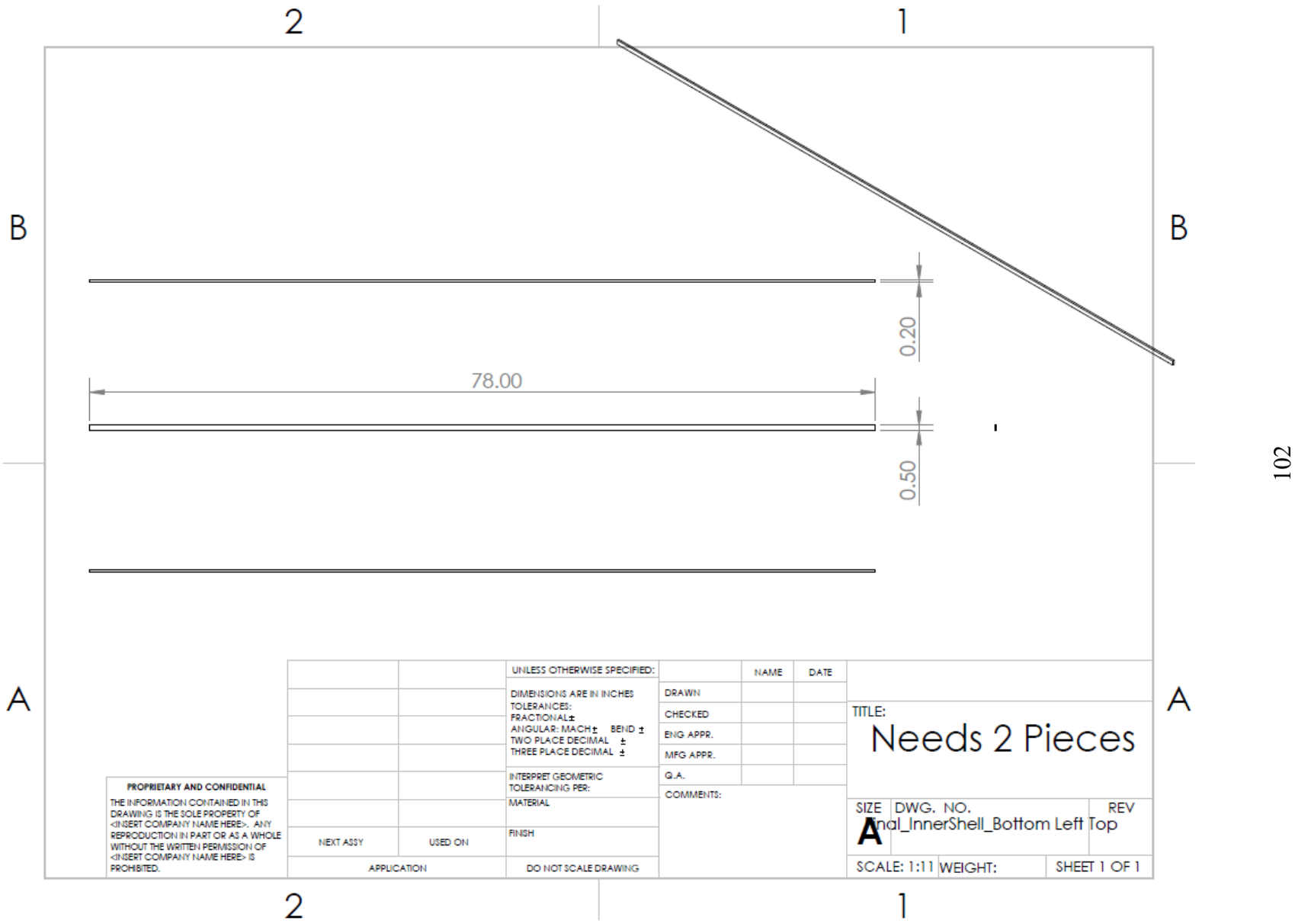

		UNLESS OTHERWISE SPECIFIED:		NAME	DATE
		DIMENSIONS ARE IN INCHES TOLERANCES: FRACTIONAL ± ANGULAR: MACH ± BEND ± TWO PLACE DECIMAL ± THREE PLACE DECIMAL ±	DRAWN		
			CHECKED		
			ENG APPR.		
			MFG APPR.		
		INTERPRET GEOMETRIC TOLERANCING PER:	Q.A.		
		MATERIAL	COMMENTS:		
NEXT ASSY	USED ON	FINISH			
APPLICATION		DO NOT SCALE DRAWING			

TITLE:

Needs 2 Pieces

SIZE	DWG. NO.	REV
A	Final_InnerShell_Bottom Left Top	

SCALE: 1:11	WEIGHT:	SHEET 1 OF 1

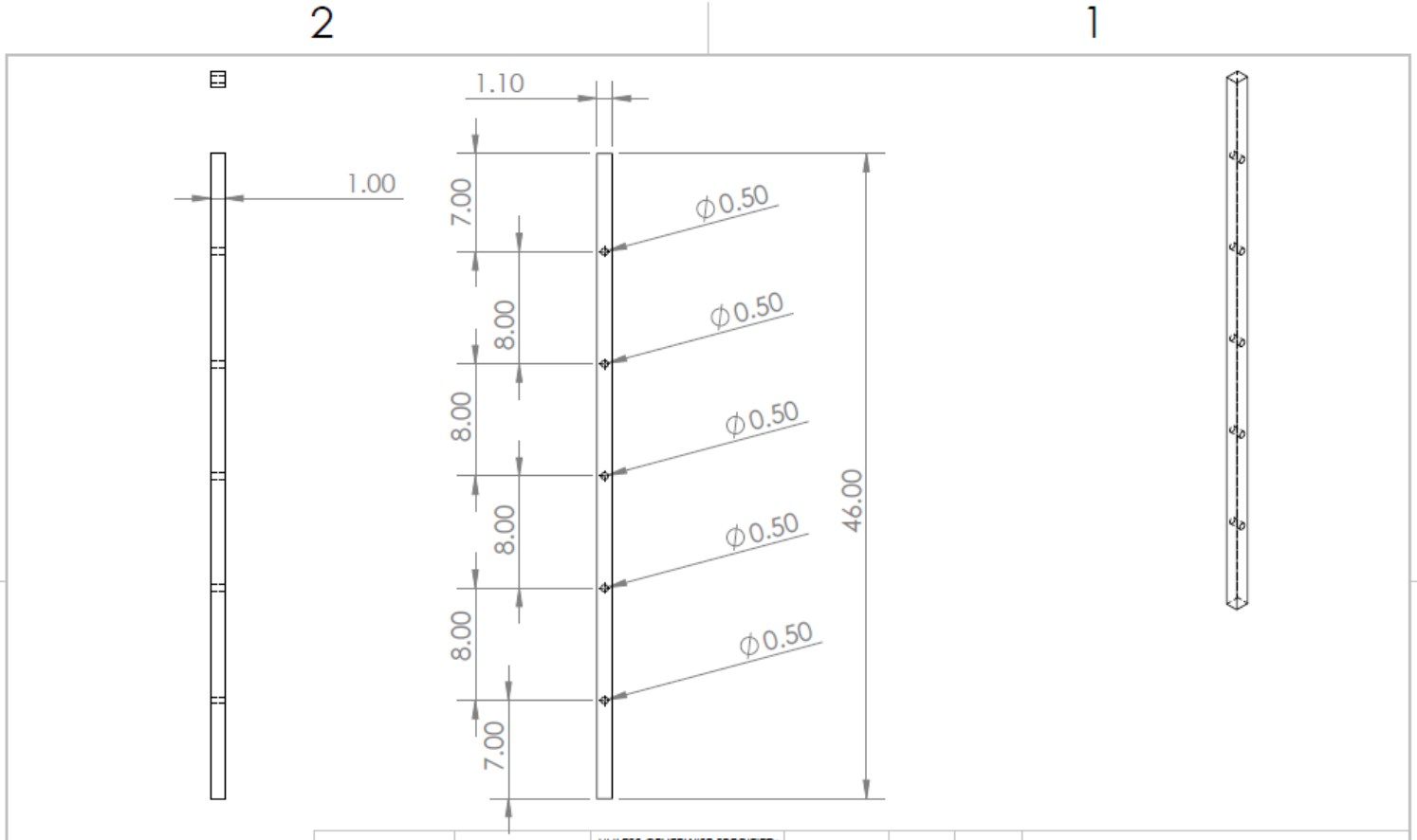

		UNLESS OTHERWISE SPECIFIED:		NAME	DATE
		DIMENSIONS ARE IN INCHES TOLERANCES: FRACTIONAL ± ANGULAR: MACH ± BEND ± TWO PLACE DECIMAL ± THREE PLACE DECIMAL ±	DRAWN		
			CHECKED		
			ENG APPR.		
			MFG APPR.		
		INTERPRET GEOMETRIC TOLERANCING PER:	Q.A.		
		MATERIAL	COMMENTS:		
NEXT ASSY	USED ON	FINISH			
APPLICATION		DO NOT SCALE DRAWING			

PROPRIETARY AND CONFIDENTIAL

THE INFORMATION CONTAINED IN THIS DRAWING IS THE SOLE PROPERTY OF <INSERT COMPANY NAME HERE>. ANY REPRODUCTION IN PART OR AS A WHOLE WITHOUT THE WRITTEN PERMISSION OF <INSERT COMPANY NAME HERE> IS PROHIBITED.

TITLE:

Needs 2 Pieces

SIZE	DWG. NO.	REV
A	Final_InnerShell_Intlet 5 holes Bottom	
SCALE: 1:10	WEIGHT:	SHEET 1 OF 1

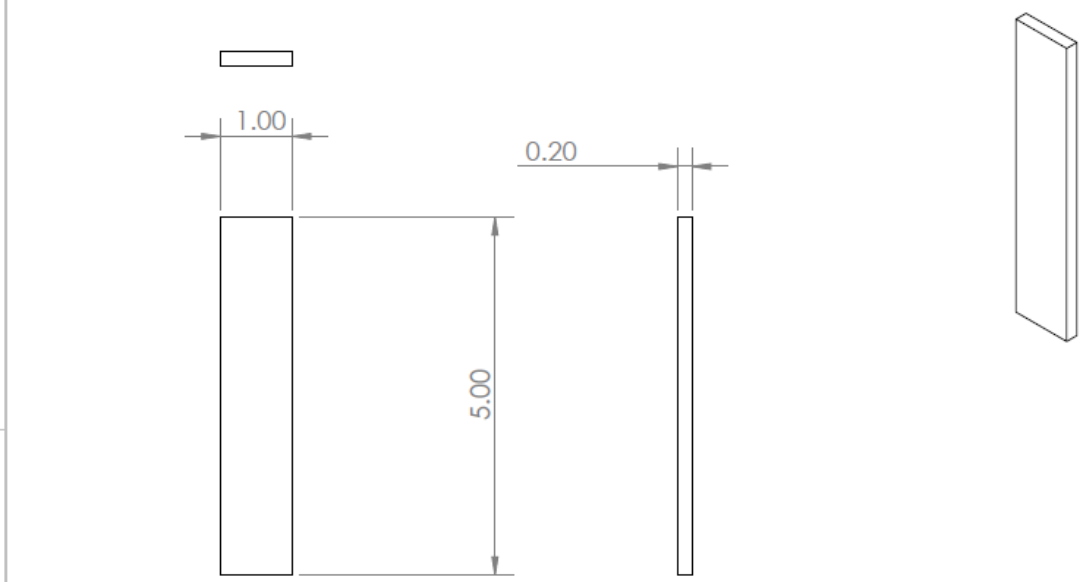

		UNLESS OTHERWISE SPECIFIED:		NAME	DATE
		DIMENSIONS ARE IN INCHES TOLERANCES: FRACTIONAL ± ANGULAR: MACH ± BEND ± TWO PLACE DECIMAL ± THREE PLACE DECIMAL ±	DRAWN		
			CHECKED		
			ENG APPR.		
			MFG APPR.		
		INTERPRET GEOMETRIC TOLERANCING PER:	Q.A.		
		MATERIAL	COMMENTS:		
NEXT ASSY	USED ON	FINISH			
APPLICATION		DO NOT SCALE DRAWING			

TITLE:

Needs 4 Pieces

SIZE	DWG. NO.	REV
A	Final_InnerShell_Intlet 5 holes Bottom 1	
SCALE: 1:2	WEIGHT:	SHEET 1 OF 1

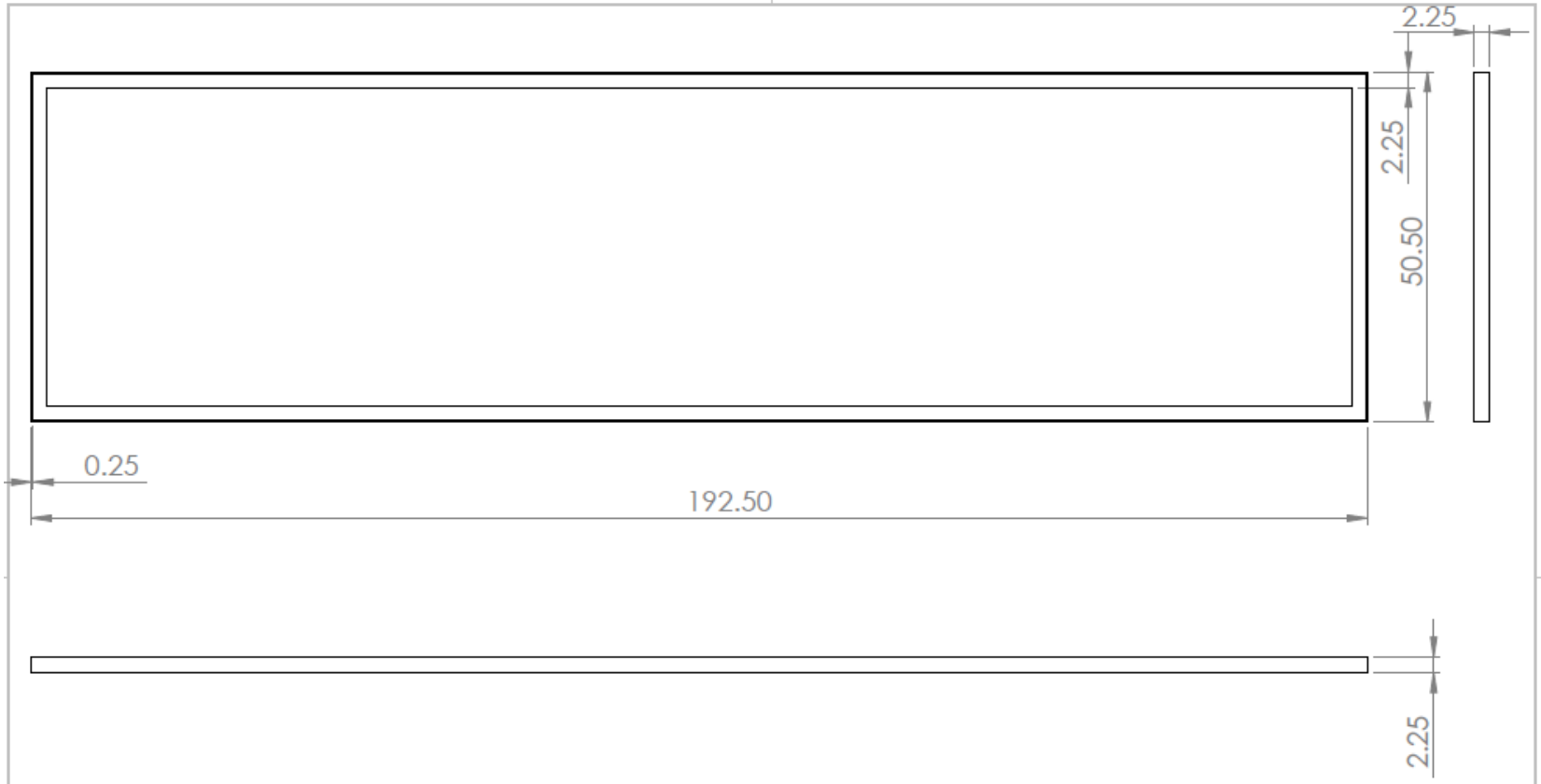

		UNLESS OTHERWISE SPECIFIED:		NAME	DATE
		DIMENSIONS ARE IN INCHES TOLERANCES: FRACTIONAL ± ANGULAR: MACH ± BEND ± TWO PLACE DECIMAL ± THREE PLACE DECIMAL ±	DRAWN		
			CHECKED		
			ENG APPR.		
			MFG APPR.		
		INTERPRET GEOMETRIC TOLERANCING PER:	Q.A.		
		MATERIAL	COMMENTS:		
NEXT ASSY	USED ON	FINISH			
APPLICATION		DO NOT SCALE DRAWING			

TITLE:

SIZE	DWG. NO.	REV
A	Steel Frame	
SCALE: 1:22	WEIGHT:	SHEET 1 OF 1

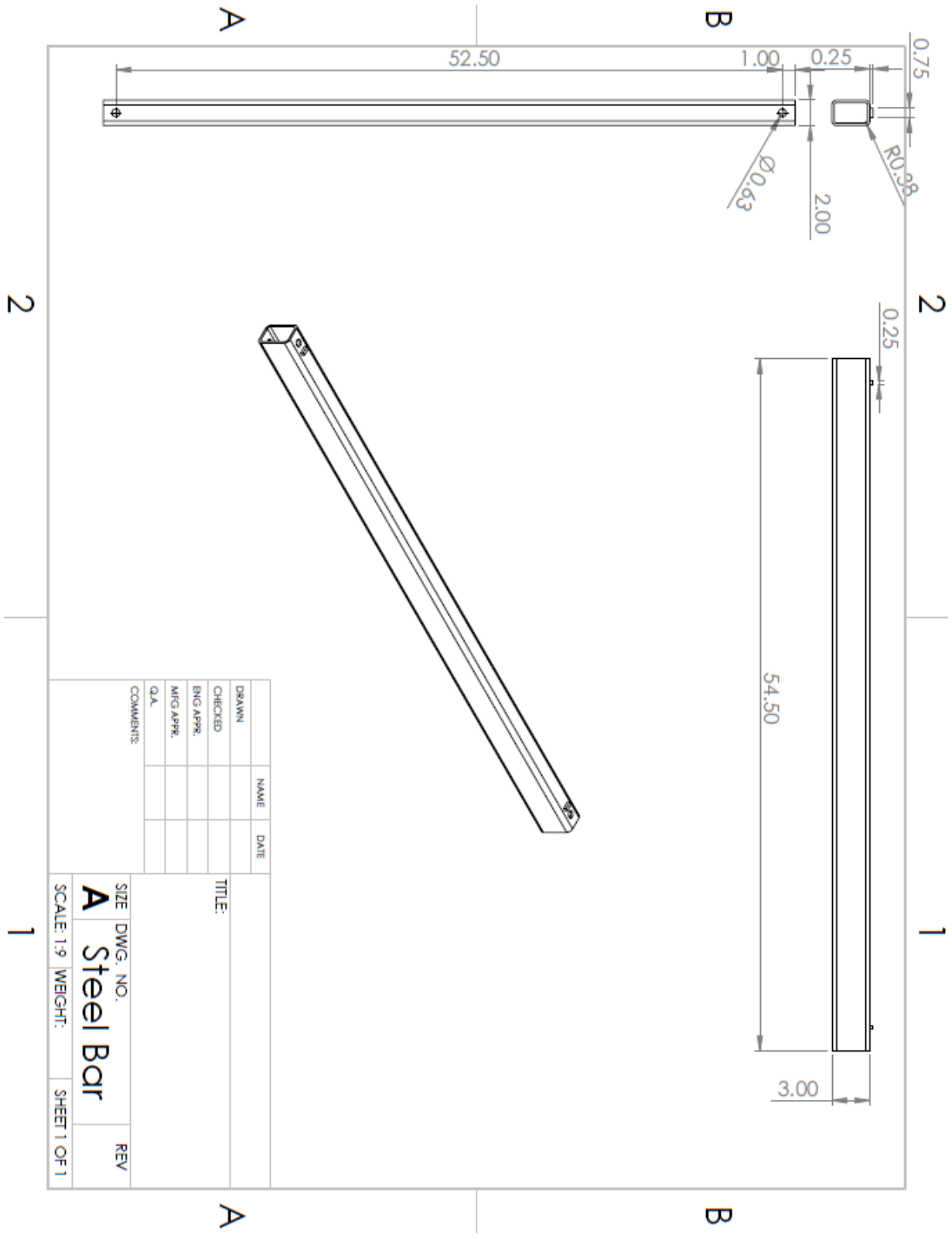
A
B
52.50
1.00
0.25
0.75
R0.38
Ø0.63
2.00
0.25
54.50
3.00
2
1
DRAWN
CHECKED
ENG APPR.
MFG APPR.
Q.A.
COMMENTS:
NAME
DATE
TITLE:
SIZE
A
DWG. NO.
Steel Bar
REV
SCALE: 1:9
WEIGHT:
SHEET 1 OF 1